ADDIS ABABA UNIVERSITY

COLLEGE OF NATURAL SCIENCES

SCHOOL OF EARTH SCEINCES

Analysis of Inter-basin groundwater flow system using Hydrogeochemical and isotope hydrology (δ^2H and$\delta^{18}O$) between Blue Nile and Awash Basins, the case of Gerado and Borkena River Catchments

A Thesis Submitted to School of Earth Sciences of Addis Ababa University in Partial Fulfillment of the Requirements for Degree of Master of Science in Hydrogeology

By: - Sadam Ebrahim

Advisor

Dr. Tilahun Azagegn

Co - Advisor

Prof. Asfawossen Asrat

September 2020

ADDIS ABABA UNIVERSITY

COLLEGE OF NATURAL SCIENCES

SCHOOL OF EARTH SCEINCES

Analysis of Inter-basin groundwater flow system using Hydrogeochemical and isotope hydrology ($\delta^{2}H$ and$\delta^{18}O$) between Blue Nile and Awash Basins, the case of Gerado and Borkena River Catchments

By: Sadam Ebrahim

Approved by Board Examiners

Dr. Balemual Atnafu .....

(Chairman)

Dr. Tilahun Azagegn .....

(Advisor)

Dr. Dessie Nadew .....

(Examiner)

Dr. Dagnachew Leggesse .....

(Examiner)

Acknowledgment

First, I would like to thank my advisor Dr. Tilahun Azagegn and Co-Avisor Prof. Asfawossen Asrat ;- your encouragement have had a vital influence on my development and your guidance helped me in the time of research and writing of this thesis.

I am also thankful for the Institutes from where data have been taken; Water Works and Design Enterprise, Geological survey of Ethiopia, Ministry of Water and Energy, Ethiopian Meteorological Agency (EMA) and Amhara Design and Supervision Works Eniterprises(ADSWE).

I would like to express my deepest gratitude to Bereket Fantaw for his constructive comments, friendly advices and his knowledge sharing as well as for providing me valuable materials and isotope data.

Finally, I would like to express my great apprciation to all my family and friends for their heartfelt inspirations, best wishes and supports:- Samson Hailu, Muluken Muhe, Eden Dessalegn, Mehari Tadesse, Tinsae Mammo, Kagnew Weldesemayat, Shishigu Biset, Seid Ebrahim and all of who has not been mentioned, thank you all.

Abstract

Hydrochemistry and environmental isotope techniques has been used to analyze inter basin groundwater flow and hydrodynamic system between Gerado and Borkena River catchments located at the southwestern block of the Afar depression where it occupies parts of the northern plateau in the northwestern part, western Afar marginal area and associated Graben.
The sratigraphy of the area is characterizes by volcanic episodes were by the extrusion of flood basalts, with interbeds of pyroclastic rocks of rhyolitic or less commonly trachytic compositions, particularly at upper stratigraphic levels and seismically active right stepping N-S trending step system of discontinuous graben that are tens of kilometers long and 5–15 km wide which follow the curving N-S trend of the western Afar margins.
Lithostructurally, Ashange basalt sequence is strongly faulted and tilted by 20° to 30° towards east. The weathering and jointing with the inclined contact is a favorable condition for ground-water flow from highly elevated plateau to the marginal graben.
Boreholes and spring in Gerado catchment are characterized mostly by low TDS (< 500 mg/l) and Ca-Mg-HCO3 water type. While the Borkena catchment show a complex groundwater type and variation in TDS (500- 938 mg/l) Based on its flow pattern. The water types in Borkena catchment generally dominated by Na and Ca cations.
Based on inverse Geochemical Modeling and ionic ratio calculations dominant reaction happened on the flow paths of Groundwater is likely to be cation exchange which Na is Exchanging Ca and dissolution of silicate minerals.
Most of the groundwater samples from Gerado and Borkena catchments have relatively depleted isotopic signature of ^{18}O and D from -2.28 to -6.83 and -2.5 to -7.8 respectively. Isotopically depleted springs found in the adjacent areas of Borkena Catchment while most of the springs found in the Gerado catchment are fall in a line of local Meteoric water.

Spring patterns suggest there is an inter-basin groundwater flow between the catchment. The springs have preferential alignment in emerging with a considerable discharge which support inter-basin groundwater flow.

Keywords: Interbasin Groundwater flow, Blue Nile Basin, Awash Basin, Gerado, Borkena

Table of Contents

Acknowledgment ..... **iii**

Abstract ..... **iv**

Table of Contents ..... **v**

List of Figures ..... **viii**

List of Tables ..... **x**

List of Acronyms ..... **x**

1 Introduction **1**

1.1 Background 1

1.2 Statement of problem 3

1.3 Objectives 4

1.3.1 General objective 4

1.3.2 Specific objectives 4

1.4 Relevance of the study 4

1.5 Literature review 5

1.6 Methodology and Materials 7

1.6.1 Data sources and collection 8

1.6.2 Analyzing Hydrogeochemical data's 8

1.6.3 Analyzing stable isotope data's 8

1.6.4 Activities 9

1.6.5 Work flow of activities 11

1.7 Materials 12

2 The study area **13**

2.1 Location 13

2.2 Physiography, soil, and land use 14

2.2.1 Physiography 14
2.2.2 Soil 16
2.2.3 Land use/cover 17
2.3 Hydrometeorology 19
2.3.1 Climate 19
2.3.2 Preciptation 19
2.3.3 Evapotranspiration 21
2.3.4 Temperature 24
2.3.5 Relative humidity, sunshine hours and wind speed 25
2.4 Hydrology 26
2.4.1 Base flow Analysis 29
3 Geology and structures 32
3.1 Regional geology and tectonics 32
3.2 Ggeology of the Gerado and Borkena catchments 34
3.2.1 Ashangie basalts/Lower Basalt 36
3.2.2 Wegel Tena rhyolitic ignimbrite 37
3.2.3 Dessie Basalt/Middle Basalt 37
3.2.4 Ancharo rhyolite ignimbrite 38
3.2.5 Tarmaber basalts 39
3.2.6 Adami basalt 40
3.2.7 Kemise Formation 40
3.2.8 Rhyolitic tuff 40
3.2.9 Quaternary alluvial deposits 40
3.3 Structures 41
4 Hydrogeology 43

4.1 Introduction 43
4.2 Hydrogeological Units 43
4.2.1 Porous (intergranular)Aquifers 44
4.2.2 Fissured/ fractured Aquifers 45
4.3 Groundwater recharge 48
4.3.1 Chloride Mass Balance 48
4.3.2 Base flow separation 49
4.4 Hydraulic parameters and Groundwater flow 50
4.4.1 Hydraulic conductivity 50
4.4.2 Transmissivity 51
4.4.3 Specific Capacity 51
4.4.4 Groundwater Flow 52
5 Hydrochemistry and Isotope hydrology 59
5.1 Hydrochemistry 59
5.2 Evaluation of laboratory results 60
5.3 Hydrochemical parameters 61
5.3.1 Total ionic concentration and pH 61
5.3.2 Major ions 62
5.4 Hydrochemical evidence of groundwater flow 68
5.4.1 Graphical representations and hydrochemical facies 68
5.4.2 TDS and EC 72
5.4.3 Chloride 76
5.4.4 Ionic ratio 78
5.5 Inverse Geochemical Modeling 81
5.6 Isotope hydrology 86

5.7 Local Meteoric Water Line (LMWL) 87
5.8 Deuterium and Oxygen-18 of Groundwater 88
6 Conclusion and recommendation 92
6.1 Conclusion 92
6.2 Recommendation 94
References 95
Appendics 102

List of Figures

Figure 1. Work flow of the study 11
Figure 2. Location Map 13
Figure 3. Physiographic map 15
Figure 4. Topographic profiles of selected line 16
Figure 5. Soil map (FAO, 1997) 17
Figure 6. Land use /cover map (FAO, 1997) 18
Figure 7. Mean monthly precipitation graph 20
Figure 8. Theissen polygons for Gerado (A) and Borkena (B) Catchments 21
Figure 9. Mean monthly calculated potential Evapotranspiration graph 23
Figure 10. Teleyeyen river (A) Lake Maybar (B) and Kelina river(C) 28
Figure 11. River network of the area 29
Figure 12. Base flow and discharge graph of Borkena at the swamp(A), Kelina (B) and Borkena at Combolcha (C) 31
Figure 13. regional geological map (Abbate et.al., 2015) 34
Figure 14. Geological map modified after ((GSE), Geology of Were Illu Area (NC 37-7), 2009) 35
Figure 15. Ashang Basalt Exposed at Teleyayen River goarge 36
Figure 16. Tossa ridge 37
Figure 17. Ignimbrite in eastern part of Kombolcha town (Multikolo locality) 38

Figure 18. Tarmaber Basalt 39
Figure 19. Structural Map Modified After (GSE, 2009) 42
Figure 20. Artesian flowing well found in Harbu town 45
Figure 21. Springs, at Kurkur (Dessie) (A) and Harbu(B) 45
Figure 22. Lithological logs from different Boreholes in the Area 47
Figure 23. Groundwater level contour map 54
Figure 24. Hydrogeological cross section of East to West 55
Figure 25. Hydrogeological Cross section From North to South 56
Figure 26. Physeographic setup of the areas which the springs are emaneted 57
Figure 27. Electrical conductivity values (Field versus laboratory) 61
Figure 28. Sample distribution of hydrochemical data 63
Figure 29. Ca versus Na graph 64
Figure 30. Ca+Mg versus SO4+HCO3 graph 65
Figure 31. Scatter plot of HCO3 versus Ca 66
Figure 32. Log of HCO3 Ion Versus TDS 67
Figure 33. Piper diagram for the classification of natural waters 68
Figure 34. Na and Ca scatter plot for Na-Ca-HCO3 and Na-HCO3 water types 71
Figure 35. TDS map 73
Figure 36. EC map 75
Figure 37. Chloride Map 77
Figure 38. Plot of Chloride versus TDS 78
Figure 39. Ionic Ratao Map of Na+K/Ca+Mg in meq/l 80
Figure 40. Log Log plot of SO4 versus Na+K 81
Figure 41. selected flow paths for inverse geochemical model 83
Figure 42. Local meteoric water line 87
Figure 43. Environmental isotope data distribution map 89
Figure 44. Groundwater sample against LMWL and GMWL 90

List of Tables

Table 1 Calculated AET using soil water balance method for available water capacity of the root zone 150 mm for Gerado catchmnet 23
Table 2 Calculated AET using soil water balance method for available water capacity of the root zone 150 mm for Borkena catchment. 24
Table 3 Average monthly Temperature(in ^{o}C) of meteorological stations 24
Table 4 Average relative Humidity in percent (%) 25
Table 5 Average monthly Sunshine hours (in hours) 26
Table 6 Average monthly wind speed (in km/day) 26
Table 7 Recharge rates estimated by other studies 50
Table 8 Summary statistics for hydro chemical parameters and ions 62
Table 9 chemical parameters for the selected flow paths 82

List of Acronyms

AET Actual Evapotranspiration

ADSWE Amhara Design and Supervision Works Eniterprises

BFI Base Flow Index

BFS Base Flow Separation

CMB Chloride Mass Balance

DEM Digital Elevation Model

EC Electrical Conductivity

FAO Food and Agriculture Organization

GMWL Global Meteoric Water Line

GPS Gobal Positioning System

GSE Geological Survey of Ethiopia

GWL Groundwater level

IAEA International Atomic Energy Agency

IGF Inter basin Groundwater Flow

ITCZ Intertropical Convergence Zone

LMWL Local Meteoric Water Line

M.a.s.l Meteres Above Sea Level

MCM Million Cubic Meter

MoWR Ministry of Water Resources

NMA National Meteorological Agency

SMOW Standared Mean oceanic Water

PET Potential Evapotranspiration

TDS Total Dissolved Solid

SWL Static Water Level

WWDSE Water Works Design and Supervision Enter

1 Introduction

1.1 Background

A groundwater basin is defined as a volume of the subsurface, through which groundwater flows from areas where the water table is recharged to a location where groundwater discharge occurs (Fetter, 2001). But the aerial extent of the groundwater basin is not necessarily the same as the aerial extent of the corresponding catchment area (Frisbee et al., 2016). Regional groundwater flow can transit underneath intervening topographic highs that define separate basins of surface water drainage.

The potential for groundwater to move from one catchment to another catchment is related to the relative altitude and geological structure of the individual basin. Where the rocks that form the boundary between adjacent basins are sufficiently permeable, there might be flow into or out of the basin. Faults cause discontinuities in rock sequences and this might control groundwater flow. Those faults and structures lead the groundwater across the surface drainage system. A fault also may set high-conducting aquifer rocks against impervious rocks, resulting in water ascent along the fault zone and formation of springs marking the fault line. Occasionally groundwater continues in its general flow path across a fault, but in different rock beds (Mazor, 2004).

Inter-basin flow is not a new scenario. It has been detected at different sites around the world (Genereuxa and Jordan, 2006). Those catchments which have interbrain groundwater flow show more complex discharge zones and characterized by the mixing of groundwater from different age and chemistry (Toth, 1963). There are also attempts of manmade inter-basin diversions, as in china it was planned and partly under construction, aiming at the allocation of water from the Yangtze River to the Hwang Ho basin in the dry northern plains around Beijing (IAEA, 2000).

As the chemical composition of groundwater is greatly dependent on natural factors:- lithologies, hydraulic conductivity, weathering, and length of the flow path. This active interaction of water with the environment helps to understand groundwater chemistry along its flow paths. Inverse modeling is very useful for interpreting the hydrochemical evolution of groundwater (Plummer et al., 1994). This mass balance approach uses two water

analyses represent starting and ending water compositions along a flow path to calculate the moles of minerals and gases that must enter or leave the solution to account for the differences in composition (Parkhurst and Appelo, 1999).

Tracing groundwater by means of environmental isotopes also offers unique and supplementary information on the origin and movement of groundwater (Geyh, 2000). By combining Hydrogeochemical data with environmental stable isotope analysis it can be produced a powerful method for understanding sources and flow dynamics of groundwater system. There are different studies in the world and here in Ethiopia which determines Interbasin groundwater flow (IGF) using a combination of Hydrogeochemical and isotope tracer methods (Nelson and Mayo,2014; Genereuxa and Jordan,2006; Asantea and Kreamerb 2018; Seifu, et al. 2008; Tenalem et al., 2007; Tilahun Azagegn.,2014; Yitbarek 2009).

The study area is characterized by a considerable difference in elevation (3800 up to 1390 m) above sea level. The highest peak is found at the Guguftu Mountain which is an extension of northwestern Ethiopian volcanic plateau. The broad volcanic plateau accounts for about 25 % of Ethiopian landmass. The Ethiopian volcanic plateau is a thick monotonous, rapidly erupted pile of locally deformed, flat-lying basalts consisting of a number of volcanic centers with different magmatic characters and with a large range of ages (Mohr, 1983). That volcanic plateau acts as a surface and groundwater water divide for the most of major drainage basins of Ethiopia. The Blue Nile and Awash basins are among those basins which are divided by those volcanic plateaus.

Structurally the area is formed in three distinct extensional phases of deformation. These are marginal faults that bound the plateau from the rift depression (NNE-SSE), the early extensional phase of deformation which is formed the highly extended rift depression and the later extensional deformation (E-NE) (GSE, 2009). Along with those structures, there is plenty of spring emanated at the foot side of the escarpment which there discharges reach up to 30 l/s. Geologically, the study area is covered by Ashange,Aiba and, Tarmaber basalts, Rhyolite and quaternary alluvial deposits. The weathering and fracturing of these basalts show a variation from place to place which plays an important role in the complexity of the groundwater flow on the study area. This study tries to understand the

flow mechanism of the area and determine the inter-basin flow between two different basins.

There are physical manifestations promising for through-flow between the two basins. The first one is:-at the boundary of the two catchments there is a wetland called Alasha which is found near to the source of the Borkena River around Kutaber town. Mostly wetlands are associated with the groundwater especially in these areas. The second manifestation identified was there is a structurally bounded lake called Maybar which is located probably at the highest elevation (2500 m.a.s.l) in Ethiopia lakes.

1.2 Statement of problem

In central Ethiopia, both highland and rift valley fractured volcanic aquifers are main sources of drinking water for urban and rural communities (Molla et al., 2008). These volcanic aquifers are more important to urban centers where demand for water supply is very high. To address both water supply sustainability and quality, understanding of the groundwater system is very essential.

Some studies have been conducted to understand the hydrogeological and hydro geochemical setup of those groundwater systems separately and even in a small catchment scales (Seifu Kebede, 2013; Tenalem et al., 2007; Seifu et al., 2005; Mesfin Sahle, 2001; BCEOM 1999; and Behailu et al.,2017). In addition to this, there are few attempts tried to study inter basin groundwater flows between Blue Nile and Upper Awash drainage systems.

However: the basin to basin interaction is not explored enough in Ethiopian major Basins because there is general assumption that surface water divides coincides with the groundwater divide. But this assumption is not always correct and such assumption leads inappropriate quantification and prediction of different scenarios in the basins, regions and nationwide.

Furthermore, as the research area is Experiancng a fast rate of population growth, urbanization and industrialization, the necessity to groundwater also increase. Groundwater for this area should be well managed. As a result, the intention of this research is to characterize geochemical evolution of the groundwater for understanding the ground water

flow system and recharge mechanism within and between the two catchments, so that it will be a good input for managing the groundwater resources for those areas.

By combining hydro geochemical data with environmental stable isotope analysis it can be help to understand sources and flow dynamics of ground water system between the two catchments. The results of this study provide an improved conceptual model that reveals the complexity of groundwater exchanges between those main basins (the two different catchments).

1.3 Objectives

1.3.1 General objective

The main objective of the study is to investigate the groundwater flow and hydrodynamic system between Gerado and Borkena River catchments using hydro geochemistry and stable environmental isotope hydrology (^{2}H and ^{18}O).

1.3.2 Specific objectives

Specific objectives are to:-

- ✓ Determine ground water flow systems within the catchments
- ✓ Conduct Hydrochemical characterization
- ✓ To model the geochemical evolution of the groundwater along its flow path
- ✓ To estimate groundwater recharge with in the catchments

1.4 Relevance of the study

The area is known for high prospect of developing groundwater sources for irrigation in the alluvial fan deposits along the foot of the rift escarpments, flood plains, valley fills and regularly recharged by seasonal runoffs and sustained groundwater flow from the highlands (ADSWE,2013). Because of this the Amhara regional government planned a huge irrigation program on the Mariginal grabens on coming years. The water demand is becoming dependant on the deep groundwater. A detail understanding of groundwater recharge in individual catchment as well as of the degree of groundwater exchange between different catchments is critical for sustainable use of groundwater. The study will help policy maker for evaluating groundwater resource development plan as well it will be also

essential for groundwater management. This study will also used as a data source for the futures researchers and concerned peoples.

1.5 Literature review

Inter-basin groundwater flow (IGF) study is becoming a prime Objective in recent years for researchers working on groundwater dynamics. Those research used different methods to investigate flow natures between different Basins. Some approaches used for the IGF are water budget imbalances, potential differences between basins, stable isotope tracer, and Lithostructural and modeling studies. There are some studies Identify IGF using Isotope and Hydrochemical Approach only and complementary with other approaches (Genereux et al.,2005; Anderson et al., 2006; Jordan, 2006; Yitbarek,2009; Nelson and Mayo, 2014; Tilahun et al., 2015; Asantea and Kreamerb, 2018; Genereuxa and; Danapou et al., 2019).

Genereux et al. (2005) quantify interbasin groundwater transfers between two watersheds using both water chemical and watershed Budget. On this work, they concluded that IGF accounted for about 66% of the water input and about 97% of the solute input to one watershed but little or none of the inputs to the adjacent watershed. They also recommended the feasibility of using multiple approaches in determining interbasin groundwater flow.

In a Ph.D. thesis, Yitbarek (2009) was successful to determine groundwater flow between awash and Abay basins by combining Lithostructural analysis, hydrochemical, and Isotope tracer methods. In this work, the author also did a groundwater modeling in order to see the scenario of IGF. According to him a permeable and porous scoraceous Tarmaber formation together with the tectonic structures is responsible for taking the recharge from the adjacent Blue Nile plateau to the Upper Awash groundwater system.

(Tilahun et al., 2015) investigates litho-structural control on inter-basin groundwater flow of the three sub-basins Middle Blue Nile basin (Guder, Muger, and Jema) and the adjacent Upper Awash River basin. They concluded that different structures have a different role in groundwater flow between those different surface drainage basins. The NW–SE trending horsts define the center of the groundwater divide and aquifer distribution within the Middle Blue Nile basin, while the E–W trending mudstone capped horst defines aquifer

distribution between the Middle Blue Nile and the Upper Awash Rivers basins. The impermeable mudstone horst located across the middle of the Muger sub-basin and extending to the southern tip of the Jemma sub-basin forms the groundwater flow barrier guiding groundwater flow to its either side to the north and south. The normal E–W oriented step faults south of the horst enhance groundwater flow rift wards to the Upper Awash basin.

There are some of the investigations in the study area which used to be determining the groundwater potential. the regional level of Upper Awash and the Blue Nile basin was studied by a number of authors determining Geology, hydrogeology, hydrochemistry, and hydrology. Some of the literatures that has been reviewed are discussed below.

On a technical report prepared by Amhara design and supervision works enterprise (ADSWE, 2013) the potential for groundwater is very high especially on the intermountain valleys like Gerado which was formed by the junction of E-W and N-S trending faults. They reported that wells drilled within Gerado valley up to 123m depth never penetrated the alluvial aquifer fully and the discharge for those wells was 35-40 l/s. Meanwhile, from drilled wells with the depth 0f around 114m on Borkana graben in Kombolcha plain, it was possible to obtain 30- 50l/s. Kombolcha plain area is a continuation of Borkena marginal graben; clearly observed a fault crossing Gerado valley running E - W direction along Borkena river and intersect with N-S major fault area and continues to Mitikolo – Cheleka stream and then to Degan area (ADSWE,2013). Those E-W direction faults allow a trough flow between Gerado and Borkena.

On the study of the hydrogeological investigation of upper and middle Borkena river Mesfin Sahle (2001) classified Two hydrogeological units (fracture and intergranular). He also suggests that the groundwater depth of the catchment is very deep based on an observation along the Borkena river discharge is decreasing suddenly. He concluded that Borkena River is recharging the groundwater reservoir. With respect to groundwater flow, he suggests that the regional groundwater flow is the same as the flow pattern of the Borkena River.

(Mola Demile, 2000) On the study of hydrology hydrogeology and hydrochemistry of lake systems of Hayk and Ardibo classified hydrostratigraphic units of the area into two which are the quaternary unconsolidated sediments and fractured volcanic units. According to him, the unconsolidated sediments are very good aquifers while fractured volcanic is classified as a poor aquifer due to morphological setup. He also suggests that the Groundwater flow direction from field observations is towards the respective lakes locally and towards Lake Hayk at the scale of the study catchment.

(GSE, 2017) On Hydrogeological and hydrochemical study of the Dessie map sheet suggested the groundwater flow in the study area is significantly influenced by geomorphology, geological structures (faults, fractures, joints, and lineament), the existence of impermeable layers and the hydraulic properties and continuity of the aquifers. According to GSE (2017), the groundwater flow in the western highlands and associated deep gorges are from north to west and south to west. Another possible groundwater flow, which can be deep and regional, is from the western Afar rift escarpment towards the deep aquifer of the Afar rift floor and they form geothermal systems. They also recommend hydrogeological investigation supported by isotope hydrology and drilling of deep wells both on the escarpment and the rift floor would help determine the hydraulic condition at the rift boundary fault and define the regional flow from the highlands to the lowlands more precisely.

Dereje et al. (2016) tried to estimate groundwater recharge on the Gerardo catchment using a water balance model. According to this study Evapotranspiration and surface, runoff is very high which is 58.1% and 27.4% of total rainfall. Groundwater on the catchment found to be 14.1% of total precipitation which is 52.2 Million cubic meters.

1.6 Methodology and Materials

The analysis of inter basin groundwater between Gerado and Borkena catchment was studied using hydro geochemical and stable isotope tracer methods. In order to achieve the objectives of this work different methods are used. The methods and activities followed in this research work are described in detail below.

1.6.1 Data sources and collection

Hydrochemical data used in this study are from boreholes, spring, Dug wells and a Lake. Those data were obtained Geological survey of Ethiopia. A total of 58 hydrochemical data have been obtained where hydrochemical analysis was done in geological survey of Ethiopia central laboratory.

During the field trip held up on from January 20, 2020- February 5, 2020 an in situ measurement of PH, Temperature, EC was done and a total of 20 samples were collected for a Stable Isotope Laboratory. The sampling was done systematically from both catchments along the possible through flow lines which were selected before the field work.

1.6.2 Analyzing Hydrogeochemical data's

Chemical data have been useful for the interpretation of inter basin groundwater (Genereuxa and Jordan,2006). This study tries to show the ratio of major ions in order to identify the mixing of water from the different aquifers. Analysis has been used to determine if the samples can be grouped into statistically distinct hydro chemical groups that may be significant in the geologic context. A number of studies have used this technique to successfully classify water samples. Comparisons based on different parameters from different samples have been done and the samples are classified according to their similarity to each other. Inverse Geochemical modeling calculations was done along the selected flow path using PHREEQC. More illustrative diagrams like Piper and Schoeller diagrams are used to show the relative concentration of major ions from the gaining and losing catchments.

1.6.3 Analyzing stable isotope data's

The application of isotope-based methods has become well established for water resource assessment, development and management in the hydrological sciences, and is now an integral part of many water quality and environmental studies. The stable isotopic data has been analyzed using scatter plot and linear/non-linear regression analysis as well as comparison of isotope values with the global meteoric line (GMWL) and local meteoric water lines (LMWL).

1.6.4 Activities

The research activities that have been followed in order to achieve the objectives are listed and illustrated on the figure below. The study has been accomplished through three phases.

i) Pre-field activities

ii) Field wok

iii) Post field activities

Pre-field work (phase-I) includes:

- ✓ Collection of Any relevant Previous data from different sources like Geo-sciences Mapping and Geo-information Centre of the Geological Survey of Ethiopia, library of the Ministry of Water Resources, Energy and Irrigation
- ✓ Review of the previous works
- ✓ Collecting the hydro - climatic data
- ✓ Analysis and interpretation of the collected data and information using different software's and tools like ArcGIS, ERDAS Imagine, Global Mapper, Surfer, aquachem and aquifer test, phreeqc

Field study

- ✓ Field survey have been conducted to obtain primary data and observation
- ✓ To collect Ground Water and surface water samples for chemical and isotope analysis will collected
- ✓ Geological structures and geomorphological observation and understanding
- ✓ Field pH, temperature, and EC measurements
- ✓ Acquisition of additional data from water bureaus at federal, regional, zone weredas and private sources

Post field activities

The post field activities include:

- ✓ Data analysis, interpretation and data organization of hydogeochemistry and Isotope hydrology data's.
- ✓ Recharge Estimation Using chloride Mass Balance
- ✓ Preparation of hydro geochemical model
- ✓ Written explanatory notes - assessment of: hydro-climatology, geology, and synthesizing their effects hydrogeology ,hydrodynamics and hydrogeochemistry

1.6.5 Work flow of activities

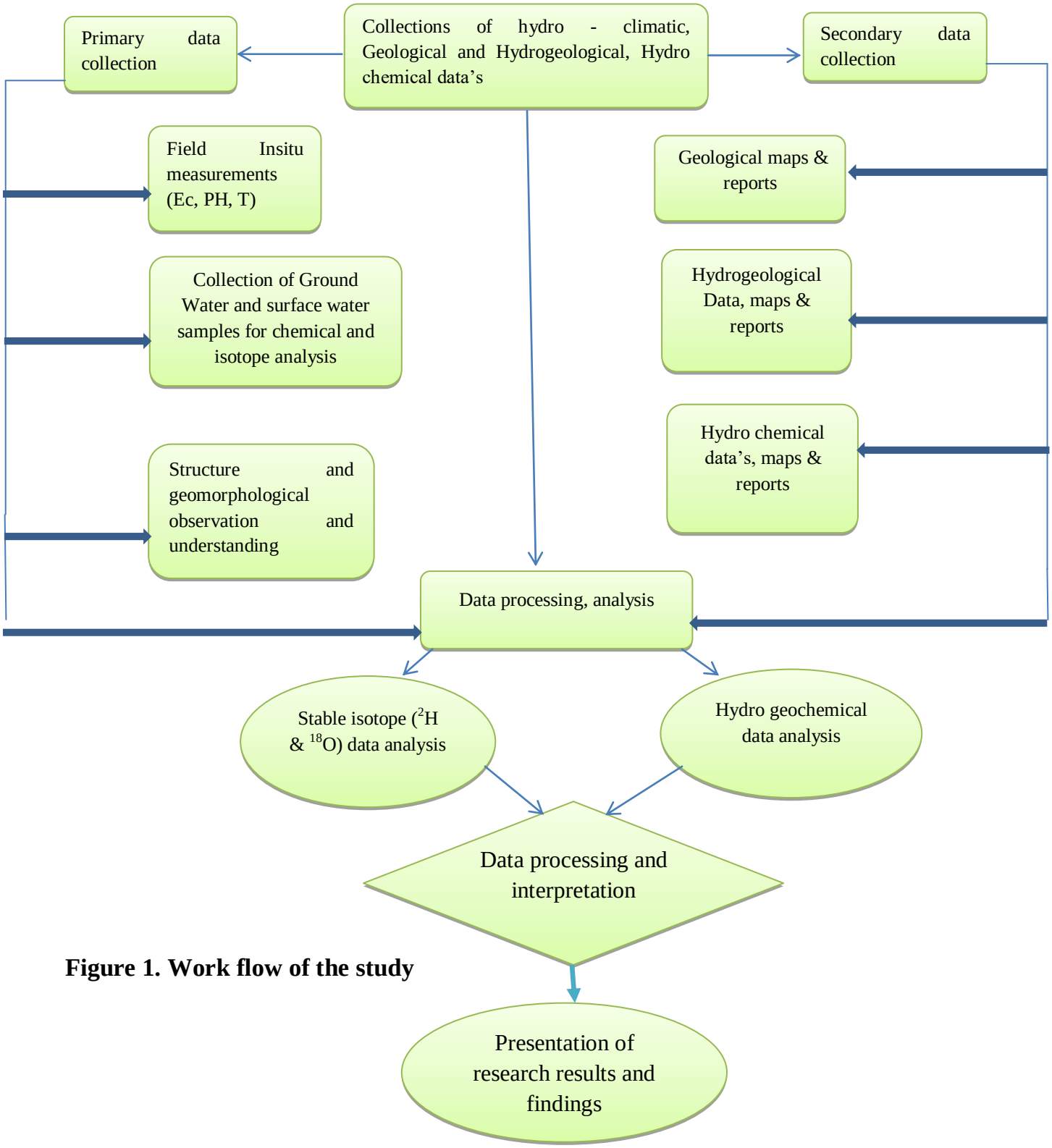

Figure 1. Work flow of the study

1.7 Materials

1. Topographic map of 1:250,000 scale used to Visualization of different topographic and geomorphologic features and assessment of access routs2.SRTM data to delineate watersheds, slope and hill shades of the research area
2. software's and tools like ArcGIS, Global Mapper, Surfer, aquachem and aquifertest, Aquachem
3. GPS used for acquiring positions
4. Geological and hydrogeological maps used as Reference/ Base map during the field work
5. Portable pH and EC meter used for Field measurement of pH and electrical conductivity of water samples
6. Solutions of known pH (4, 7, and 10) and concentration of dissolved salt (KCl of 1N concentration) for Calibration/ adjustment of pH and EC meter
7. Distilled water for washing the electrodes of pH and EC meters to prevent sample contamination
8. Plastic sample bottles for Collecting and storing representative water samples.

2 The study area

2.1 Location

The study area is found around Dessie Area which the capital of South Wollo. It can be accessed along Addis Ababa to Dessie a 401 km asphalt road. It is approximately bounded to 10^{o} 24' 0'' up to 11^{o} 30' 0'' N and 39^{o}24'0' up to 39^{o} 54' 0'' E. The study area is elongated in the NNW to SSE direction with a total length about 118 km and the maximum width not more than 41 km East-West direction. The total area considered in this study is about 3030 sq. /km.

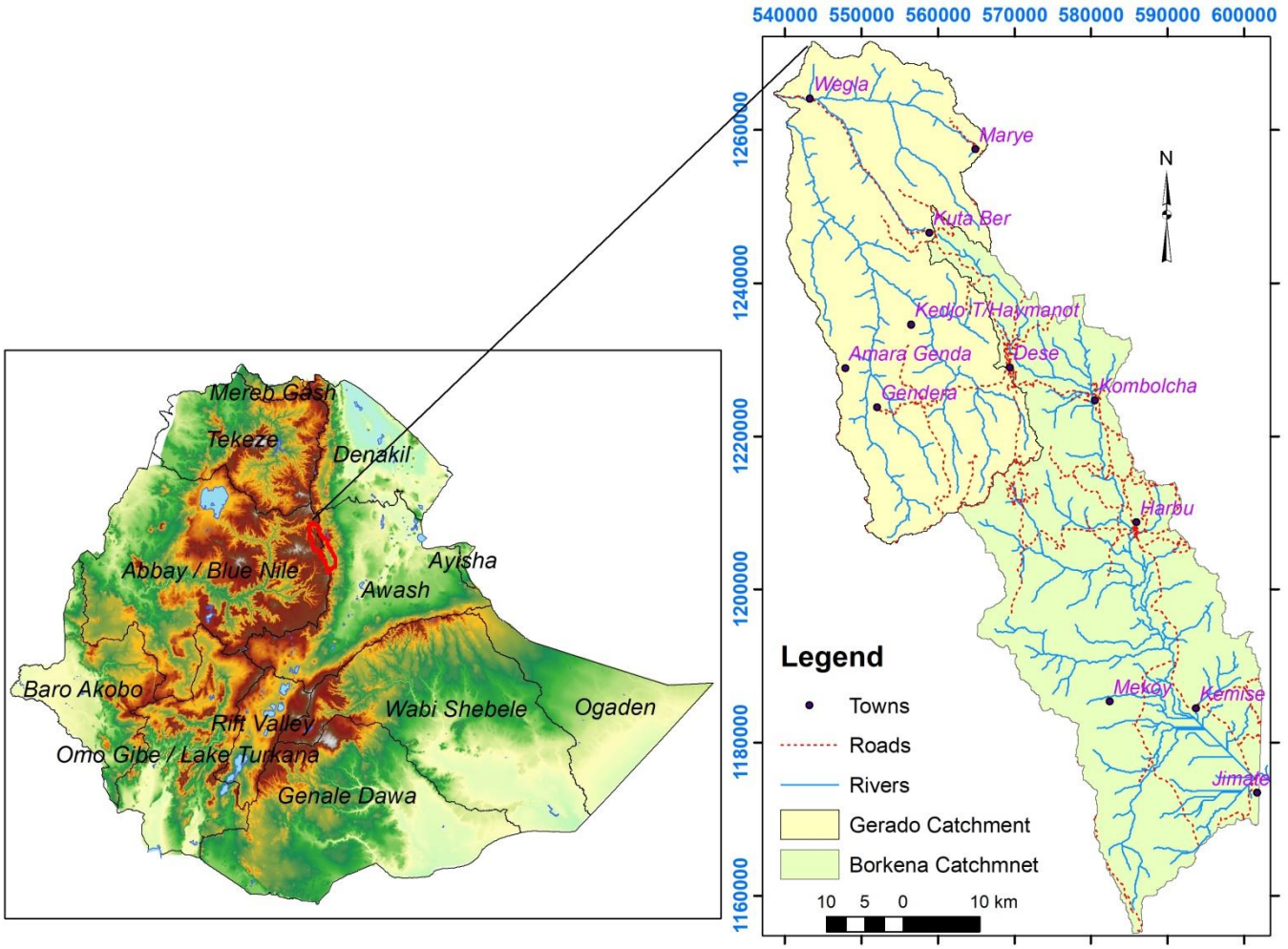

Figure 2. Location Map

2.2 Physiography, soil, and land use

2.2.1 Physiography

The physiography of the area is highly variable and is generally the result of repeated volcanic and tectonic events with the associated erosion of volcanic rocks and deposition processes. The tectonic activity and lithological variation in the area also control the drainage density and drainage pattern. The physiography comprises of the western Afar marginal graben and highland plateau. The N-S trending Borkena graben is an extension of Afar Mariginal graben includes Robit, Ataye, Mersa, Hayk, Ardibo,and Kobo. Borkena graben is characterized with hilly terrain of the rift ward tilted faulted blocks (GSE, 2009). The western highlands, part of the northern-central Plateau, forms typical plateau topography, which is extensively eroded and dissected by deep gorges. The eastern part is part of the southwestern block of the Afar Depression and is separated from the western plateau by NNW-SSE striking western Afar escarpment. The elevation varies from approximately 3800 to 1390 m.a.s.l. Highland plateau forming the shoulder of the Afar Depression abruptly fall into lowland plains towards the center of the Afar Depression. The highland is dissected by deep V-shaped NW trending Gerado River and its tributaries. Most of the rivers start from the high lands of the plateau situated in the central part of the study area.

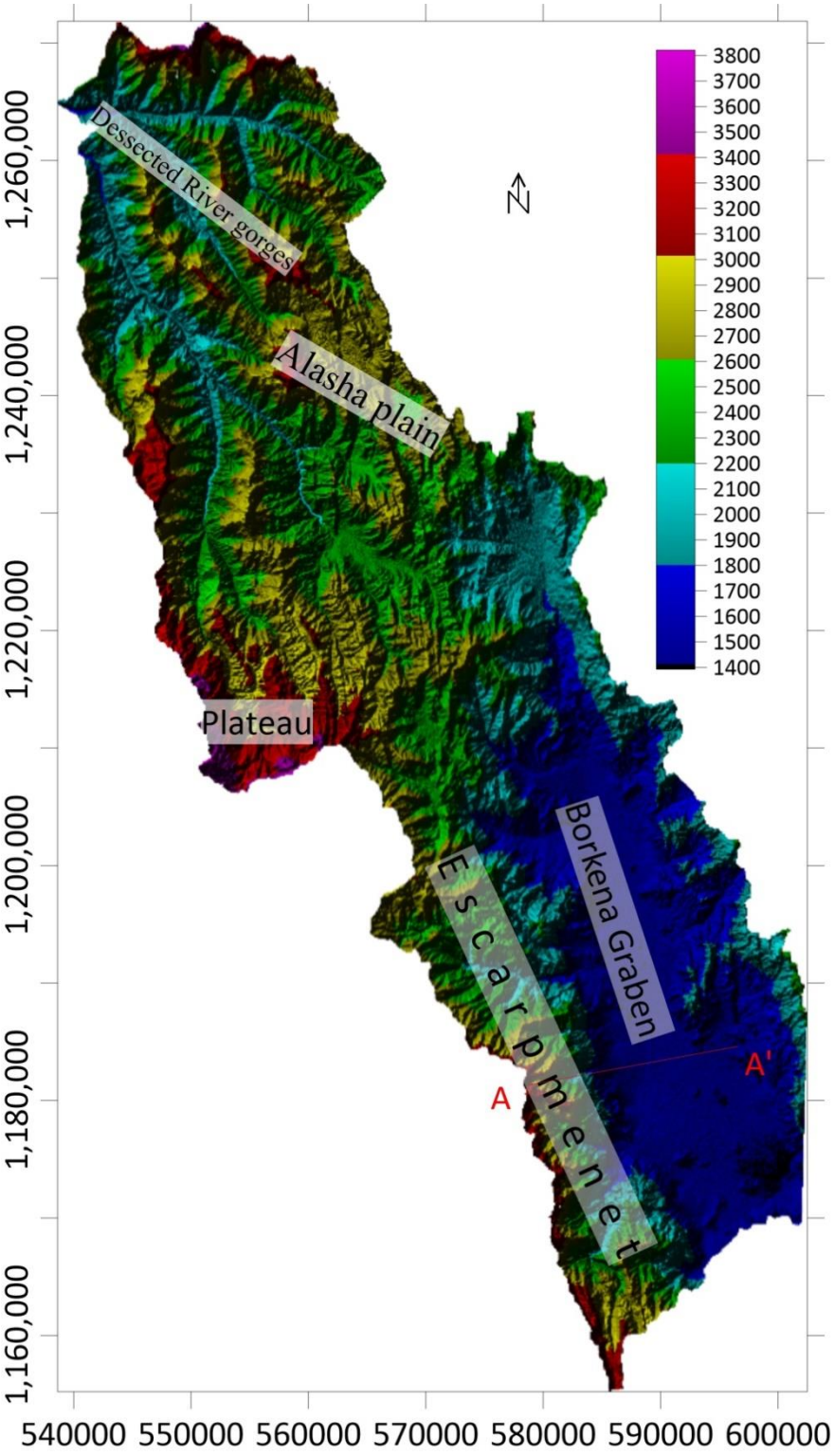

Figure 3. Physiographic map

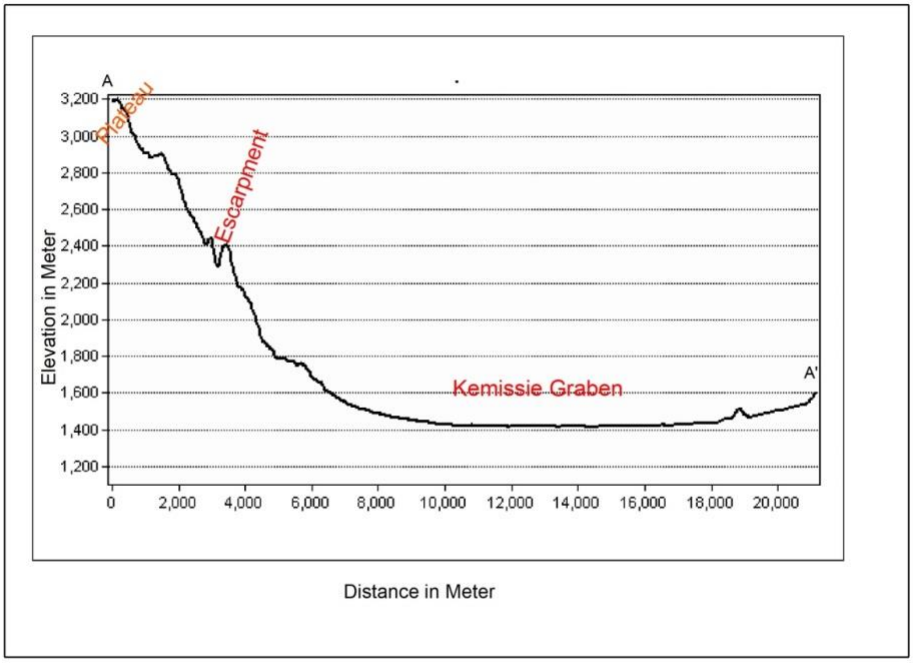

Figure 4. Topographic profiles of selected line

2.2.2 Soil

Bare soil has much lower infiltration capacity than soil with vegetative cover. Consequently, bare soil is much more easily eroded by surface runoff. Soil types also have a significant effect on the recharge and surface runoff mechanisms of the catchments. Sandy soils favors infiltration because of their porosity. In general, the infiltration rate decreases with increasing clay content in the soil. Initial soil-water content and saturated hydraulic conductivity of the soil also have an effect on infiltration process.

A considerable area for both catchments' covered by silt loam which accounts 1449 km^2 of the study area. Areas of adjacent to mountain are covered with sandy soil and some flat lying areas are covered clay soil.

Most of mountainous areas of Gerado catchment are covered with leptosols which are the most extensive soil types on the earth. Those soil types have thickness less than 10 cm. which are very favorable for runoff on the catchment.

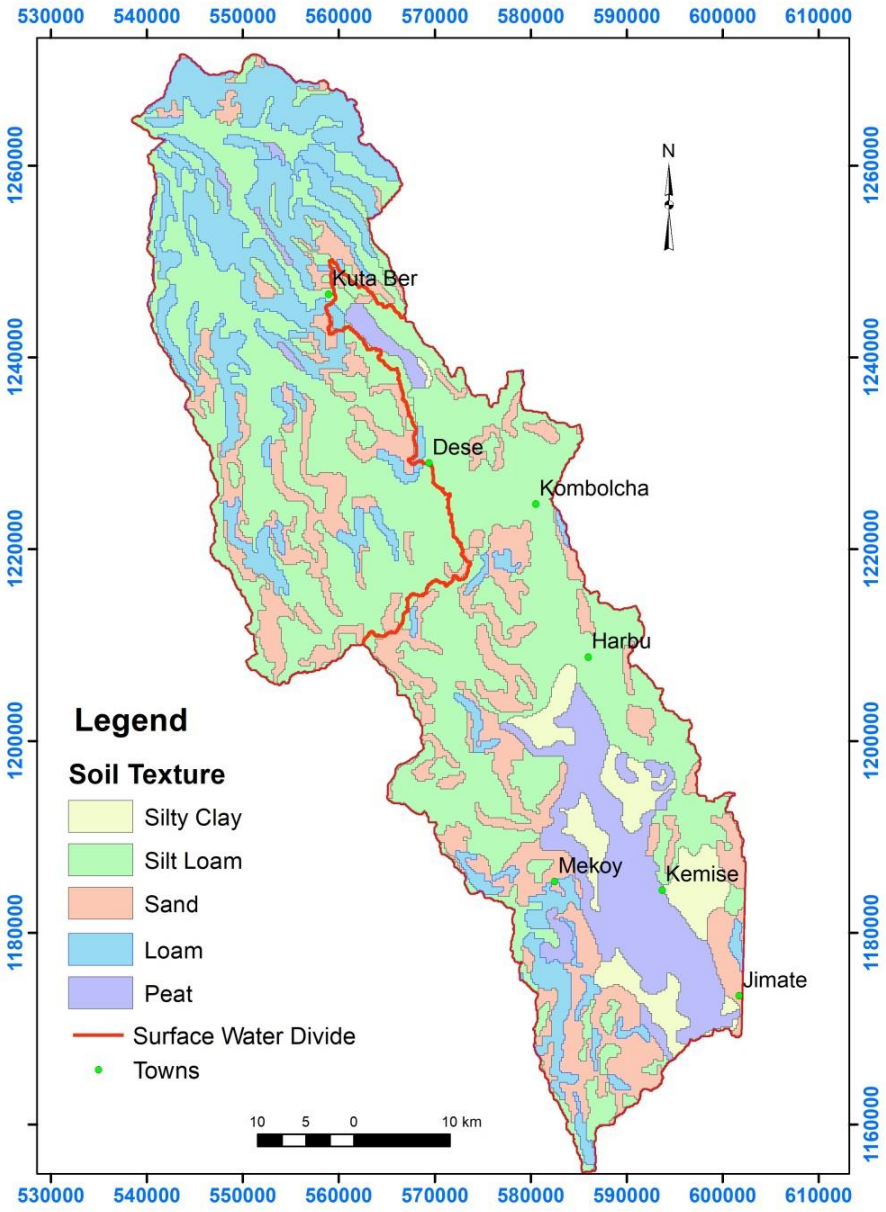

Figure 5. Soil map (FAO, 1997)

2.2.3 Land use/cover

It is obvious that the presence of vegetation protects the soil surface from the impact of rainfall. Root systems of vegetation tend to enhance soil porosity and permeability (Kresic, 2007).Urban areas and development generally decrease infiltration rates and increase

surface runoff because of the increasing presence of various impervious surfaces (rooftops, asphalt, concrete). Urban areas are facilitating the water runoff other than percolation.

Most of the area of both Gerado and Borkena basin has covered by annual crops. The area is also considerably covered with sparse forests. The study area has the following land covers (FAO, 1997).The map (Fig 6) Show land use/covers of the study area.

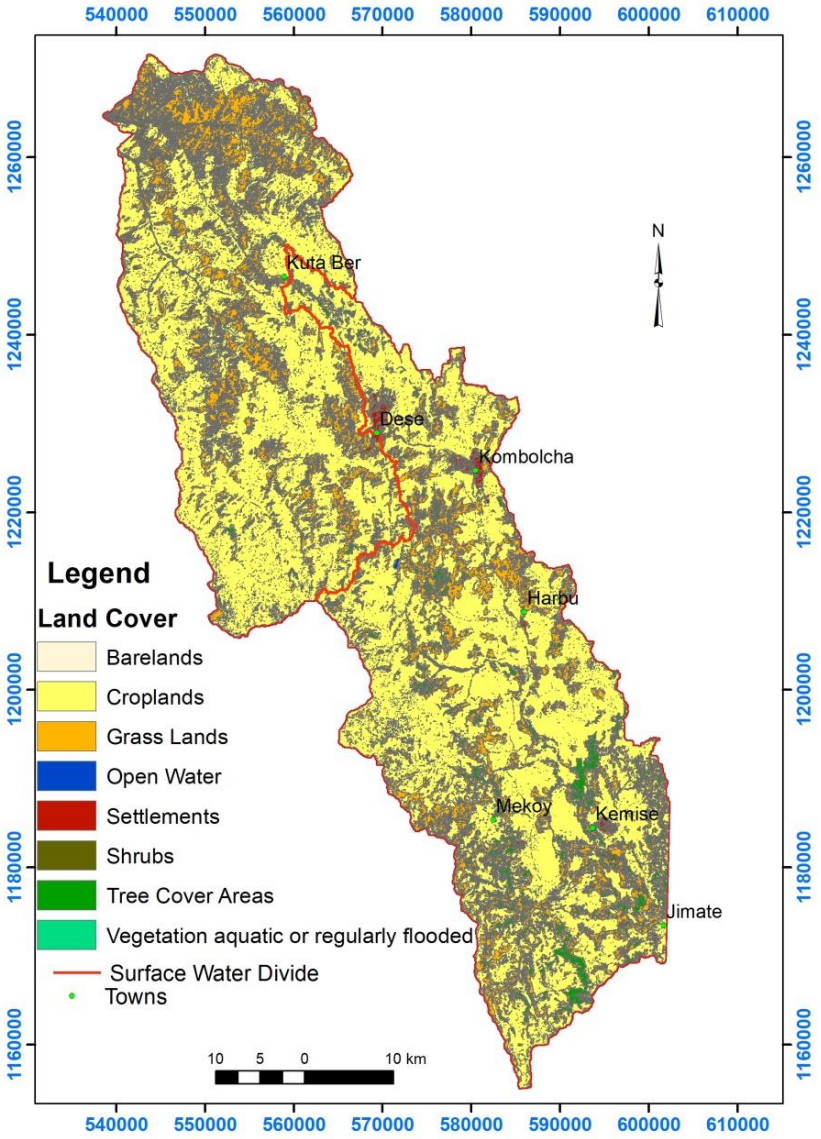

Figure 6. Land use /cover map (FAO, 1997)

2.3 Hydrometeorology

2.3.1 Climate

The climate of Ethiopia is mainly controlled by the seasonal migration of the Intertropical Convergence Zone (ITCZ) and associated atmospheric circulations as well as by the complex topography of the country. Landscapes with contrasting characteristics in terms of physiographic and elevation, such as the highlands and the lowlands, experience a variety of climates from desert climate to that typical of equatorial mountains (Fazzini et al., 2015).

The climatic condition of the country is conventionally classified into five climatic zones based on the elevation and temperature variation. It ranges from the high cold area named as “wurch” to the highly hot climatic condition area known as “Berha.

In order to understand the different features of the climatic conditions of the study area the monthly mean meteorological measurements were collected from the National Meteorological Agency (NMA). The data considered include monthly mean rainfall, maximum and minimum temperature for all stations, relative humidity, sunshine hours and wind speed. Even though the data is inconsistent it will provide basic information regarding the climatic conditions of the area. Each of the climatic features is discussed in brief below.

2.3.2 Preciptation

Amount of precipitations varies both spatially and temporally. Despite the fact that Ethiopia is gifted with a considerable amount of water resources it’s economy is mainly dependent on rain-fed agriculture; the failure of seasonal rainfall is incredibly devastating to the country’s socio economic functioning- in particular, food production (Kassa, 2015). There have been a noticeable famines happened due to seasonal failure in rain fall in the country. Particularly the study area is prone to drought because of the variability of rainfall. All meteorological stations shows same trend of annual precipitation, and the year 2015 and 2004 were the lowest annual rainfall recorded in all stations.

On the rainfall analysis ten meteorological stations from year 1986 to 2018 have been analyzed. Most of these stations have long year’s records with very good data quality. Data with missing records greater than 3 months have been omitted. From the analyzed data the lowest annual rain recorded on the study area was 502 mm which was recorded in a year of

2015 on the Harbu station. Mean monthly precipitations of ten meteorological stations are shown in the figure below. Most of the rainfall occurs during the months of July and August for all stations.

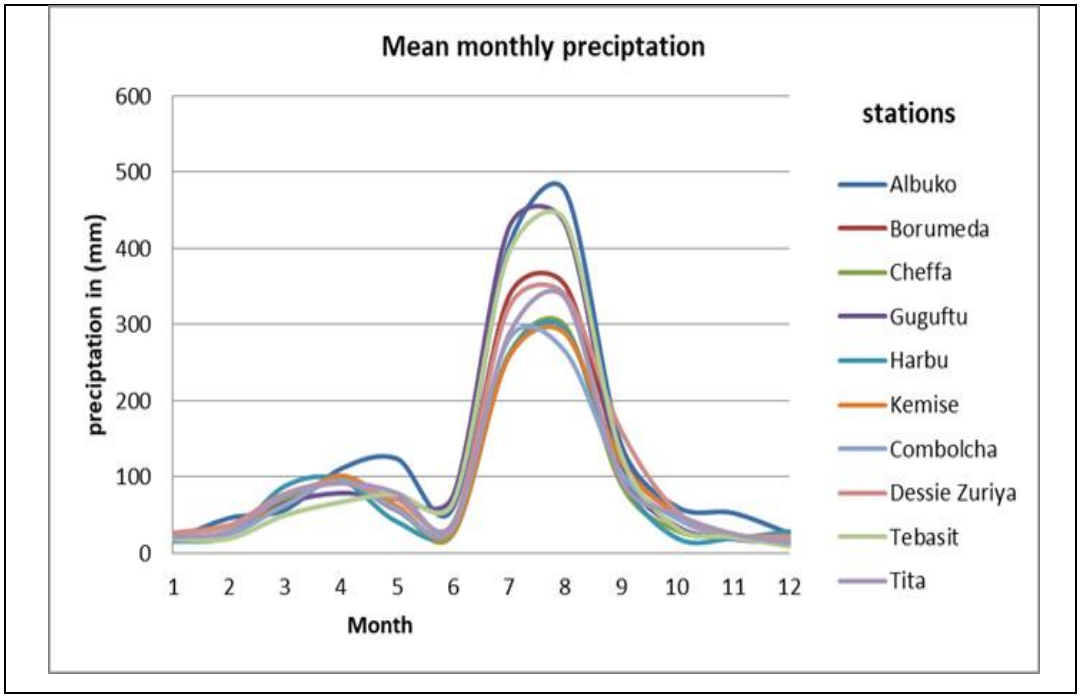

Figure 7. Mean monthly precipitation graph

The distribution of precipitation varies spatially. There is some difference between highlands and lowlands due to large difference in altitude. However, there are stations such as Albuko and Dessie Zuriya, with relatively high precipitation values unlike their relatively lower altitude. Thiessen polygonal averaging method was also used to calculate annual precipitation (fig 8). Annual precipitation is calculated separately for the two catchments and the annual precipitation for the Gerado is 1291.3 mm/year and 1156.7 mm/year for the Borkena catchment. Hence Gerado has much precipitation than Borkena because its topography is favorable for runoff. The runoff for the Gerado catchment is 27.4% of total precipitation (Dereje et al., 2016).

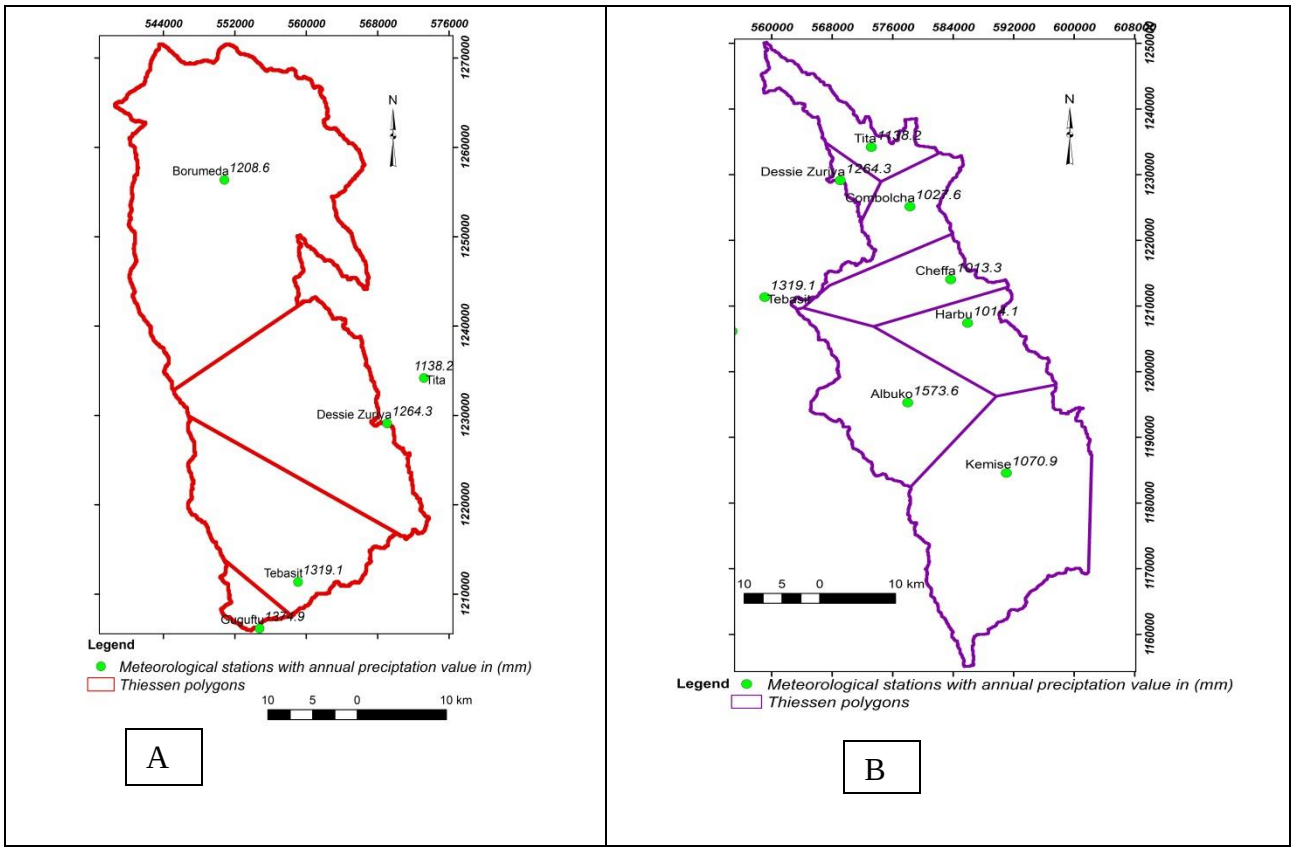

Figure 8. Theissen polygons for Gerado (A) and Borkena (B) Catchments

2.3.3 Evapotranspiration

Evapotranspiration is known as a loss of water or moisture through the process of transpiration by plants and evaporation of water from the soil and water bodies. If sufficient moisture is available for the need of vegetation covering the area under the given set of atmospheric conditions, the resulting evapotranspiration is called potential evapotranspiration. Potential evapotranspiration is a measure of maximum possible water loss from an area under a specified set of weather conditions.

The mean monthly potential evapotranspiration (ETo) has been estimated for the two catchments using Penman-Monteith method with the help of the FAO (2009) software known as Cropwat version 8.0. Estimated meteorological stations with in Gerado catchments are Guguftu, Amba Mariyam and Borumeda. The stations belongs to Borkena Catchments are Combolcha, Tita, Cheffa, and Albuko. FAO Penman-Monteith method is a combination of energy, aerodynamic and surface resistance equations and is given below

$$ETo = \frac{0.408\Delta (Rn-G) + \gamma (900/T+273)\, u2\, (es-ea)}{\Delta + \gamma (1+0.34\, u2)}$$

Where,

ETo = reference evapotranspiration (mm/d)

Rn = net radiation at the crop surface (MJ/m2d)

G = soil heat flux density (MJ/m2d)

T = mean daily air temperature at 2m height (ºC)

u2 = wind speed at 2 m height (km/d)

es = saturation vapor pressure (kPa)

ea = actual vapor pressure (kPa)

es-ea = saturation vapour pressure deficit (kPa)

Δ = slope vaspour pressure curve (kPa/ ºC)

γ = psychometric constant (kPa/ ºC)

Mean annual Potential evapotranspiration is relatively low in Gerado (1346.3 mm/year) catchment than Borkena (1462.1 mm/year). This is because Borkena is found in low land area with respect to Gerado.

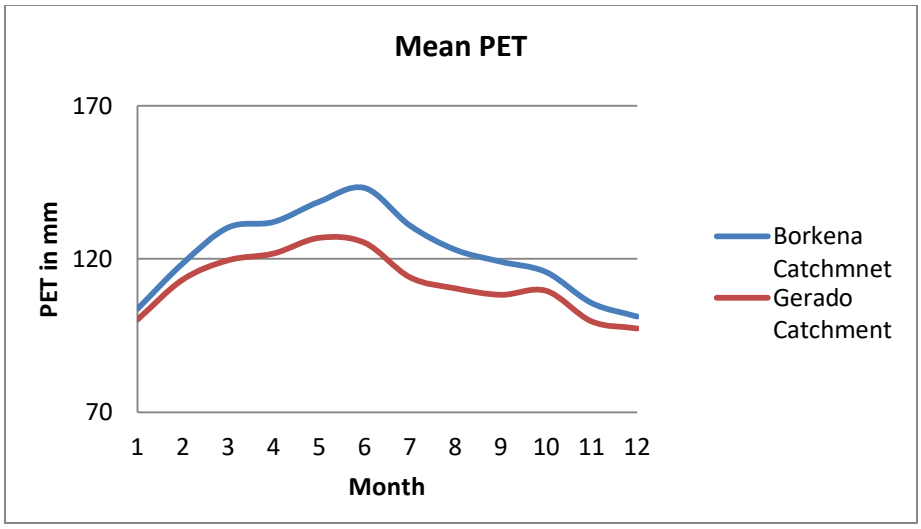

Figure 9. Mean monthly calculated potential Evapotranspiration graph

Soil moisture balance was applied to obtain actual evapotranspiration using the dominant soil types and respective land use for both catchments separately. Accordingly, the annual calculated average AET is 878.4 and 890.9 mm/year for Gerado and Borkena catchments respectively.

Table 1 **Calculated AET using soil water balance method for available water capacity of the root zone 150 mm for Gerado catchment. All values are in mm**

	Jan	Feb	Mar	Apr	May	Jun	Jul	Aug	Sep	Oct	Nov	Dec	Annual
P	20.3	26.3	64.7	82.9	68.5	53.7	370.6	390	132.6	43.4	20.5	17.8	1291.3
PET	100.2	113.3	119.6	121.8	126.9	125.3	114	110.4	108.3	109.6	99.6	97.3	1346.3
P-PET	-79.9	-87	-54.9	-38.9	-58.4	-71.6	256.6	279.6	24.3	-66.2	-79.1	-79.5	
APWL	-304.7	-391.7	-446.6	-485.5	-543.9	-615.5				-66.2	-145.3	-224.8	
SM	19.6	11	7.6	5.8	3.9	2.4	150	150	150	96.4	56.9	33.5	
Change I SM	-13.9	-8.6	-3.4	-1.8	-1.9	-1.5	147.6	0	0	-53.6	-39.5	-23.4	
AET	34.2	34.9	68.1	84.7	70.4	55.2	114	110.4	108.3	97	60	41.2	878.4

Table 2 Calculated AET using soil water balance method for available water capacity of the root zone 150 mm for Borkena catchment. All values are in mm

	Jan	Feb	Mar	Apr	May	Jun	Jul	Aug	Sep	Oct	Nov	Dec	Annual
P	21.1	30.6	70.6	97.2	69.9	36.1	296.2	327.9	116.5	44.2	26.2	20.2	1156.7
PET	103.7	118.6	130.3	132.1	138.7	143.2	130.9	123	119.1	115.7	105.6	101.2	1462.1
P-PET	-82.6	-88	-59.7	-34.9	-68.8	-107.1	165.3	204.9	-2.6	-71.5	-79.4	-81	
APWL	-317.1	-405.1	-464.8	-499.7	-568.5	-675.6			-2.6	-74.1	-153.5	-234.5	
SM	18.1	10	6.7	5.3	3.3	1.6	150	150	147.4	91.5	53.9	31.4	
Change in SM	-13.3	-8	-3.3	-1.4	-1.9	-1.7	148.3	0	-2.6	-55.9	-37.6	-22.4	
AET	34.4	20.5	63.8	91.8	66.5	34.4	130.9	123	119.1	100.1	63.81	42.6	890.91

2.3.4 Temperature

Monthly maximum and minimum temperatures data (2008-2018) have been obtained for seven stations within the study area. The mean monthly temperatures have been calculated for each station. The mean monthly temperature data for Combolcha, Harbu, Guguftu, Cheffa,Tita , Marye and Amba Mariyam stations are given in Table below.

Temperature varies in the study area and does show relationship with altitude. The mean annual temperature for these stations vary from the minimum 9.6 ℃ for Guguftu station in december to the maximum of 25.7 ℃ for Cheffa station in June.

Table 3 Average monthly Temperature(in ^{o}C) of meteorological stations

Stations	Jan	Feb	Mar	Apr	May	Jun	Jul	Aug	Sep	Oct	Nov	Dec
Mariye	13.9	15.5	16.8	17.8	18.6	19.4	18.2	17.3	17	15.6	14.4	13.6
Amba Mariyam	13	14.2	14.7	14	14.9	15.1	13.1	12.5	12.8	12.5	12.5	12.4
Tita	13.1	14.43	15.5	16.5	17.4	18.78	18	17	16.5	14.7	13.7	12.9

Combolcha	17.8	18.8	20.2	21.3	22	23.2	22.2	21.3	20.7	18.9	17.8	17.1
Harbu	19.3	19.8	21.1	21.4	22.1	22.4	21.8	20.7	19.9	19.1	18.7	18.6
Guguftu	10.5	10.3	10.8	11	11.1	11	10.6	10.7	10.5	10.1	9.9	9.6
Cheffa	19	21.2	22.6	23.6	24.3	25.7	24.5	23	22.4	20.5	19.4	18.6

2.3.5 Relative humidity, sunshine hours and wind speed

Relative humidity was measured five times a day, which is at 6:00, 9:00, 12:00, 15:00 and 18:00 hours. Relative humidity is found to be higher at Amba Maryam station (60.9 %) and lower for Combolcha station (58.6 %). Generally, relative humidity is higher during rainy seasons than dry period in all stations (table 4).

Daily sunshine hours are low during wet season than during dry period in all stations. Amba Mariyam station has the highest mean annual daily sunshine hours (8.2 hours) while Cheffa station has the lowest sunshine hours (7.8 hours) (Table 5).

Wind speed is measured at 2 m above the ground surface. The highest wind speed (119.2 km/d) is recorded for Amba Mariyam station and the lowest (52.4 km/d) is for Combolcha station. Wind speed is generally high during summer season in all stations.

Long term (2004- 2015) mean monthly relative humidity, sunshine hours and wind speed data for three stations are given in Tables below (table 4, 5 and 6).

Table 4 Average relative Humidity in percent (%)

Stations	Jan	Feb	Mar	Apr	May	Jun	Jul	Aug	Sep	Oct	Nov	Dec
Cheffa	62.3	55.72	55.6	57.21	56.1	42.6	58.2	71.2	68.8	61.3	59.3	57.9
Combolcha	62.81	55.6	55.4	59.6	54.76	44.3	57.4	67.8	64.5	60.1	61.3	60
Amba Mariyam	53.9	49.1	54.7	57.7	59.4	53	75.1	81.2	70.1	61.8	59.7	55.4

Table 5 Average monthly Sunshine hours (in hours)

Station	Jan	Feb	Mar	Apr	May	Jun	Jul	Aug	Sep	Oct	Nov	Dec
Combolcha	8.1	9	8.3	8.3	8.6	7.5	6.3	6.4	6.9	8.2	8.8	8.4
Cheffa	7.5	8.5	8.1	8.1	8.9	7.2	6.1	6.6	7.2	8.5	8.8	8.3
Amba Mariyam	9	9.2	8.5	8.3	8.9	7.1	5.4	6.2	7.7	9.5	9.3	9.3

Table 6 Average monthly wind speed (in km/day)

Station	Jan	Feb	Mar	Apr	May	Jun	Jul	Aug	Sep	Oct	Nov	Dec
Combolcha	57.9	63.8	60.8	58.6	58.2	67.6	61.4	49.4	36.9	33.2	37.3	43.7
Cheffa	117.5	133.8	139.1	132.9	131.6	138.2	135.7	106.3	84.3	84.1	96.8	105.4
Amba Mariyam	114.2	132.2	135.2	139.8	137.8	116.4	98.7	83.8	96.5	129.2	126.3	121.2

2.4 Hydrology

The drainage system in the study area is mainly controlled by topography and geological structures. Borkena and Gerado are among the perennial rivers found in the study area which flow towards Northwest and southeast directions. Borkena River is flowing to the Awash river Basin while Gerado belongs to Blue Nile river Basin. The western Afar Margin which forms the water divides between the eastern Awash River and the western Abay basins. There are many streams that feed Gerado River some of them are Indode, Kelina, Yito, Teleyayen and kechem rivers. The streams are characterized by a dendritic to sub parallel drainage pattern. On the other hand the tributary of Borkena River are mostly intermittent and seasonal streams while Borkena is a flowing throughout the year. The tributary streams of upper Borkena River are Werka, Luyele, Arawele, Wefkele and Werkwuha, While the rivers Bisheya, Sal, Duben, Beteho, Felana, Dirma, and Halko streams which emerge from western and eastern part of the horst and drain to Harbu and Kemissie plain, and join with Borkena river in the lower course of the catchment. Some of the researchers suggest that Borkena River is recharged by the groundwater (Mesfin, 2001). Base flow index (BFI)

calculated at the swamp outlet of Borkena is became 0.52 which also confirms this assumption of gaining river.

In addition to the rivers Borkena catchments is also known for fault bounded seasonal and permanent plains and marsh areas. These plains are Boru plain, Felana plain, Alansha plain and large Kemissie plain and wetlands. Recharge to these plain comes out as seepage and from the contacts of different basaltic flows along the fault scarp (Ketema Tadesse,1980). There is also structurally bounded lake called Maybar which is located probably at the highest elevation (2500m.a.s.l) in Ethiopia Lakes.

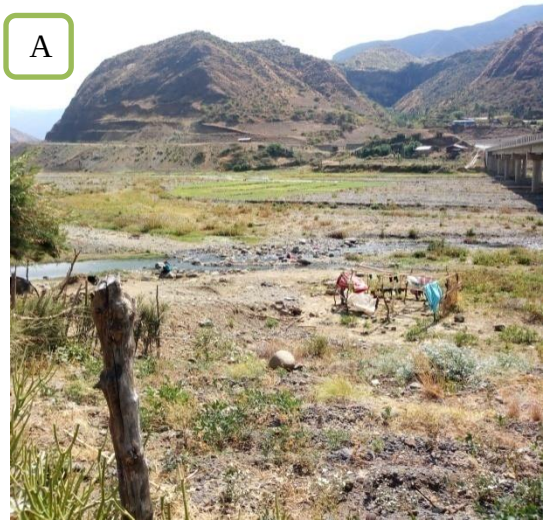

Figure 10. Teleyeyen river (A) Lake Maybar (B) and Kelina river(C)

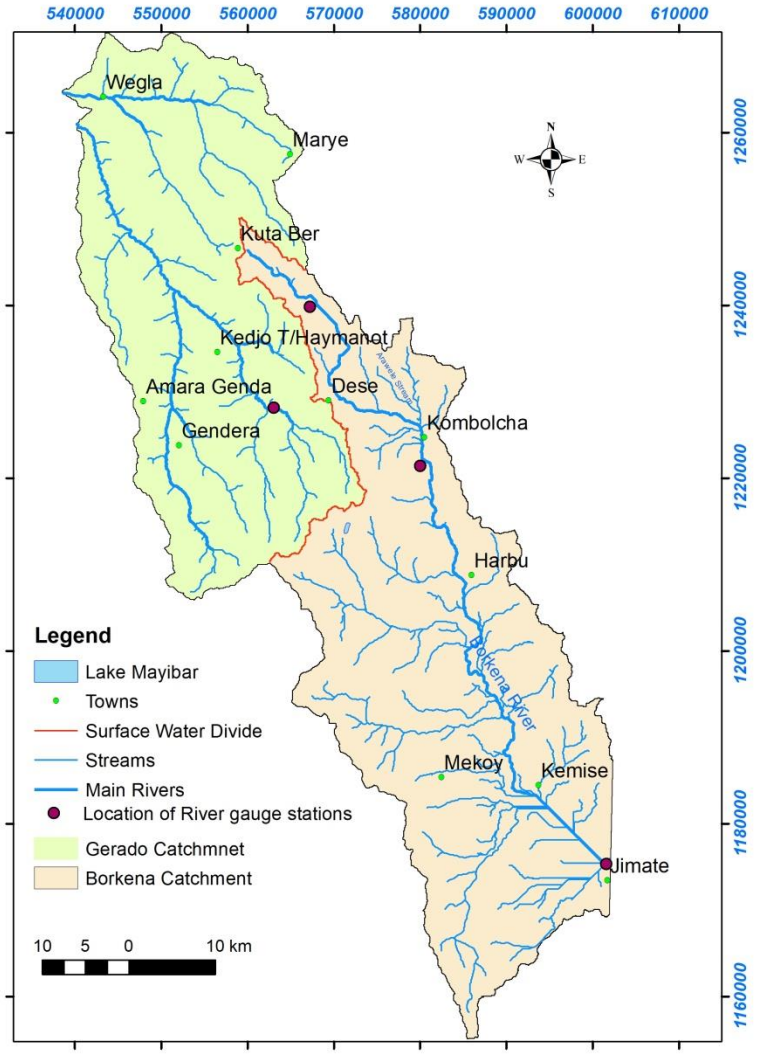

Figure 11. River network of the area

2.4.1 Base flow Analysis

Estimation of base flow and direct runoff is useful to understand the hydrology of a watershed. Baseflow varies spatially and temporally influenced by several factors including geology, topography, climatic season, and anthropogenic activities (Smakhtin, 2001). Baseflow can nurture river flows during periods of dry weather. Although dry season flows are significantly reduced and in some rivers approach zero flow, this water can be a vital life source for those who depend on it (Smakhtin, 2001).

There are some river gauging stations within the Blue Nile and Awash River basins. Most of the gauging stations have not adequate data and they lack the consistency to be fully interpreted. However, river gauge data have been obtained from the Ministry of water resource (MoWR) for four river gauge stations. The year of gauging data shows a certain variation.

River discharge records from river gauging stations show the fact that the river discharge is directly proportional to the intensity of rainfall within the basins. There is a high discharge fluctuation between the wet and dry seasons of the year. The first high flow period is in April, the highest flow period is from July to September, and the peak flow for all rivers is usually recorded in August. The period from December to March is characterized by low flow, and most of the small streams become completely without water on this period.

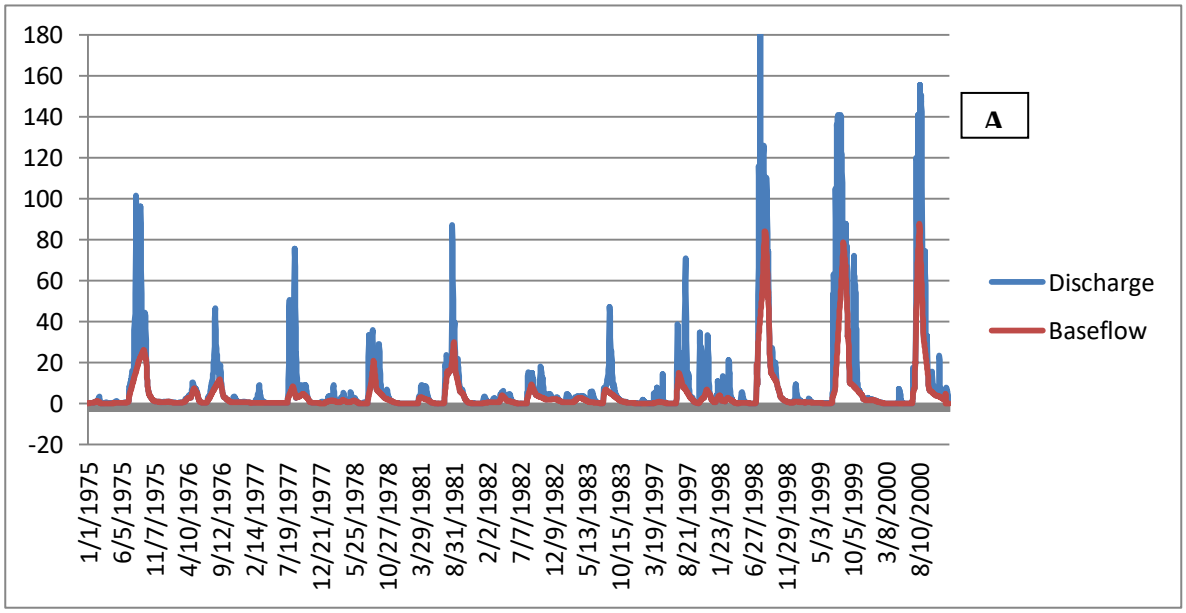

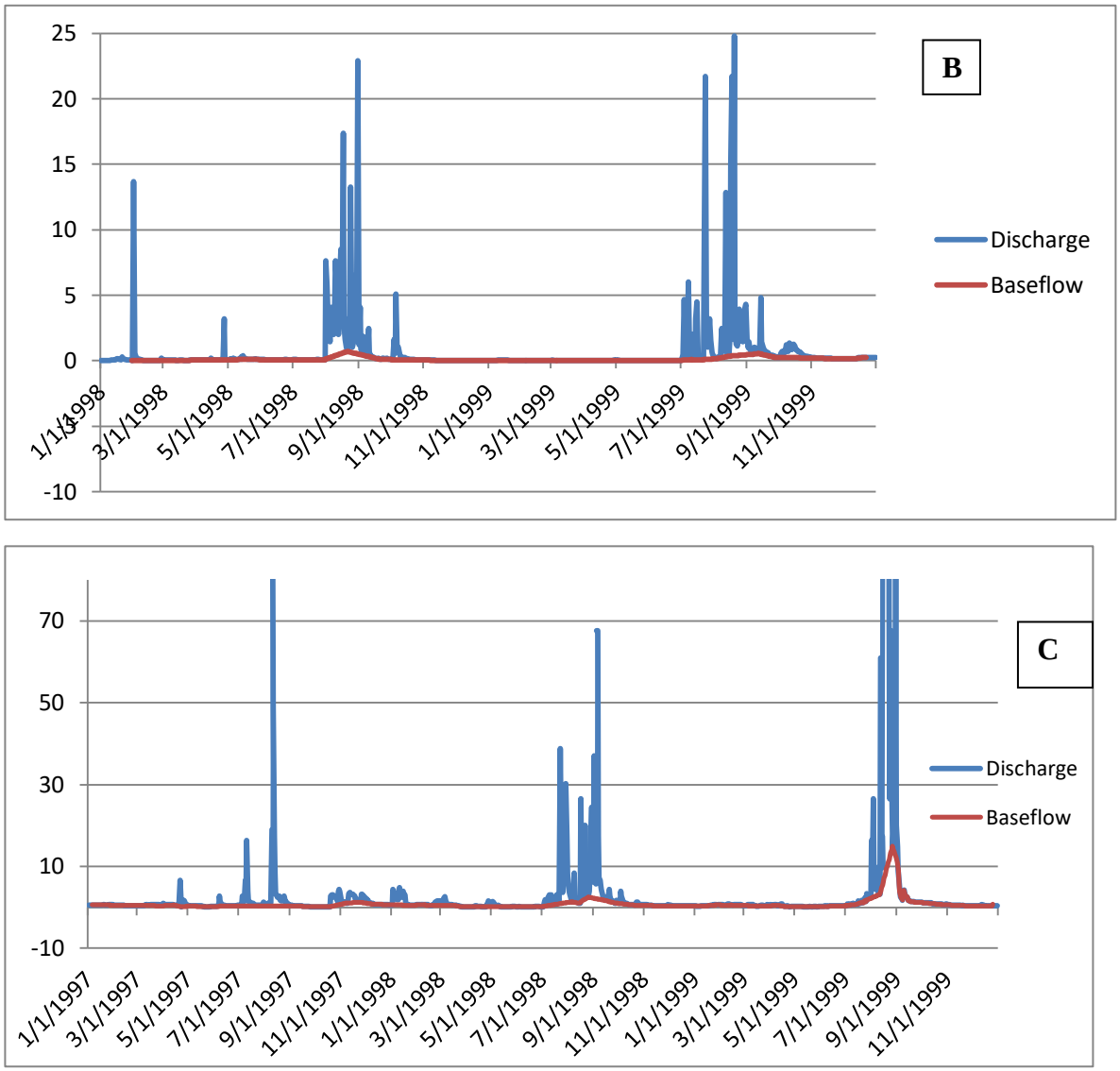

Figure 12. Base flow and discharge graph of Borkena at the swamp(A), Kelina (B) and Borkena at Combolcha (C)

Results of an assessment of data from the Borkena River catchment from the river gauge at the outlet from the swamp show a mean river flow of 7.3m^3/s, which represent a total flow of Borkena 230.2 MCM per year. On the other hand the flow of Gerado River has become 4.6 m^3 /s which represent 148.5 MCM per year of annual flow.

3 Geology and structures

3.1 Regional geology and tectonics

The study area is located at the south-western block of the Afar depression where it occupies parts of the northern plateau in the north-western part, western Afar Margin, and associated Graben.

The Northern Ethiopian plateau is characterized by the prolific eruption of basalt and subordinate other lavas during the Oligocene which built up a sub-aerial volcanic pile, typically 500-1500 m thick and locally attaining 3000 m (Mohr, 1983). These Trap Series represent the whole pile of the Oligocene – Miocene flood basalt sequence with intercalation of silicic rocks. Ethiopian plateau was started by the eruption of Ashangi basalt during the Oligocene, and then followed by extrusion of Aiba basalts and Alaje Formation during the Oligocene-Miocene. These volcanic episodes were characterized by the extrusion of flood basalts, with interbeds of pyroclastic rocks of rhyolitic or less commonly trachytic compositions, particularly at upper stratigraphic levels. These fissural volcanics were followed by central-type eruptions of alkaline Tarmaber-Gussa basalts during the Middle to late Miocene. The Ashangi and Aiba pulses consist of dominantly basalts whereas the Alaje Formation is represented by bimodal rhyolite (ignimbrite) and basaltic volcanism. Silicic rocks of the Alaje cycle are mainly restricted to the plateau-rift border (GSE, 2009). Rooney (2017) also suggests that Ethiopian volcanism appears in Oligocene is equivalent to 1 to 2 km thick sequences of dominantly basalt that is observed from Turkana in the south to Yemen in the north, to Sudan in the west, and the margin of the Somali plateau to the east. The mineralogical compositions of the basalts are spatially variable but all the basalt types contain dominantly olivine and clinopyroxenes with minor but variable amounts of plagioclase, K–feldspars, and brown glass (Pik et al., 1998).

The Western Afar Margin is lying west of the present-day Red Sea–Gulf of Aden–Main Ethiopian rift triple junction zone. The triple junction is associated with the Afar plume and Eocene-Oligocene flood basalt province lying atop the uplifted Ethiopia-Yemen plateau (Wolfenden et al., 2005). The Western Afar margin is bounded by a seismically active right stepping N-S trending step system of discontinuous graben that extends for 500 km (GSE, 2009). These grabens are Kemise, Ataye, Jewha, Borkena, Robit, Kobo, and Hayk basins. Individual marginal grabens are tens of kilometers long and 5–15 km wide. Topographic profiles across the plateau and Marginal grabens show an elevation drop of up to 2500 m between them (Samson and Woldai, 2013). The marginal grabens follow the curving N-S trend of the Western Afar Margins (Zwaan et al., 2019). However, most of the grabens oriented NNW-SSE and arranged in a right-stepping pattern, except the Robit graben and the northern part of the Kobo graben which have a NNE-SSW orientation (Zwaan et al., 2019). There are many tectonic models that were aimed to investigate the genesis of marginal grabens. One of the models was done by Mohr (1962) which suggests grabens were formed simply due to isotactic compensation after the material was removed by the erosion of the plateau margin.

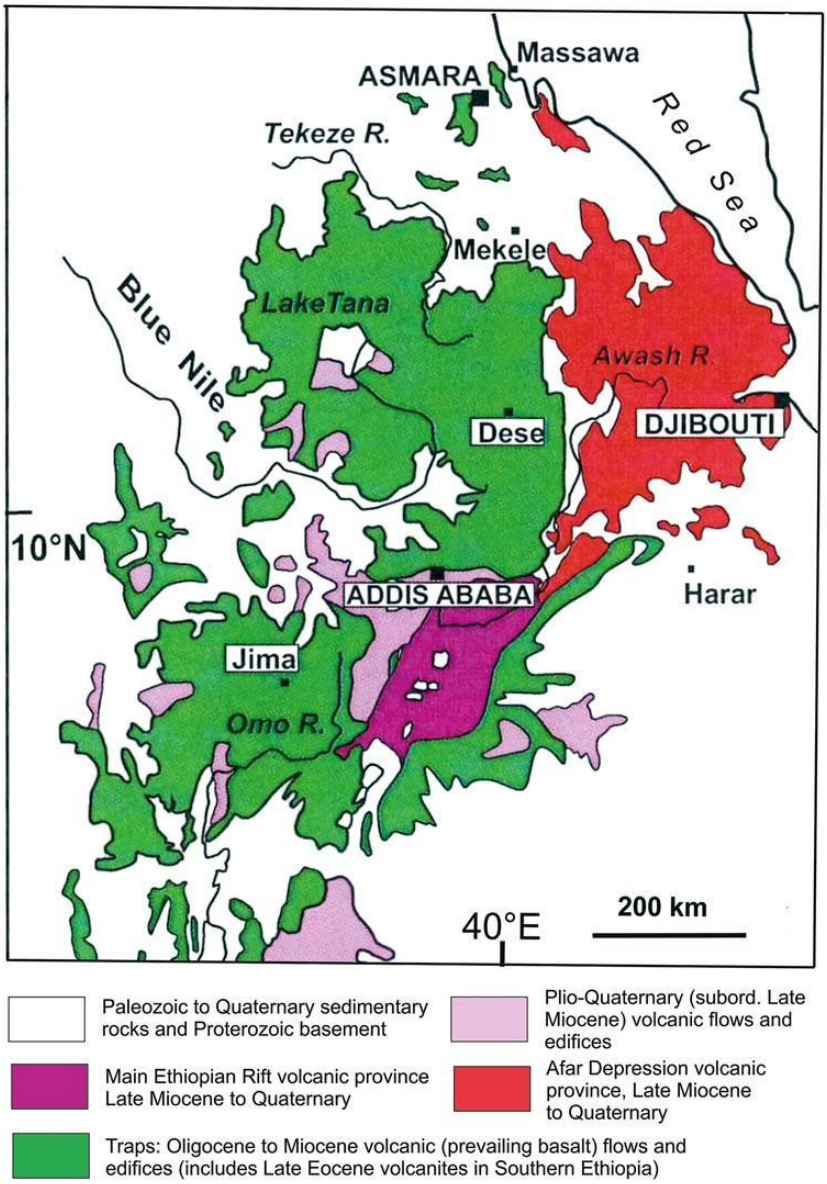

Figure 13. Regional geological map (Abbate et.al., 2015)

3.2 Geology of the Gerado and Borkena catchments

The study area comprises two litho-stratigraphic units. These are: - Cenozoic and Quaternary volcanic rocks and alluvial deposits. A total of 9 different rock types are identified (Fig 14). These units are then shown on the geological maps of the study area.

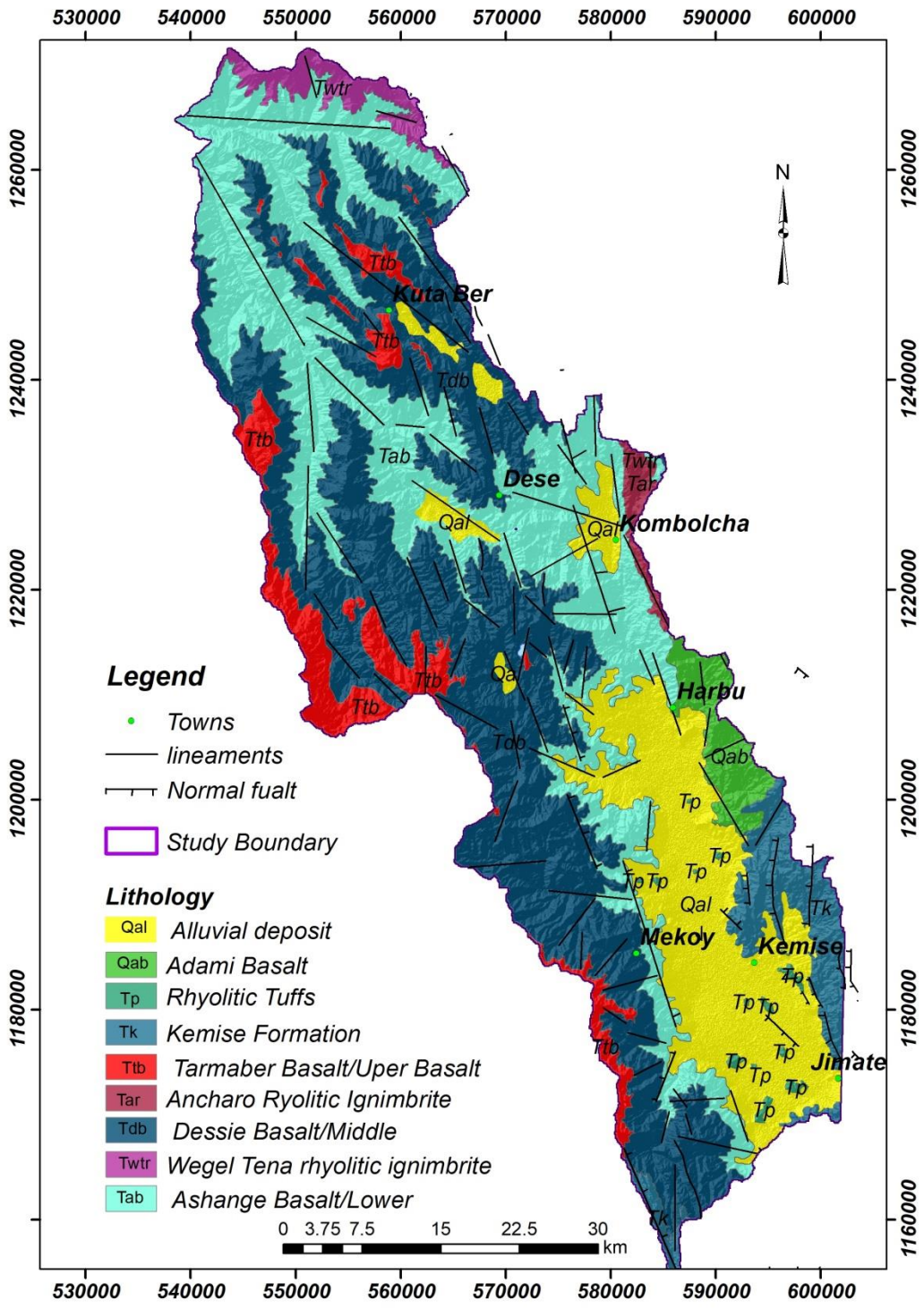

Figure 14. Geological map modified after (GSE,2009; 2010)

3.2.1 Ashangie basalts/Lower Basalt

Ashangie basalt was defined as being the lowest basalt on the northwest Ethiopian plateau. It is dominantly composed of basalt with minor interlayering of pyroclastic towards the top part of the succession (GSE, 2009). The basalts attain a maximum thickness of ~1000 m along Beshilo river section. Its thickness decreases towards south (< 200 m) along Dessie Kombolcha road. These basalt flows represent the lower most parts of the volcanic successions. They are exposed along the deep river gorges of NE-SW trending Zita and Beshilo and NW-SE trending Gerado rivers and their tributary streams in the western plateau area.

Ashangi basalts are strongly weathered, intensely fractured and jointed, friable and rarely vesicular (Fig 15). Generally, the flows are horizontally bedded while exposures along the escarpment and within the marginal grabens are inclined with amount of dip measured between 20^{o} and 60° towards northwest and southeast (GSE, 2009). On the other hand ADSWE (2013) also reported the Ashange basalt sequence is strongly faulted and tilted by 20^{o} to 30^{o} towards east. The weathering and jointing with the inclined contact might have been a favorable condition for ground-water flow from highly elevated area to the marginal graben.

Figure 15. Ashang Basalt Exposed at Teleyayen River goarge

3.2.2 Wegel Tena rhyolitic ignimbrite

It is exposed on Ajibar road, north of Wegel Tena town and Gishen Mariam and Ambassel sections. It typically forms a flat topography but north of Wegel Tena town it is extensively eroded and dissected by the deep gorges forming sharp cliffs. In the Mekdela and Gishen Mariam area it is found on the hill top with sharp slopes overlying the Ashangie basalts. Along Wegel Tena-Beshsilo river road section it forms plains. It forms NW – SE trending hill at the Ambassel section. The maximum thickness of the Wegel Tena ignimbrite is about 500 m. The rock is pink, white, light gray and fine to coarse grained. The unit is layered or bedded and individual flows vary in thickness from < 3 m up to 15 m. The individual layers show variation in texture, they are dominantly porphyritic with microlitic or glassy matrix. Densely welded ignimbrites have a glassy appearance and exhibit a well-developed columnar jointing (GSE,2010).

3.2.3 Dessie Basalt/Middle Basalt

The Dessie basalt covers parts of west, southwest, and northeast part of the area, which accounts considerable area of the study area. It is exposed in the western plateau area forming chain of ridges like Tossa Mountain (Fig 16 A), cliffs along the escarpment and river cuts of Zita and tributary streams of Gerado River. It has columnar joint structure which makes it favorable for vertical flow (Fig16 B).

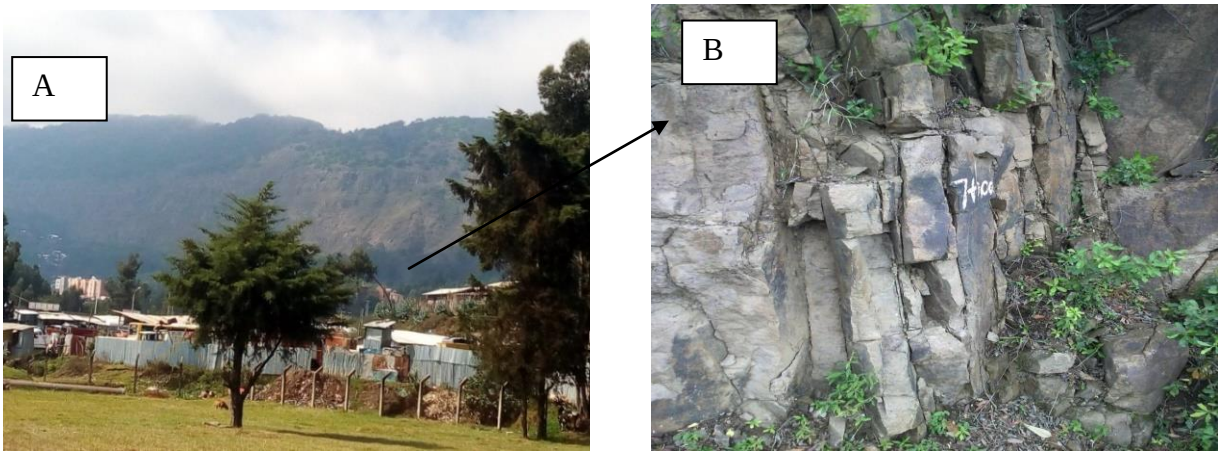

Figure 16. Tossa ridge

The contact with the underlying Ashangie basalt is marked by about 20 m thick plagioclase phyric basalt marked by 50 cm thick paleosol from top and bottom as seen along Dessie-Kombolcha and Dessie-Hayk road (GSE, 2010).The Lower (Ashangi) and Dessie (Middle) basaltic units are separated by an angular unconformity. Petrographically, it is aphanatic basalts dominated by fine microcrystalline matrix consisting fine plagioclase microlites (GSE, 2010).

3.2.4 Ancharo rhyolite ignimbrite

This unit forms a north-south trending hill east of Kombolcha, which is named after the locality called Ancharo. It is well exposed in quarry site (fig 17) along Kombolcha-Bati road, where the exposed thickness is about 50m. The rock is white, pink, gray and medium to coarse grained. This unit is columnar jointed and shows three major layers. The bottom part (~ 15 m thick) is pink, yellowish white and massive. According to GSE (2009) this unit contains plagioclase, alkali feldspar phenocrysts, glass shards and pumice rock fragments. The middle part (~ 20 m thick) is vesicular and the vesicles are mostly rounded with maximum diameter of 15 cm. The top part (~ 15 m thick) is white and compositionally similar with the bottom one, except that it sometimes contains secondary calcite.

Figure 17. Ignimbrite in eastern part of Kombolcha town (Multikolo locality)

3.2.5 Tarmaber basalts

Termaber basalt exposures are mostly found on high altitude but also outcrop on down-faulted blocks of the western escarpment. Termaber basalt is well exposed on ridges greater than 3000 m.a.s.l like Borumeda - Kutaber, Tita – Sulula, Tebasit - Guguftu, Tosa felana ridges. It has conformable contact with the Dessie basalt (GSE, 2010). It is reported that this Formation attains a thickness greater than 1000 m. There are thin layers of ignimbrite inter bedded within the flow and it is cut by sets of E-W and N-S trending aphanitic basaltic dykes having 170 cm and 80 cm width respectively. Some of these dykes show vesicles which are filled by secondary silica. Petrographically, it is composed of 95 % groundmass and 5 % phenocrysts. The phenocrysts include plagioclase (4 %) and alkali feldspar (1 %). The groundmass is dominantly constituted by oriented microlites of plagioclase. The rock shows aphanitic, porphyritic and trachytic textures (GSE,2009).

Figure 18. Tarmaber Basalt

3.2.6 Adami basalt

The unit forms small to big hills and flat-lying topography and well exposed along hill sides, roads and stream sections. Adami basalt is 350 m thick, consists of fractured and weathered aphanitic basalt, pyroxene - olivine -plagioclase phyric and plagioclase-phyric basalts, scoriaceous basalt and agglomerate (GSE,2009).

3.2.7 Kemise Formation

The Kemise Formation consists of rhyolite, ignimbrite, tuff and ash with subordinate basalt. They crop out as discontinuous tectonic block bounded by normal- and reverse-slip faults. Along the footwall of the low-angle normal-slip (detachment) fault, the rocks are strongly deformed, and variably sheared and folded. The beds are inclined (25°-60°) to overturn. It has a tectonic contact with the Ashangi basalt (GSE, 2009). It is exposed in ridges and hills, and road cuts along Kemise-Shewa Robit high way, and in stream beds and cliffs. It is affected by faulting, folding, shearing and jointing. It shows thin laminations of flow layering. Around Bora calcite and minor opal infillings are observed. Along the main Dessie-Addis Ababa high way about 2 km south of Kemise town the rock is cut by basaltic dyke, and deformation folded both the tuff and the basalt.

3.2.8 Rhyolitic tuff

This unit is exposed in the south central part of the area within the Borkena graben and formed dom shaped hills and ridges. These flows consist of cluster of plugs, and localized lava flows ranging in diameter from about 250 m to 3 km occur along northwest- and northeast- trending faults.

3.2.9 Quaternary alluvial deposits

The Quaternary deposits are exposed in the eastern low land plain of Borkena graben and intermountain low lands of Gerado Kutaber. This soil is mostly covered with extensive farming. The yellowish gray sandy to silty and clayey soil occupy low land plain of the rift floor. When the solid supply of a stream is high and the transfer capacity is not adequate for the transportation of the corresponding solid material, flow speed is reduced and deposition of the heavier solid material (boulders, gravels) begins to be deposited in the upstream areas (towards the western sector of the marginal grabens near to the Escarpments). As one goes towards downstream due to a decrease in inclination of the

terrain, a decrease of a water stream's transfer capacity occurs and as a result finer and lighter materials (sand, silts, and clays) are deposited on the eastern part of the marginal grabens forming wide alluvial plains.

3.3 Structures

The structural architecture of the Western Afar Margin is dominated by normal faulting and the extensive occurrence of eastward tilted fault blocks with dips increasing towards Afar (Zwaan et al., 2019). Those faults are responsible for a series of fault-bounded grabens.

The structures in the area are characterized by normal faults; lineaments represented by fractures and/or joints of variable strike and length. According to GSE (2009), normal faults in the study area are of two types. The first one is low angle normal-slip (detachment) faults which are SW- to NW and WNW- trending and dipping to the north and northeast.

The prominent big detachment faults are the Bati-Kombolcha-Dessie fault. The length is more than four-kilometer and characterized by top to NW and SW sense movement. This fault separates the Ashangie basalt at the footwall with Ancharo rhyolitic ignimbrite at the hanging wall. The second form of normal fault is high angle normal fault which separates the plateau and Afar depression. The trend and the amount of displacement along the escarpment vary along the strike. They have an overall NNW general orientation, long, widely spaced, and have a large vertical offset (> 1000 m).

Lineaments related either to fractures and/ or joints are common in the area. They are N-S to NE, NW, and E-W striking with the N-S and NE lineaments predominating. These predominating lineaments are long and subparallel, suggesting they are reactivated older structures. The E-W striking lineaments crosscut both the NE and N-S striking lineaments as observed during the fieldwork and DEM interpretation, suggesting they are of younger age (Fig 19).

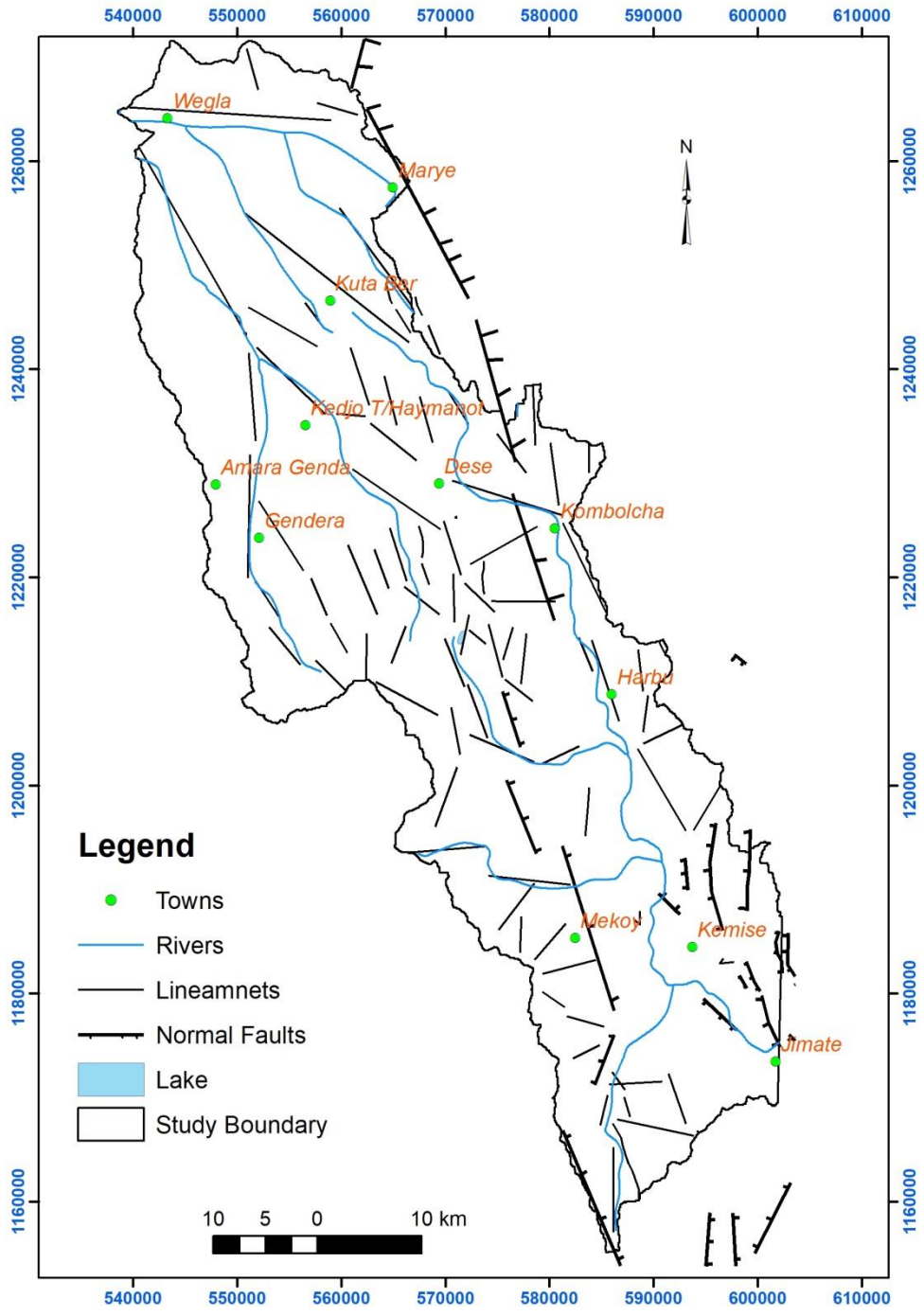

Figure 19. Structural Map Modified After (GSE, 2009)

4 Hydrogeology

4.1 Introduction

Rock beds at the saturated zone that host flowing groundwater are called aquifers. the size and number of voids and thus the degree of interconnection between those pores and fissures define the qualities of the aquifers. Those properties also define infiltration efficiency and the capacity of the intake of recharge water (Mazor, 2004). Less permeable rocks, that retard water, are termed as aquitards (Gilvear & Bradley, 2009). When the aquitards situated below an aquifer they'll restrict the downward movement of water, hindering drainage or if they situated above an aquifer act to confine water within the aquifer. Different types of Rocks have variable hydrogeological properties relying on their permeability. Most of the Basalt and other extrusive lava have no primary porosity; however, they might get permeability to circulating water from fractures. Rocks often occur in bedded structures, alternating with paleosoils. Thus, basaltic terrains may have lateral flow conductivities. Unconsolidated deposits have primary porosity which is typically governed by grain size distribution. The more uniform (well sorted) the grain sizes are, the upper the porosity and thus the coarser the material, the upper its permeability and hydraulic conductivity (Fitts, 2002).).

4.2 Hydrogeological Units

The nature and distribution of aquifers and aquiclude in a geologic system are controlled by the lithology, stratigraphy and structures of the geologic deposits and formations (Freeze and Cherry, 1979). The area is characterized by volcanic rocks and intermountain graben alluvial deposits. Hydraulic properties of volcanic rocks are determined by their primary and secondary porosities as well as their openness and interconnections. It is also highly dissected by NNE-SSW, NE-SW, EW trending faults.

Numbers of intermountain Graben are formed elongated in north-south and NW-SE directions. The volcanic rocks form the mountains, escarpments and rugged terrain which act as recharge area for those intermountain valleys. The intermountain graben is dominantly composed of poorly compacted quaternary basin fill deposits. The alluvial deposit’s origin is considered to be local tectonic development forming an intermountain

channels. Those alluvial deposits have different permeability from the volcanic rocks. The groundwater availability and flow in alluvial deposits is highly dependent on grain size, sorting, type of cementing material and thickness of the Aquifer.

There are different literatures which have been studied the groundwater potential of the area (GSE, 2017; Ketema 1980; (ADSWE) 2013;, Mesfin 2001, Mola 2000). Based on those studies the area have classified within three hydro geological units. Those hydro geological units are porous aquifer, fissured aquifers and low permeability hydro geological units.

4.2.1 Porous (intergranular)Aquifers

Hydrogeological units with porous permeability: where groundwater is accumulated in and flows through the pours of unconsolidated material. The Quaternary alluvium and lacustrine sediment represent porous materials. The groundwater availability and flow are highly dependent on grain size, sorting, type of cementing material, and thickness of aquifers.

The main groundwater prospective intermountain Grabens within the study area are Gerado, Boru-Meda-Alansha, Kombolcha, and Harbu-Cheffa–Kemissie. The marginal grabens are sites of the highest potential of groundwater storage and availability (Seifu, Kebede, 2013). According to ADSWE (2013), the alluvial Porous aquifers are unconfined, semi-confined, and confined (fig 20). The thickness shows certain variability from place to place (fig 22). The sediment thickness of the deposit in different parts of the deposit is not similar: - the thickness alluvial deposits reached up to 250m and the area yields greater than 30 lit/sec (ADSWE, 2013).

Figure 20. Artesian flowing well found in Harbu town tapping from alluvial deposit

4.2.2 Fissured/ fractured Aquifers

Those aquifers unit mainly covers the western and elevated part of the study area. Hydrogeological properties of the basaltic aquifers have been computed from drawdown data and recovery pumping tests and from the yields of springs issuing from the aquifers. Very high yielding springs along deep faults on the western escarp of Borkena graben are typical representatives of the high groundwater potential (GSE, 2017). The variability of spring discharges from these aquifers shows the diverse hydrogeological and hydraulic properties of the basaltic aquifers. Volcanic rocks outcrop surrounding the valley plains are so highly fractured and weathered that are good recharging zone for the alluvial filled plain areas.

Figure 21. Springs, at Kurkur (Dessie) (A) and Harbu(B)

The potential water bearing horizon of these units is concentrated to the fractured and weathered surfaces. Boreholes drilled at Dessie penetrating Dessie basalt aquifer to depths of more than 100 m show transmissivity values in the range of 90 to 318.5 m2/d and yield of 5 – 12 l/s.

On the contrary, acidic volcanic rocks cover the eastern block of marginal graben is considered as very low productive aquifers. Because those rocks are massive and fresh rocks with less fractured and weathered surfaces. The slope which those units exists is mainly steep and there is no considerably developed soil cover which favor a runoff other than infiltration.

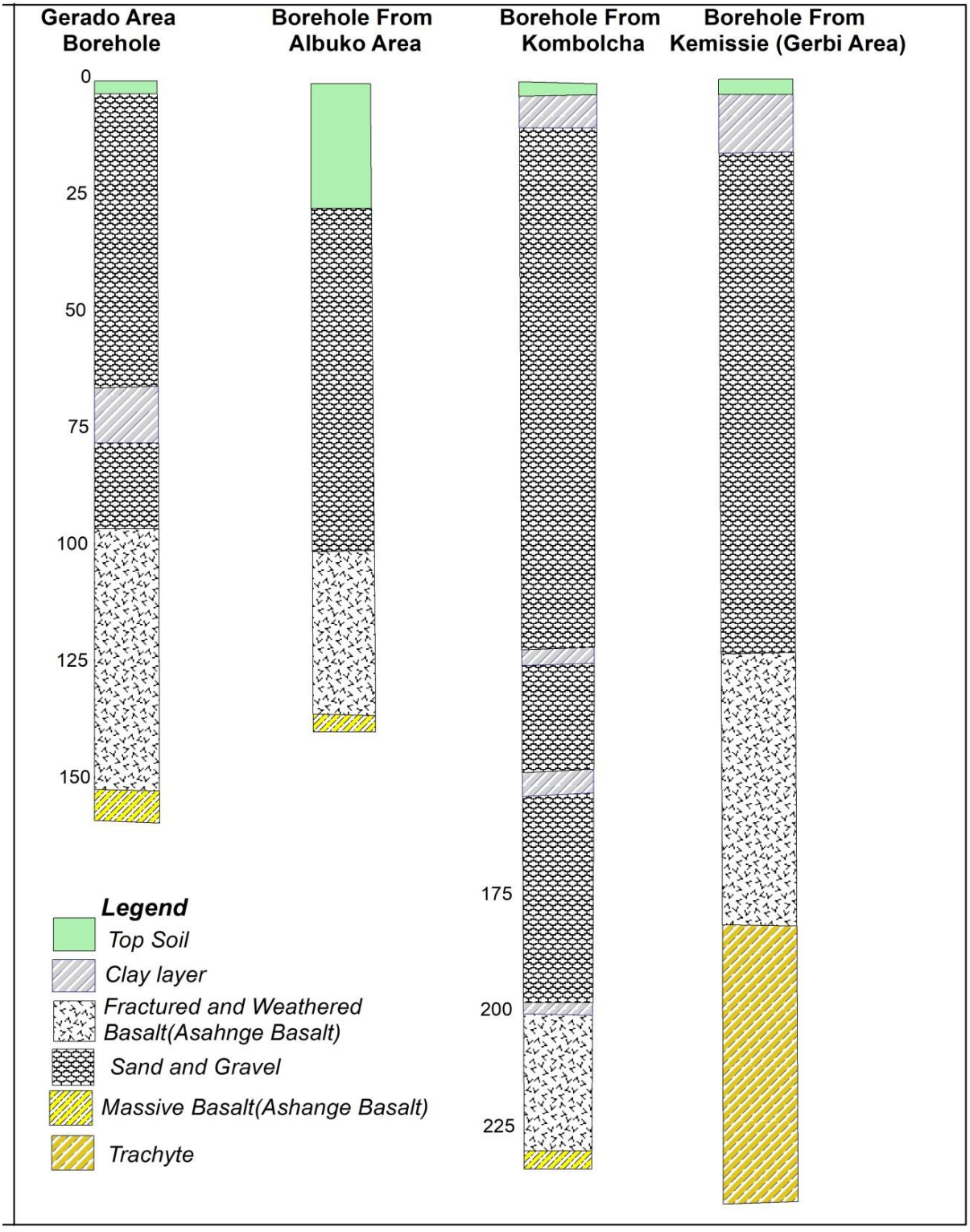

Figure 22. Lithological logs from selected Boreholes in the Area tapping groundwater from both volcanic and alluvial aquifers

4.3 Groundwater recharge

The rate at which groundwater is recharged is influenced by several factors including rainfall or surface water bodies, climate, topography, soil, and aquifer hydraulic properties and vegetation cover (AGBRS,2007). It is essential to know the rate of groundwater recharge in order to sustainably manage resources. There have been different methods of estimating groundwater recharge with different spatial scales. Among several methods of estimating groundwater recharge, two of them are used in this study to compare the results between those methods and to obtain an average value of recharge. Chloride mass balance and Base flow separation has been used.

4.3.1 Chloride Mass Balance

Chloride mass balance is considered an appropriate environmental tracer since its highly soluble, conservative, and not substantially absorbed by vegetation (Marei et al., 2010). The chloride mass-balance method is convenient and cheap due to its simple data requirements.

$$R=P\times Clp/clgw$$

Where R is recharge (mm/year); P is rainfall (mm/year); ClP is a mean chloride concentration in rainfall (mg/L); and Clgw is a mean chloride concentration in groundwater (mg/L). The recharge estimation has been done for both catchments separately. Precipitation samples from Gonder, Dessie, and Debre Birihan are used for the estimation because there's no enough precipitation data within the study area boundary. The mean concentration of chloride for rainfall is 0.94 mg/l. a mean chloride for groundwater in

Gerado is 6.87 mg/l while in Borkena its 13.67mg/l calculated recharge has become 176.6 and 80 mm/year for Gerado and Borkena catchments respectively. The recharge for Gerado seems realistic and it coincides with values estimated in other approaches while Borkena's is under estimated. This might be because of there is additional chloride source to the groundwater from the factories found in Dessie and Kombolcha towns. Agricultural activities might be also additional sources for chloride within Borkena Catchment.

4.3.2 Base flow separation

The base flow separation method was applied so as to get recharge from the entire flow of a river. Base flow separation techniques use the time-series record of stream flow to derive the base flow signature. The common separation methods are either graphical which tends to target defining the points where base flow intersects the rising and falling limbs of the fast flow response or involves filtering where data processing of the whole stream hydrograph derives a base flow hydrograph. Among several base flow methods on this paper Base flow index (BFI) was used. BFI has usually divided river flow sequences into many small units according to a given time-step and subsequently, the minimum value in each unit is chosen to get the bottom flow via linear interpolation (Kelly et al., 2019). A mean annual base flow has become 2.5, 0.76, and 0.11m3 /s for Borkena River at the swamp and Combolcha and of Kelina River of Gerado basin respectively. Comparing to chloride mass balance the recharge is high in Borkena catchment calculated using Baseflow separation which becomes 132.5 mm/year which represents 11.4% of Average precipitation on the catchment. This result can tell us the previous assumption is convincing and therefore the source additional chloride concentration to the groundwater needs an assessment. Recharge of Gerado catchment calculated using base flow separation also has become 177.2 mm/year which represents 13.7% of total precipitation. There are few attempts tried to estimate groundwater recharge of the world using the water balance method. The result of a number of the studies has been discussed during a table below.

Table 7 Recharge rates estimated by other studies

Study	Catchment	Estimation Method	Recharge mm/year
Dereje et.al (2016)	Gerado	Water Balance	173.6
ADSWE (2013)	Gerado	Water Balance	168
Kidist (2018)	Gerado	Water Balance	148.5
ADSWE (2013)	Borkena	Water Balance	134
Mesfin (2001)	Borkena	Water Balance	155.6

4.4 Hydraulic parameters and Groundwater flow

4.4.1 Hydraulic conductivity

Hydraulic conductivity is the ease with which water can move through pore spaces or fractures (Fetter, 2001). It is dependent on the intrinsic permeability of the aquifer material and the degree of saturation. The hydraulic conductivity of fractured rocks depends largely on the density of the fractures and the width of their apertures. Fractures can increase the hydraulic conductivity of solid rocks by several orders or magnitude (Kruseman and de Ridder, 1994).

Many empirical and experimental methods have been developed to determine the hydraulic conductivity. Among them, a pumping test is the most reliable method to calculate the coefficient of permeability. From calculated values using pumping test data on different boreholes, the alluvial aquifers in the central parts of the Kombolcha sub-basin have relatively very high values of hydraulic conductivity (10.01-30.00 m/d). Relatively high hydraulic conductivity values (7.51-10m/d) have also been encountered from alluvial aquifers in the northern and southern limits of the Kombolcha sub-basin. Moderate values of hydraulic conductivity (5.1-7.5m/d) have been depicted by alluvial aquifers in the southern tip of the Kombolcha area.

Low hydraulic conductivity values (2.51-5.0 m/d) have been indicted by the alluvial aquifers in the area surrounding Kemissie. Very low hydraulic conductivity values also

(0.06-2.5 m/d) have been revealed by the alluvial aquifers in the central parts of Gerado and Harbu areas.

4.4.2 Transmissivity

The transmissivity of an aquifer is a measure of how much water can be transmitted horizontally. It is the Product of the hydraulic conductivity times the thickness of the aquifer (Dricoll, 1986)Transmissivity (T) is a hydraulic parameter of an aquifer that is known employed in most Groundwater flow equations to understand the flow dynamics and is generally estimated from Pumping tests (Freeze and Cherry, 1979).

The transmissivity values in the Area calculated from pumping test ranges from 10 m2/d to about 1750m2/d. data obtained from ADSWE (2013) and MoWIE (2018) show that transmissivity of alluvial aquifer found in Kemisse area of Borkena river catchments has relatively high transmissivity values (>500 m2/d). While most of the area of an alluvial aquifer of Gerado and upper Borkena river catchment have range of transmissivity values (100-500 m2/d) Low transmissivity values (10-50 m2/d) correspond to the volcanic rock aquifers surrounding the alluvial aquifer in the western and eastern side of the alluvial aquifers

4.4.3 Specific Capacity

Specific capacity is material physical properties that characterize the capacity of an aquifer to release groundwater from storage in response to a decline in hydraulic head. The Specific Capacity of a well is simply the pumping rate (yield) divided by the drawdown. It is a very valuable number that can be used to provide the design pumping rate or maximum yield for the well. It can be used to identify potential of well, pump, or aquifer problems, and accordingly to develop a proper well maintenance schedule.

From data obtained from ADSWE (2013) an average specific Capacity of wells from the four well fields become 107, 143, 35 and 470 m3/day/m for Gerado, Kombolcha, Harbu and Kemissie well fields respectively.

4.4.4 Groundwater Flow

Groundwater in the saturated zone is always in motion (Kresic, 2007). It moves through the porous media under the influence of fluid potential (Fetter, 2001).The most driving factor for the movement of groundwater is hydraulic gradiant. groundwater flow takes place from the higher hydraulic head towards the lower hydraulic head.

For the reason that groundwater is hidden it is not possible to directly measure the groundwater rates within an aquifer.However,observation piezometers can be constructed to determine the elevation of the water level in the piezometer. This water level offers information about the groundwater head at the open section of the piezometer. Groundwater head gradients can be used to estimate the extent and direction of groundwater velocities (Rushton, 2003).

Toth (1963) classifies groundwater flow regimes in to three flow systems which are local, intemediate, and regional. He also suggests understanding of groundwater movement in adjacent small basins makes possible an accurate representation of the motion of groundwater.

The study area lies in two surface water Basins which are the Blue Nile and Awash. Previous studies are tried to understand the flow dynamics of the catchments separately. The study area is studied with the number of authors that try to conceptualize a groundwater flow but specifically, Between Borkena and Gerado there is no study conducted to understand a flow. However, on a study of groundwater flow Ethiopian rift volcanic within a selected transects Seifu et al. (2008) concluded groundwater inflow originating from the plateau accounts for greater than 50% of water inflows to the deep rift aquifers. They also determine the transverse faults that dissect the rift margin channel groundwater from the plateau to the rift floor the marginal graben and faults bounding the rift as a major groundwater barrier that shifts the water to the rift valley system. But on the case where the rift floor is bounded by marginal graben, the waters infiltrating into the plateau emerge in the alluvial sediments (Tenalem et al., 2007).

.

Groundwater flow on the study area controlled by the low angle normal-slip faults which are SW- to NW and WNW- trending and dipping to the northeast create the pattern for groundwater flow from the western escarpment towards the northeast. Minor lineaments that are related either to fractures and joints are common in the mapped area. They are N-S to NE, NW, and E-W striking with the N-S and NE lineaments is predominating. Those lineaments are transected by the E-W striking lineaments. These lineaments also have a favorable condition for groundwater flow across the surface water divide.

Despite there is a lack of adequate deep well data on the Gerado Basin. 15 spring elevation data that have been collected during the field trip and 35 deep well static water level data are obtained from Ethiopian water work design and supervision has been used to do groundwater level contour map (fig 23).

Groundwater flow direction has been determined from the groundwater level contours which is the direction of the groundwater flow perpendicular to the equipotential lines. Kriging with the help ArcGIS 10.7 software was done to interpolate groundwater level data's through the study area which is a linear geostatistical approximation method that enables the estimation of a regionalized variable at any point in space based on its measured values at other locations. Most of the wells found in the alluvial graben deposits found to be semi-confined and confined. Those wells can represent an intermediate groundwater flow while spring at the higher elevated areas representing local groundwater flow. The topographic gradient, Stratigraphy, and structures are responsible for the flow pattern in the study area. The graben is recharged by sub-horizontal flow from Western and Eastern escarpment areas. Recharge from the escarpment area is also a reason for the artesian character of the graben aquifers. Alluvial graben reaches a thickness of more than 200m in some areas and they provide a great amount of water for the communities in the area.

Groundwater Existence in Gerado catchments is limited on the springs emanated from the highly elevated mountain ranges to the river dissected gorges and depressional areas. Apart

from the Gerado well field, there is no borehole encountered in the catchment.

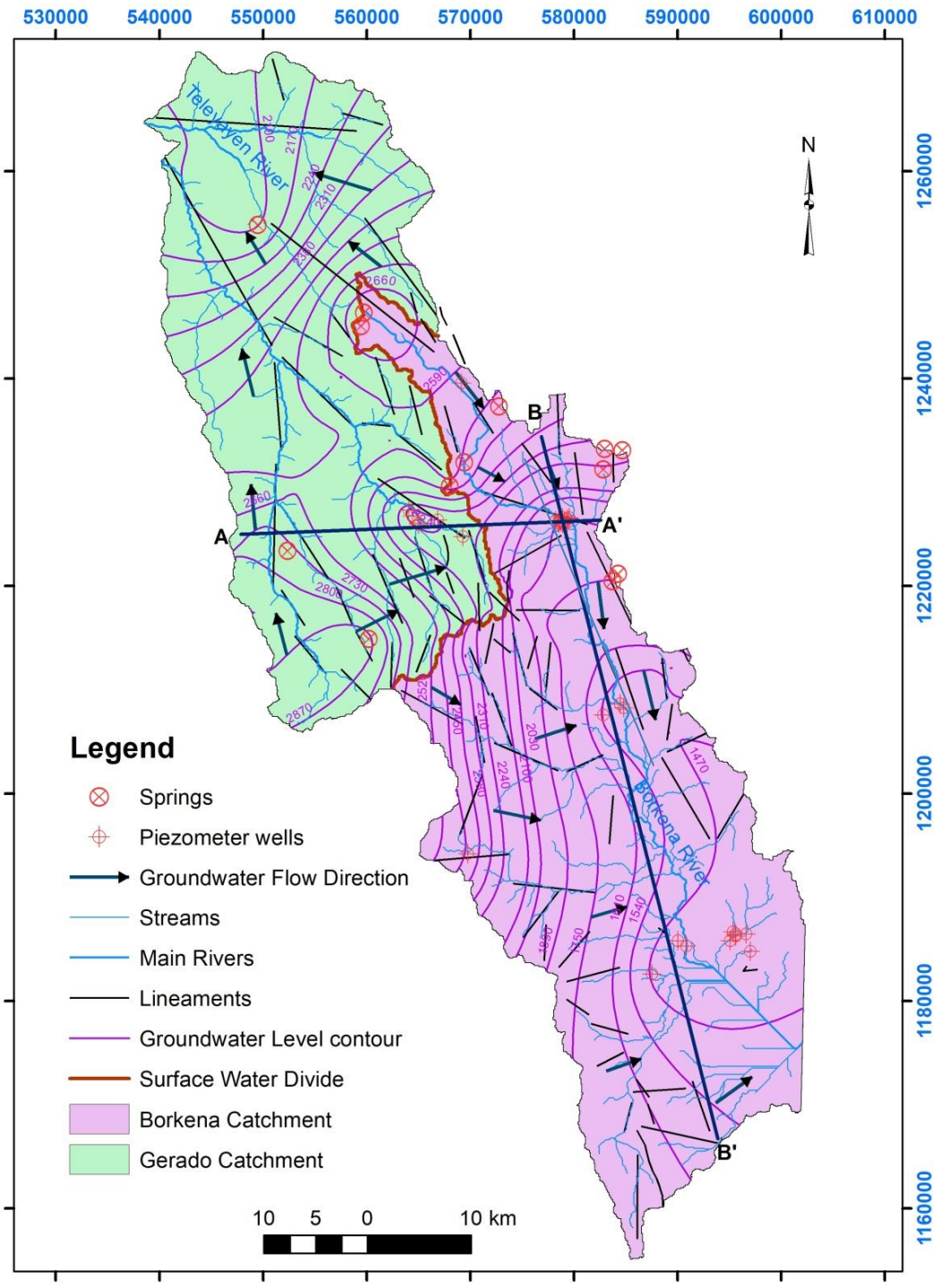

Figure 23. Groundwater level contour map

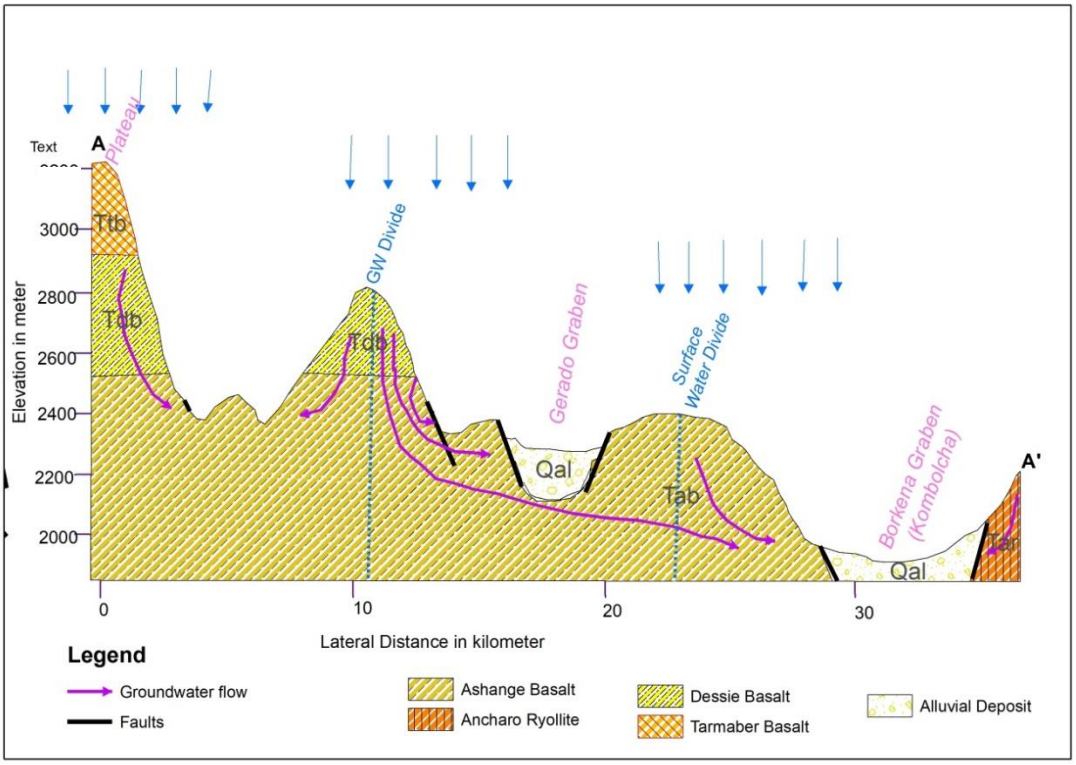

Figure 24. Hydrogeological cross section of East to West

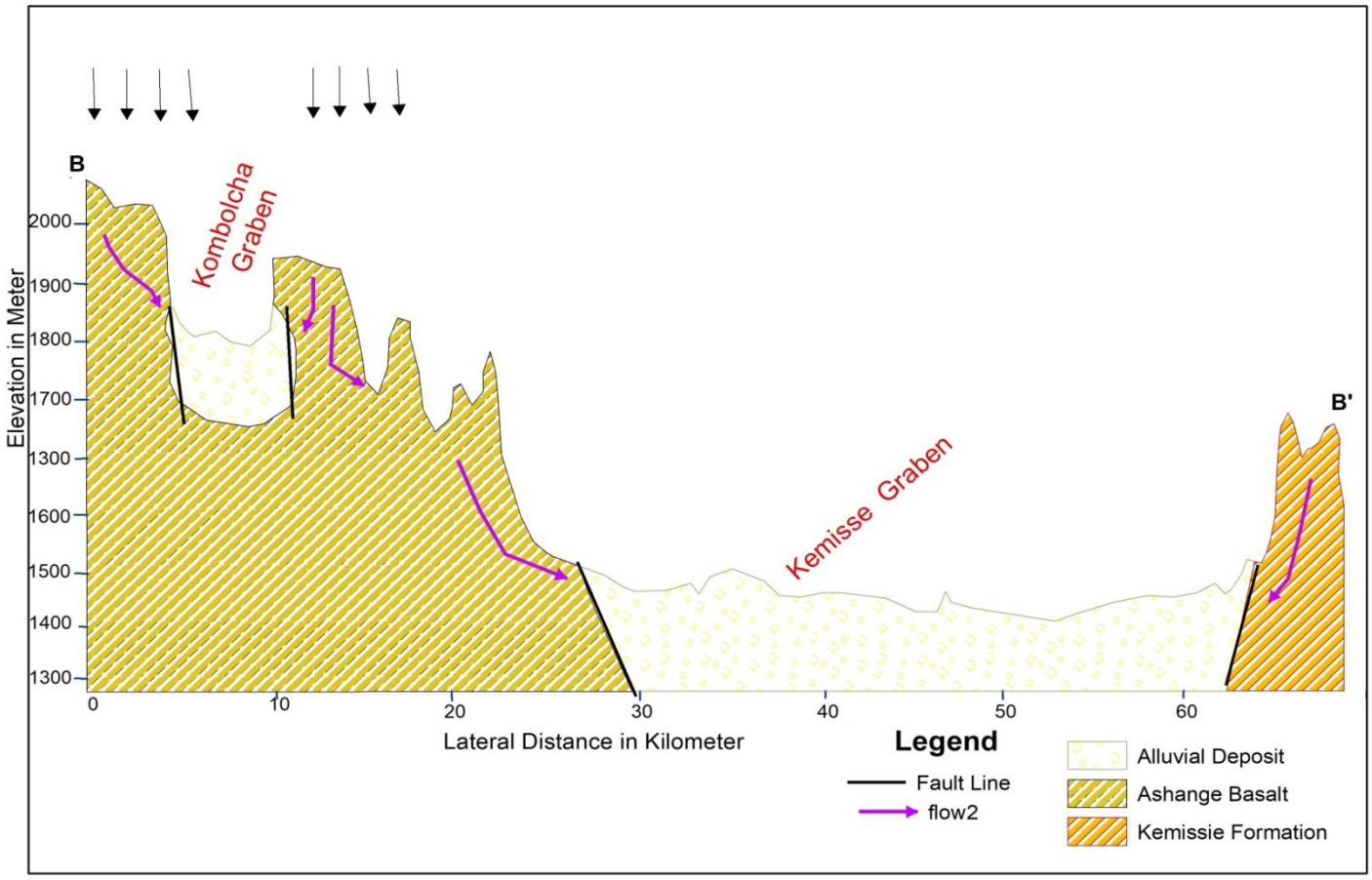

Figure 25. Hydrogeological Cross section From North to South

In addition to groundwater level and structural evidence, geomorphological spring patterns also suggest there is an inter-basin groundwater flow between the catchment. The springs have preferential alignment in emergences with a considerable discharge which support interbasin groundwater flow. Most of the springs in Borkena catchment emerge from Western and northwestern sides which are adjacent to the divide. The tributary streams of Borkena catchments are mostly flowing from west to northeast which is in the direction of groundwater flow. Lake Maybar which is structurally controlled found

immediately after the surface divide may also be good evidence of through flow. This lake is found with an elevation of 2500 m. a. s. l. `

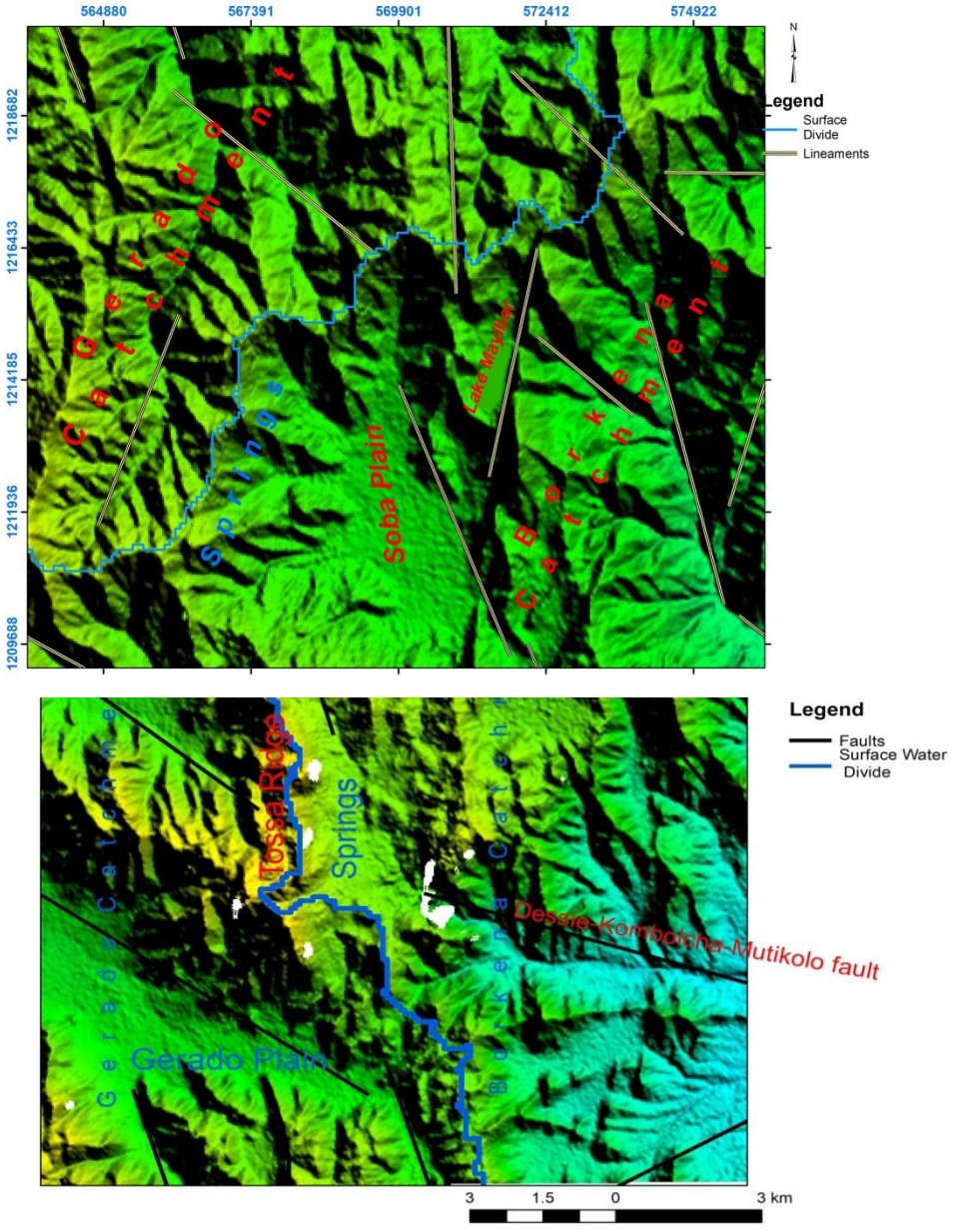

Figure 26. Physeographic setup of the areas which the springs are emaneted

.

Water flows from high points to low points, and therefore a water level gradient is an important condition for groundwater flow. Reconstructing groundwater flow directions based on water level gradients is a compulsory but inadequate to characterize groundwater flow and dynamics. Consequently, this paper also tries some Hydrogeochemical and environmental isotope tracers to confirm the conventional method of determining groundwater flow.

5 Hydrochemistry and Isotope hydrology

5.1 Hydrochemistry

The chemical composition of groundwater is greatly dependent on natural factors chemical reactions, lithologies, meteorological factors, hydrology, weathering, residence time and length of flow path. As the groundwater becomes older and slowly circulating it develops more complicated subsurface histories through rock water interaction (Clark, 2015). The active interaction of water with the environment helps to understand groundwater chemistry along its flow paths.

Geochemistry is a major tool to understand groundwater recharge, evolution and flow processes since last century. Theories and conceptual models that have been developed helped us to describe the solute concentrations and chemical characteristics of water. Numerical Reaction models also have been developed that assists for furthers deep understanding of the concentration limits and the variations in the behavior of the dissolved substance.

Mass balance approach uses two water analyses represent starting and ending water compositions along a flow path to calculate the moles of minerals and gases that must enter or leave solution to account for the differences in composition (Pankhurst et al., 1980). Before doing reaction models it is essential to understand the possible reactions that could happen in the groundwater system. The chemical reaction that has alter the chemical composition of groundwater are Acid base reaction, Precipitation/dissolution reactions, Redox reactions, Sorption reactions, Aqueous complexing, Gas transfer, Ion filtration and osmosis and Radioactive decay (Kovalevsky et al.,2004).

In addition to geochemical studies, environmental isotopes have proved extremely useful in groundwater studies. The distribution of isotopic species in water provides additional information on sources of groundwater, on flow paths and mixing, and on chemical reactions and sources of ions. The variation in the ratio of stable isotopes is governed by chemical reactions and phase changes due to the energy difference between chemical bonds involving different isotopes of an element (Kovalevsky et al., 2004). Distribution of isotopes is controlled by fractionation of isotopes during any physical or chemical reaction,

and the distillation of isotopes from reactant reservoir as the reaction proceeds (Clark, 2015). The most important physical reactions that cause variations in isotope compositions of natural waters are evaporation and condensation.

A number of studies have been carried out on the research area tries to understand the hydrochemistry of the Borkena and Gerado catchments separately. Some of the studies are GSE, 2017; Dereje Gidafe, 2012; Ketema Tadesse, 1980. There are also studies that have been done on a regional scale tries to understand the flow processes and Hydrogeochemical evolution of both Awash and Blue Nile basin.

This study tries to investigate a groundwater flow process of both catchments and analyze IGF using different chemical approaches such as hydrochemical analysis, ionic ratios, TDS and Chloride ion concentration. Inverse geochemical modeling has been also applied in certain selected groundwater flow paths.

5.2 Evaluation of laboratory results

Water samples were collected for chemical analysis during the field work and field in situ measurement of EC, PH and were done as well. In addition, available chemical data have been collected from previous studies (Dereje Gidafe,2012; GSE,2017).Thirteen parameters have been analyzed in the laboratory:- TDS, EC, pH, , Na+, K+, Ca^{+2}, Mg^{+2}, NO^{3}-, , HCO^{3-}, $SO4^{-2}$, Cl, SiO4 and Br.

The accuracy of hydro chemical laboratory analysis was checked by calculating the cation-anion balance. According to the principle of electro neutrality, the sums of cations in meq/l have to nearly be equal to the sum of anions in meq/l for the chemical data to be dependable for further geochemical characterization and interpretation (Freeze and Cherry,1979). The accuracy of chemical analysis results was evaluated Based on electro neutrality obtained from using aquachem software. Water samples with electro neutrality below + or – 10 % regarded as acceptable. A total of 56 samples were pass cation- anion reliability check less than ten percent.

Other method of checking the accuracy of Laboratory result is by checking resemblance of field measured parameter with laboratory measurement. In this case field measured Electric

conductivity is showing a good correlation with R^2 of 0.84 which shows the result of laboratory is reliable (Fig 27).

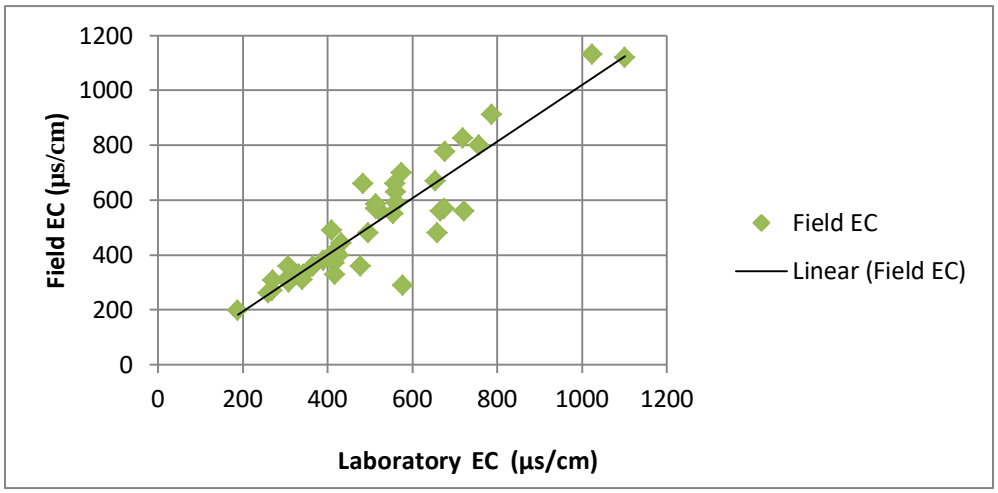

Figure 27. Electrical conductivity values (Field versus laboratory)

5.3 Hydrochemical parameters

5.3.1 Total ionic concentration and pH

The residence time of the water within the aquifer determines the concentrations of dissolved ions. The short residence time in the fractured aquifers leads to lower dissolved ions and vice versa.

The total ionic concentration is expressed in terms of electric conductivity (EC) or total dissolved solids (TDS). From the chemical analysis result the total dissolved solids and Electrical conductivity from different lithological units show variation from 165- 938.1 mg/l and 188 -1394 µS/cm respectively. The lowest TDS was recorded on a spring at the foot of the escarpment around Mekoy town south western part of the area. Maximum TDS and EC were obtained deep wells from Kemissie plain. The high TDS and EC samples are characterizes with relatively a long flow path and residence time.

pH is a measure of how acidic or basic water is. The pH in an aqueous solution is controlled by interrelated chemical reactions that produce or consume hydrogen ions (Hem,1989). Despite the fact the PH values doesn't show a systematic variation along flow path on the

study area the values have a range between 6.64- 8.9. Most of the values are fall under PH value of 8.3.

Table 8 Summary statistics for hydro chemical parameters and ions

Parameter	Ca	Mg	Na	Cl	HCO3	SO4	pH	Electrical Conductivity	NO3	calc TDS	Total Hardness
Unit	mg/l	mg/l	mg/l	mg/l	mg/l	mg/l		uS/cm	mg/l	mg/l	mg/l
Min	0.3	0.8	0.2	0.6	100.0	3.9	6.6	188.0	0.1	165.1	7.9
Max	167.2	41.5	267.3	163.1	477.0	192.0	8.9	1394.0	86.4	938.2	547.5
Average	53.0	14.4	47.5	20.7	277.7	23.4	7.4	537.6	9.9	451.4	197
St. Dev.	32.3	8.6	47.5	27.6	97.2	34.8	7.3	234.1	15.9	186.8	111
Sample Num	56	56	56	56	56	56	56	56	56	56	56

5.3.2 Major ions

Total of 58 samples have been analyzed from both catchments for hydro chemical parameters. Those samples were collected from Rivers, boreholes, shallow dug well and springs found on the study area.

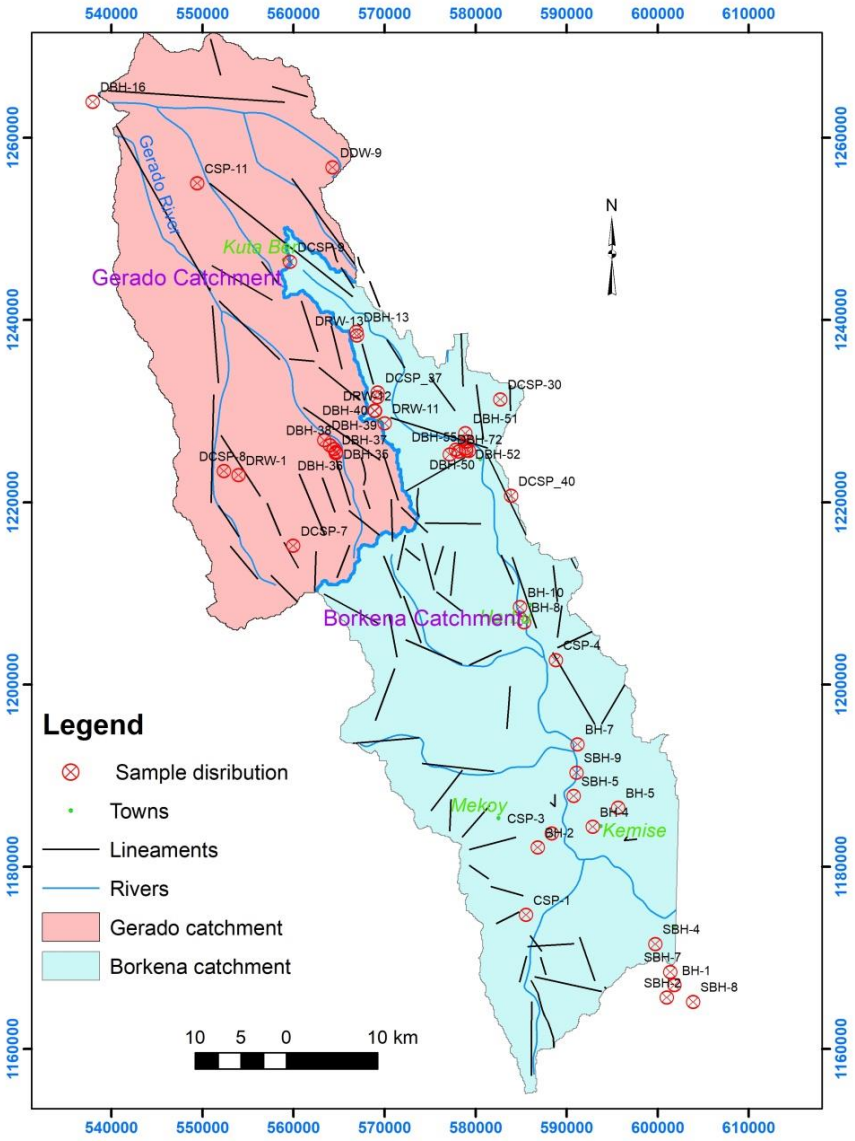

Figure 28. Sample distribution of hydrochemical data

Different processes play a role in shaping the chemistry of groundwater. Samples from northwestern area have high Ca^{2+} when compared southeastern areas of Borkena catchment. Ca^{2+} shows some decreasing trend along groundwater flow direction although locally high and low values are found due to variation in depth of boreholes, geochemical reaction, and presence of deep groundwater system.

Cations exchange is a reaction in which the calcium and magnesium in the water are exchanged for sodium that is adsorbed to aquifer solids such as clay minerals, resulting in higher sodium concentrations. The molar concentration of Na^{+} plotted against Ca^{2+} is shown in Fig 29 .The linear trend shows the chance of two ion exchange systems with different original water quality.

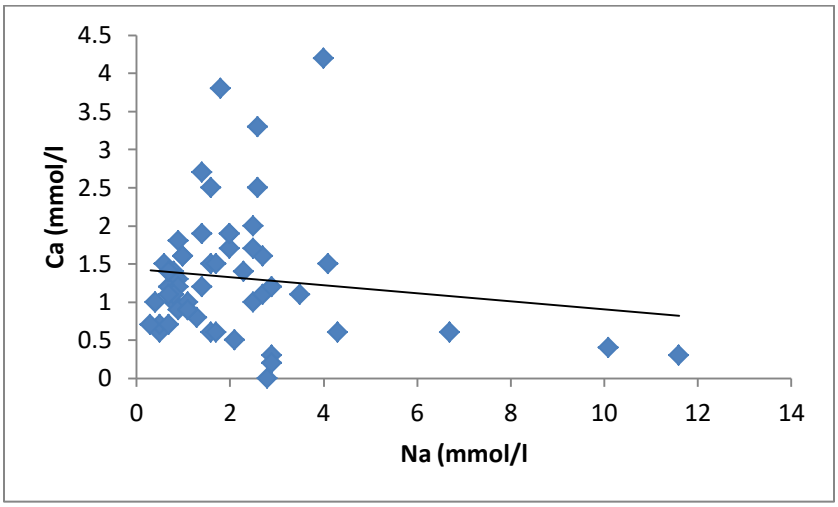

Figure 29. Ca versus Na graph

Plots of (Ca + Mg) vs. (HCO3 + SO4) were studied to identify the relative importance of ion exchange and weathering processes. If Ca, Mg, SO4 and HCO3 are derived from a simple dissolution of calcite, dolomite and gypsum, a 1:1 stoichiometry of (Ca+Mg) to (SO4+HCO3) will exist;- If ion exchange is the process, it will shift the points to the left due to a large excess of Ca+ Mg over SO4 + HCO3. Most of the samples are plotted toward ion exchange process (fig 30).

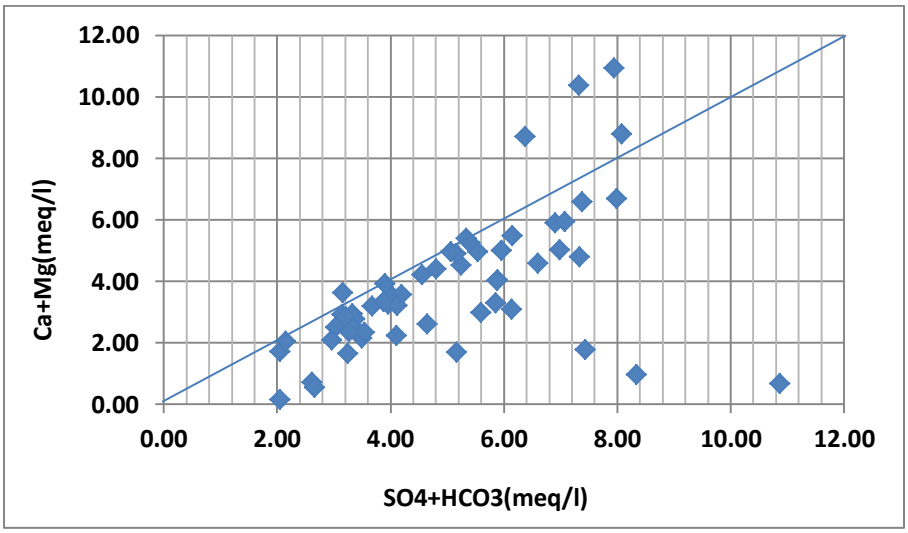

Figure 30. Ca+Mg versus SO4+HCO3 graph

Ca^{2+} versus HCO3 plot indicates that some of the samples have relatively excess Ca^{2+} than HCO3 that can be contributed by calcite. However calcite dissolution is not a dominant reaction on groundwater evolution (Fig 31).

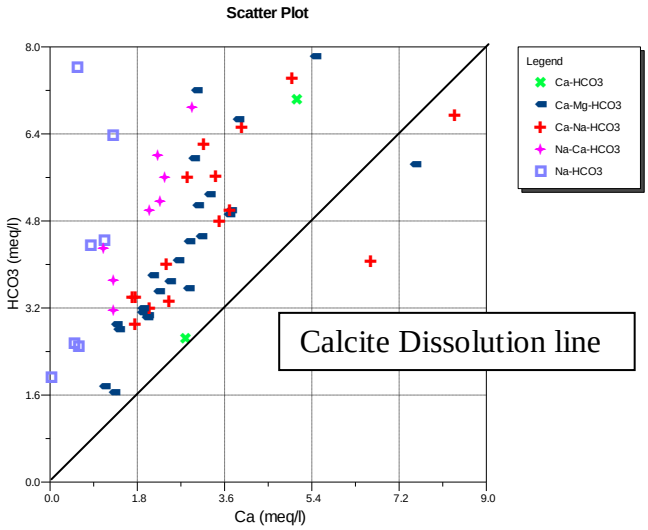

Figure 31. Scatter plot of HCO3 versus Ca

The most dominant anion in all groundwater samples is HCO3 which is a dominating anion in most fresh waters. However most the samples have a TDS concentration not exceeding 600 mg/l. Those types of water have not passed evaporates. The nature of rocks interacted with can be deduced from the cations. Na and Ca- HCO3 waters have interacted with feldspar, plagioclase, and pyroxene contained in volcanic rocks.

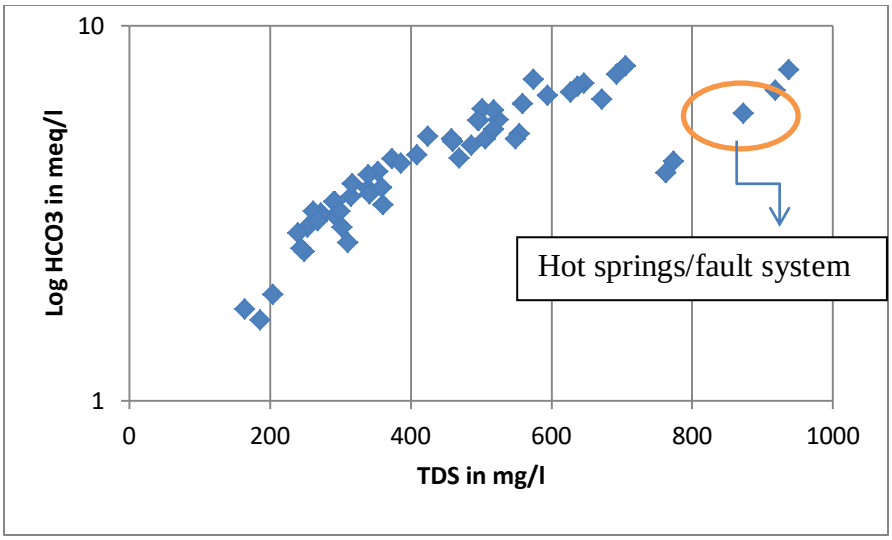

Figure 32. Log of HCO3 Ion Versus TDS

The dissolution of feldspars, micas, and other silicate minerals is strongly influenced by the chemically aggressive nature of water caused by dissolved CO2. When CO2 charged waters that are low in dissolved solids encounter silicate minerals high in cations, aluminum, and silica, cations and silica are leached, leaving an aluminosilicate residue. This residue is usually a clay mineral such as kaolinite, illite, or montmorillonite. The result of this process of incongruent dissolution is a rise in HCO3 concentration (Freeze & Cherry, 1979) (Fig 32).

$(Ca,Fe,Mg)\ (SiO_3) + 2H_2O\ 2CO_2 \rightarrow (Ca,Fe,Mg)\ (HCO_3)_2 + SiO\ (OH)_2$

5.4 Hydrochemical evidence of groundwater flow

5.4.1 Graphical representations and hydrochemical facies

The chemical properties of water can be represented in graphical illustrations. The common graphical representation of hydrochemical facies of water is the piper diagram. This diagram permits the cation and anion compositions of many samples to be represented on a single graph in which major groupings or trends in the data can be discerned visually (Freeze and Cherry, 1979). It also can define the patterns of spatial change in the water chemistry along a line of a section or along a flow path. Hydrochemical facies are distinct zones that have cation and anion concentrations describable within defined composition categories (Freeze and Cherry, 1979).

Hydrochemical facies are useful tools for tracing a groundwater flow and reaction in the subsurface. Geochemical reactions along ground-water flow paths can lead to regional differences in water composition that change in the direction of flow. Iso concentration contours of reacting dissolved constituents drawn on maps of water composition tend to align normal to the direction of ground-water flow (Glynn and Plummer, 2005).

The dominant cation in the study area are Ca and Na which approves the fact that in volcanic aquifers the dominant cations range from Ca–Mg to Na–K dominance while HCO3 is almost exclusively the dominant anion (Seifu Kebede,2013). Waters in the study area classified into 5 different hydrochemical facies using aqua-chem software based on the dominant anion and cations: Ca-HCO3, Ca-Mg- HCO3, Ca-Na-HCO3, Na-Ca-HCO3 and Na-HCO3(Fig33).

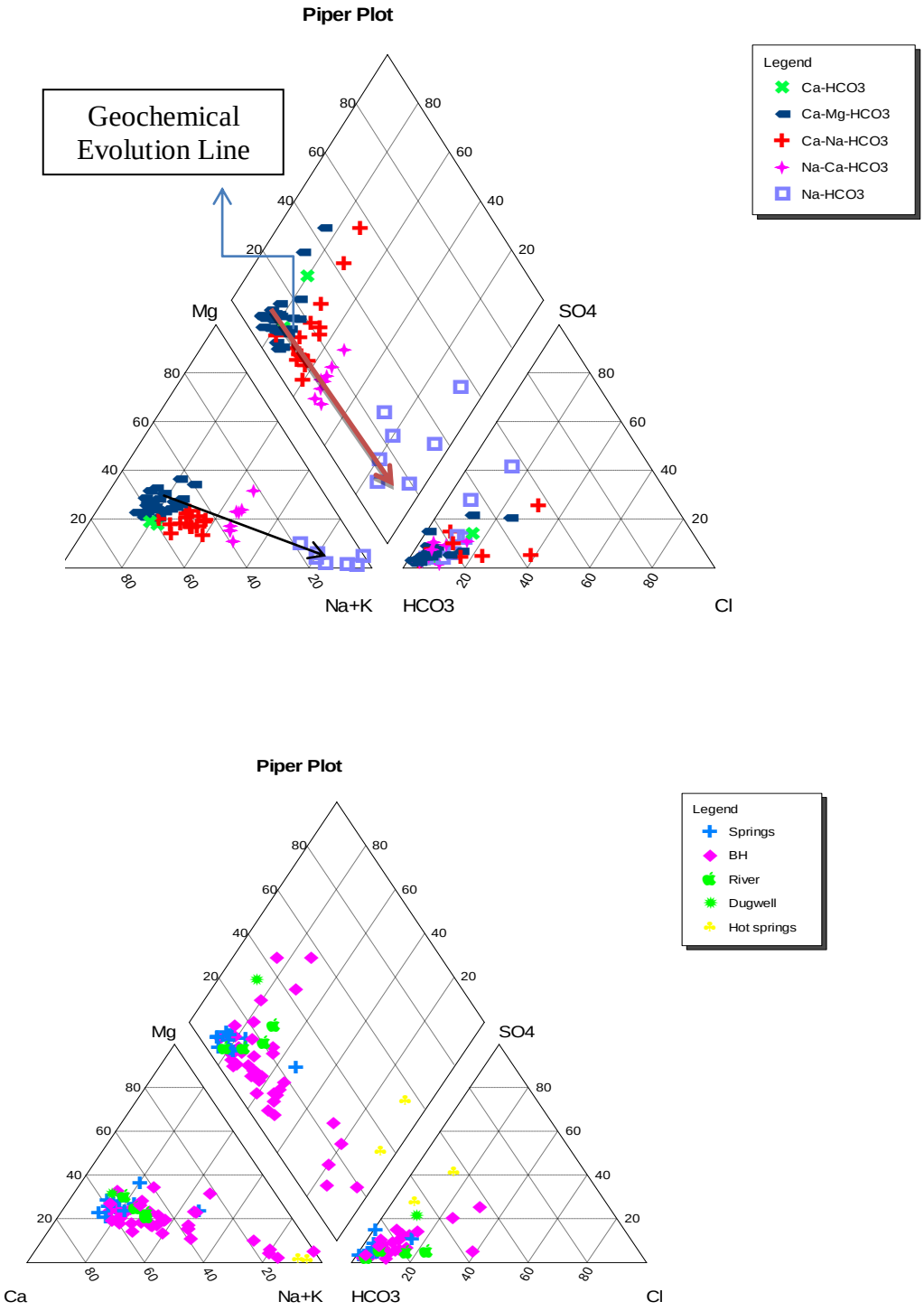

Figure 33. Piper diagram for the classification of natural waters

Ca-HCO3 type waters are associated with less evolved water types. They also have a relatively low residence time in the subsurface, without significant water-rock interactions. In the study area, those water types found on the shallow boreholes which have been developed along the fault lines. The fracture is facilitating the flow which gives no much time for the water to interact with the environment. These types of water have a TDS between 311 and 646 mg/l.

Water groups represented by Ca-Mg-HCO3 are associated with the shallow systems. Those types of waters are localized in the highland basic volcanic areas. The high Mg content is related to preferential leaching of host basalts (Tenalem et al., 2007). Samples that belong to this group are springs, Rivers, and some wells. There TDS is generally low which is below 500 mg/l. It is also characterized by relatively higher TDS values 706 and 873 mg/l recorded on two of the borehole samples. This group also includes Ca-Mg-Na-HCO3 which shows a considerable mixing of groundwater from different sources.

The other types of water groups are Ca-Na- HCO3 which are more mineralized and evolved types of water with the TDS ranging from 300- 918 mg/l. This water type is found in relatively deep wells found at the Gerado graben and some of the Boreholes found at the foot of the eastern block of Borkena graben. As the eastern part of the graben mostly dominated with acidic volcanic rocks, this might be the result of the weathered and fractured rocks rich in Ca- and Na- plagioclases.

Na-Ca-HCO3 groups are represented by intermediate groundwater evolution which relatively long travels a distance from the recharge source and more residence time. These types of water are found at the Kombolcha area along the fault line of Dessie- Muti kolo-Bati. These types of water in the study area not highly mineralized with the TDS value ranging from 272- 637 mg/l. those low mineralized Na dominated water might be the result of cation exchange.

The last hydrochemical facies found is Na-HCO3. Water samples in this group were obtained from wells and thermal fault springs. The group has a range of TDS values from 204- 938 mg/l. those water types found at the Kemise plain on the deep wells and hot springs found in the Harbu area. For the borehole with low TDS Cation exchange at clay

layer interfaces as water percolates to deeper zones could be a possible explanation. The silicate mineral such as albite (NaAlSi3O8) weathering in volcanic rocks produces Na, HCO3, and clay. When freshwater with Ca-HCO3 type enters into the aquifer, the Na in the aquifer will substitute Ca leading to a rise in Na concentration in the water and Na-HCO3 type water. This assumption can be seen from the scatter plot of Na^{+} and $Ca2^{+}$ which Na^{+} shows a negative correlation with Ca^{2+} (Fig 34).

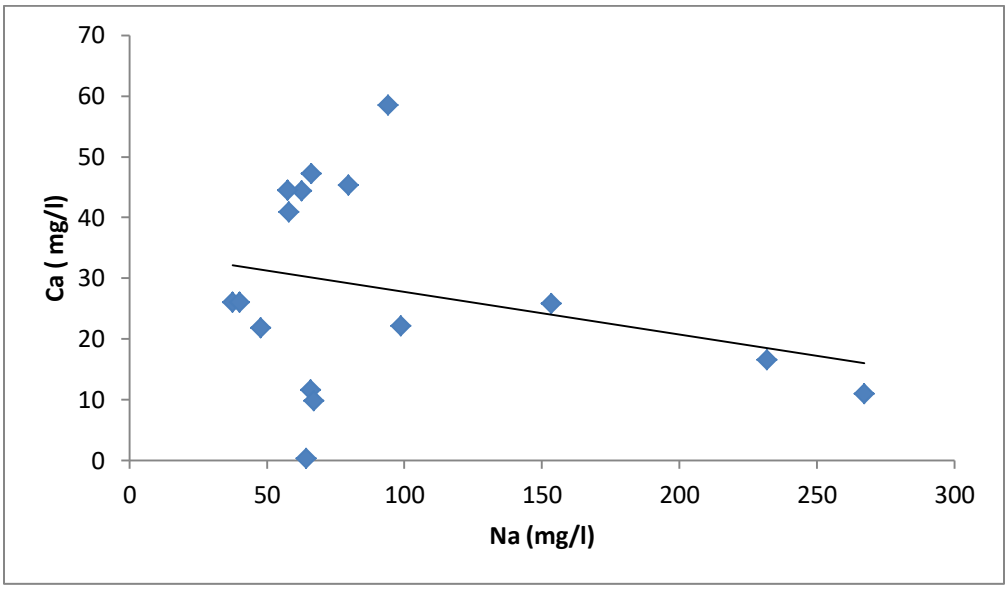

Figure 34. Na and Ca scatter plot for Na-Ca-HCO3 and Na-HCO3 water types

5.4.2 TDS and EC

Groundwater moves along its flow paths in the saturated zone, increases of total dissolved solids, and most of the major ions normally occur. TDS also may increase due to the dumping of wastewater, metropolitan runoff, and increased erosion due to land-use changes in the drainage basin. TDS in water is an essential factor to describe the changes groundwater undergoes along the flow path (Tilahun Azagegn, 2014).

Measured TDS value in the study area has varied from 165 to 938 mg/l. The lower values belong to springs and shallow boreholes which have less evolved in the groundwater system. The highest value is recorded from hot sprig found in Harbu area which is thermal spring associated with the fault system.

Moderately evolved groundwater systems with TDS value above 500 mg/l found from Boreholes and river samples Adjacent to Tosaa ridge in Borkena river catchment while adjacent to the ridge in Gerado river catchment; boreholes have a TDS value less than 300 mg/l. There are also boreholes with TDS value up to 800 mg/l found along N- S the fault lines. These waters have substantial rock-water interaction, with long sub-surface path length and residence time. This suggests there might be a groundwater interaction between two catchments.

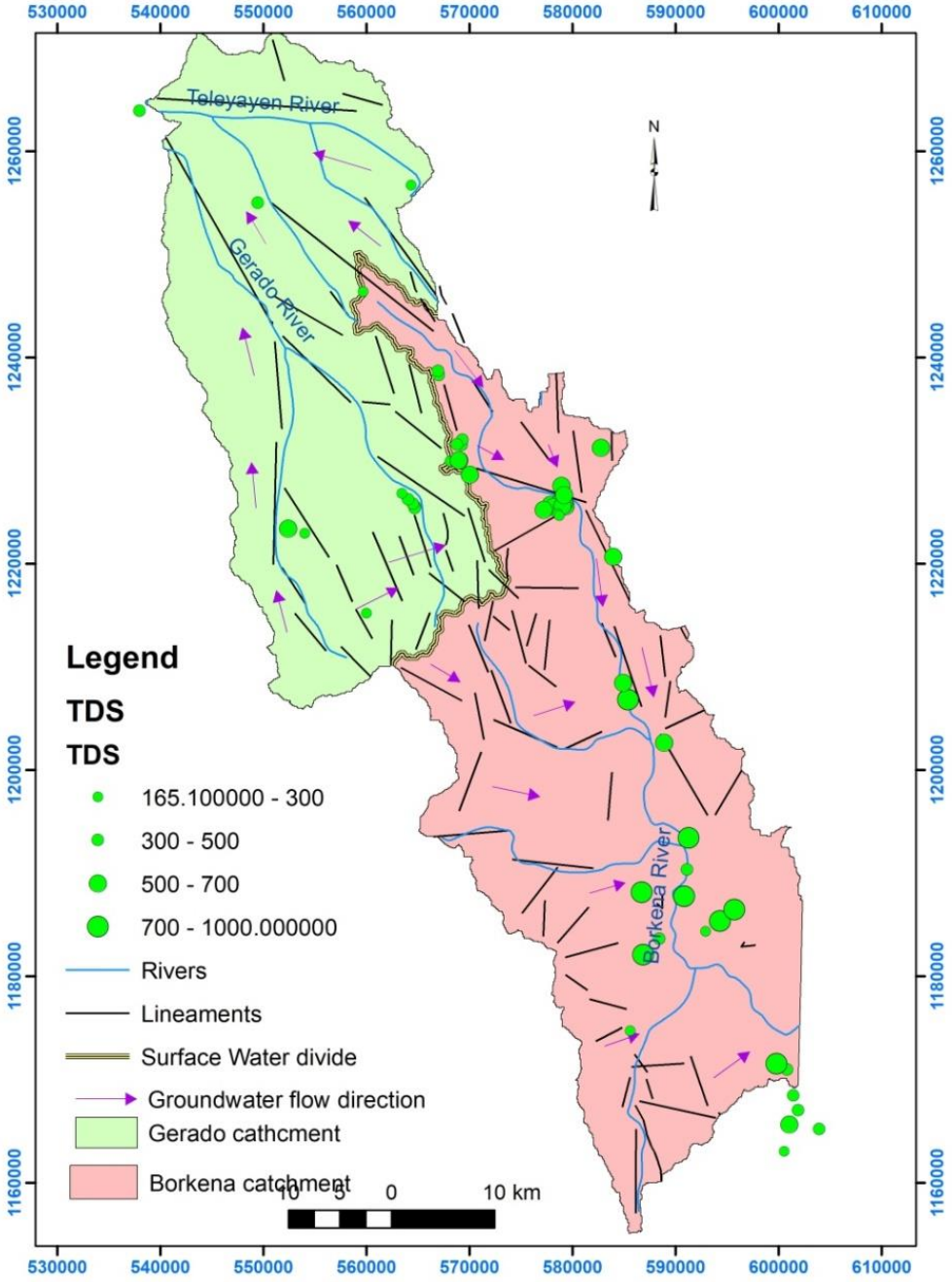

Figure 35. TDS map

Electric conductivity is the ability of the water to conduct an electric current. The presence of charged ionic species in water makes the water conductive. As ion concentrations increase, conductance of the water increases. Therefore, the conductance measurement provides an indication of ion concentration in the water (Hem, 1989).

Electrical conductivity of water in the study area shows some variation with respect to flow process of a groundwater. It can also be used as an evidence for studying a groundwater evolution. EC values of the water samples of the investigation area are in the range from188 μs/cm to 1394 μs/cm. The electrical conductivity (EC) values in the investigation area showed an increasing trend from recharge to discharge area as showed on the spatial distribution map of EC (Fig 36). The groundwater and spring samples found in Gerado catchments have the lowest value of EC while the springs on the foot escarpments in the Borkena river catchment have relatively high EC values. Therefore, this shows that the change and rise of EC values comes after series of interaction of water with different lithologies along the flow path. The rise of the EC also coincides with the direction of groundwater flow mapped on the area.

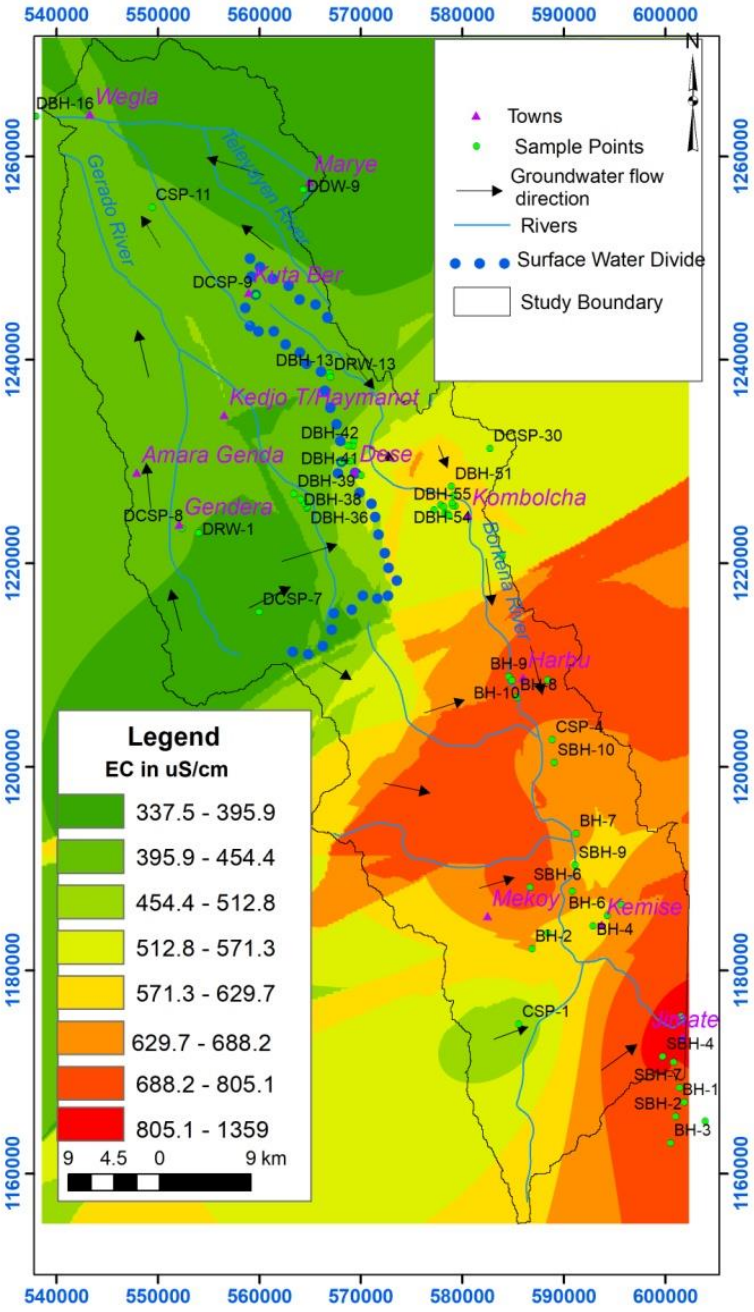

Figure 36. EC map

5.4.3 Chloride

Chloride is possibly the most informative ion from a hydrochemical viewpoint, since it is common in groundwater, has a limited number of identifiable sources, and is hydro chemically conservative. These properties turn chlorine into a most useful hydro chemical indicator.

Since chloride is conservative ion which never reacts once ionized and inters to a solution but its value increase along groundwater flow direction new chloride inters to the solution due to libration of geochemical reaction.

Generally, igneous rocks cannot produce very high concentrations of chloride to natural water. Considerably more important sources are associated with sedimentary rocks, particularly the evaporites (Hem, 1989). There is also chloride bearing minerals found in igneous rocks like feldspathoid sodalite and phosphate mineral apatite (Hem, 1989).

The chloride concentration on the study area ranges from 0.5 to 163 mg/l. highly elevated areas that have been considered as a recharge area have a low concentration of chloride with the exception of areas that have been found on Borkena river catchments near to the surface divide possess a high amount of chloride concentration (up to 60 mg/l). Since chloride concentration and TDS have some correlation (Fig 38) the possible explanation of high concentration of chloride found adjacent areas of the groundwater divide is possibly the groundwater have relatively greater travel time from the adjacent Gerado catchment

During the flow, there is a considerable contribution of chloride from erosion of the rocks that underlies most of the area. Some boreholes found at Kemissie plain area which is found in the lower course of Borkena River catchment and hot springs also have chloride concentration more than 100 mg/l. Chloride source from industries might also have an

impact on the high concentration of chloride on the lower course of Borkena catchment.

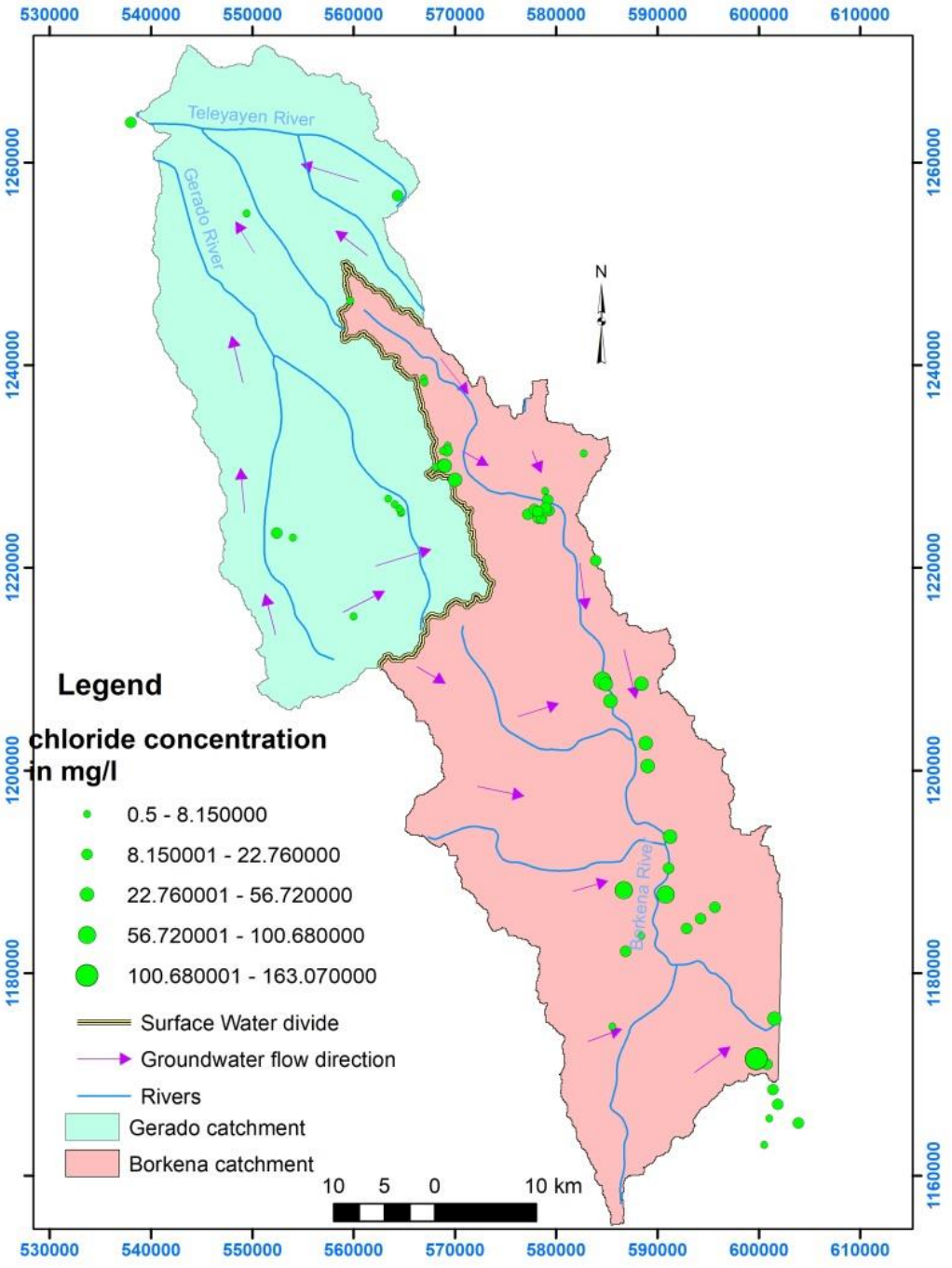

Figure 37. Chloride Map

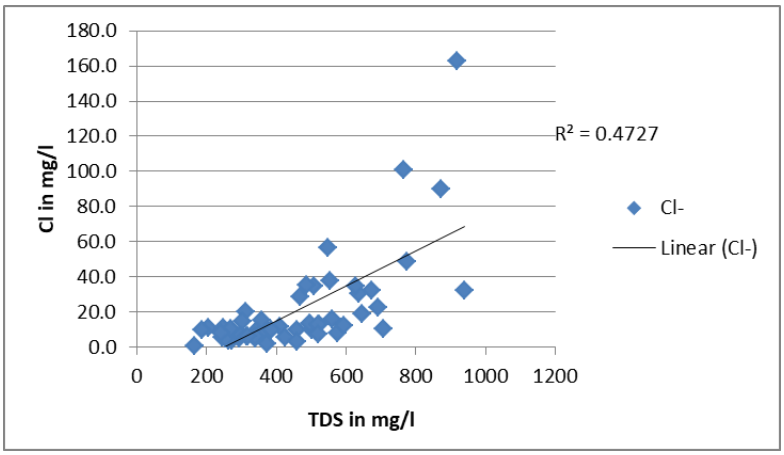

Figure 38. Plot of Chloride versus TDS

5.4.4 Ionic ratio

Na^{+} and Ca^{2+} molar ionic ratios are useful for determining the groundwater flow path. Since the sources of sodium and calcium in the groundwater are from the minerals corresponding silicates, feldspars, pyroxenes, and amphiboles rock types of the study area. The Na/Ca ratio is higher where there are deep groundwater circulation and long residence time. In the study area, the groundwater becomes rich in sodium as it circulates through the aquifer. Under such conditions, the cation exchange reaction of calcium by sodium, which comes from the host aquifers and intercalated clay soil, increases the sodium concentration over the calcium. The systematic changes in the cation composition of groundwater can be interpreted as direct evidence of exchange reactions. The chemical composition of groundwater might, therefore, be used to trace groundwater flow (Varsanyi,1989).

Some of the boreholes found in the Kombolcha area have Na/Ca ratio values more than 20 which have been considered as relatively long traveled groundwater from the recharge area. On the other hand, fault-controlled hot springs also have a high value of the ratio of about 40. Therefore, areas with a high Na/Ca ratio are the possible discharge areas, whereas those with a low ratio can be considered as recharge areas.

The molar ratio of dissolved ionic species and their relationship with TDS also helps to trace the origin of solutes as well as the environment and major processes that generate the observed composition of groundwater (Hem, 1989). Along the groundwater flow paths, the

concentration of, Na+ and K+ increases with increasing TDS. From samples analyzed on the study area TDS and Na+K/Ca+Mg ratio have a correlation factor 0.48 (fig 39). Low Na+K/Ca+Mg ratio has been found on springs and boreholes found at Gerado catchment in Gerado well field. Those samples also have a low TDS from 189 up to 365 mg/l. the high amount of Ca and Mg for those areas might be due to dissolution reactions from silicate weathering in volcanic aquifers. High ratio of Na+K/Ca+Mg with a relatively increasing TDS (>500 mg/l) value obtained from Boreholes found in Dessie town which is found at the foot of Tossa ridge dividing the surface drainage of Borkena and Gerado. Water from Kombolcha town also has a high ratio of Na+k/Ca+Mg (3-7) with an increasing TDS. This might suggest there is a trough flow of groundwater from Gerado to the Borkena Catchment.

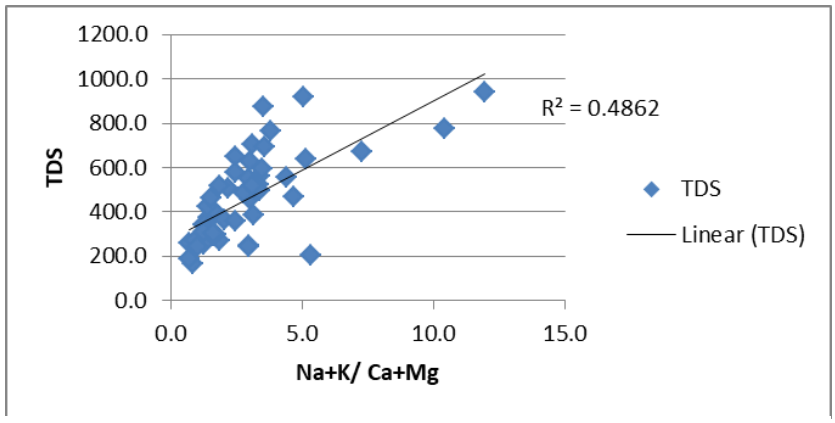

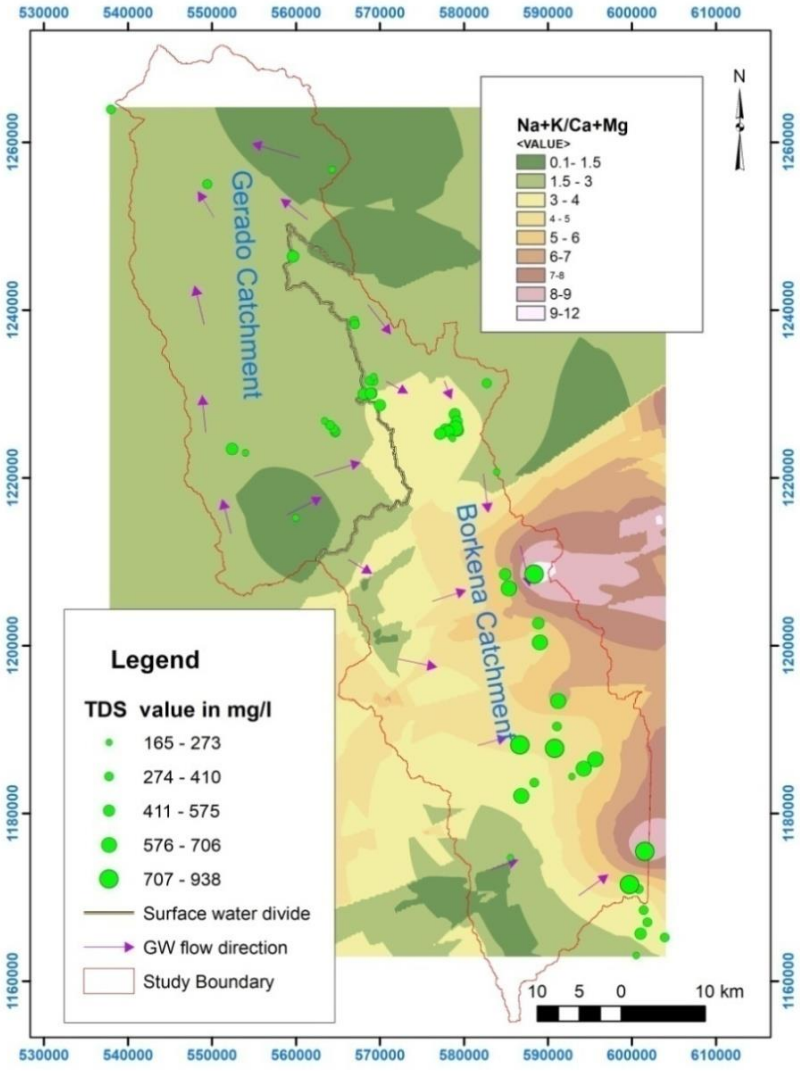

Figure 39. Ionic Ratao Map of Na+K/Ca+Mg in meq/l

Other ionic ratio which have been used for the tracers are Na+K against SO4. The log- log plot of Na+K versus SO4 shows a good correlation. Accordingly the Concentrations of Na^{+}, Cl^{-}, and $SO4^{2-}$ in the areas of discharge of those Na-HCO3 type is relatively high than an areas which have been considered as a recharge areas (fig 40).

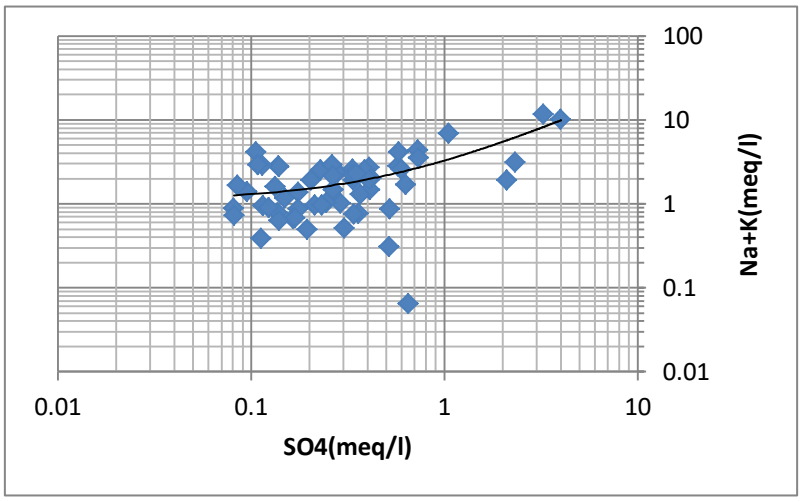

Figure 40. Log Log plot of SO4 versus Na+K

5.5 Inverse Geochemical Modeling

The mass balance concept is a means of keeping track of reacting phases that transfer mass during water flow. Inverse mass balance models are one of the geochemical mass balancing techniques which are useful tools in constraining flow paths where a reasonable set of mineral dissolution or precipitation reactions must be found. However, such models do not establish flow paths, but they can infer that such paths are reasonable. Instead, they can rule out certain paths if there is no sensible evolutionary path for the solutes (Nelson and Mayo, 2014)

Inverse geochemical modeling was done using PHREEQC model. The program calculates all the possible mass balance models that can create the final solution from the initial solution and all conceivable combinations of available reactants. This is particularly useful when modeling a well-constrained system such as a column experiment where the initial

and final solution chemistry is well known and the solid phase can be well characterized (Parkhurst and Appelo, 1999).

The flow paths were chosen based on the pattern of variation of the hydrochemical facies, the physiographic location of the sample in the basin and the hydraulic head variation within the flow system. In the modeling, it is presumed that groundwater flows from west to East which is from Gerado Catchment to the Borkena Catchment since the hydrochemical evolution shows indications. Finally, the flow path is selected from north to south which is considered as a general flow within a Borkena catchment. Three distinct flow paths have been selected from topographically high areas (Fig41). All initial input of groundwater for all three paths considered in the inverse geochemical model is Ca-Mg-HCO3 type waters. Initial (I) and final (F) water types and there corresponding hydro chemical parameter for all three flow paths P) are shown in table (9).

Table 9 chemical parameters for the selected flow paths

model		ID	pH	EC	Na	K	Ca	Mg	Cl	SO4	HCO3	F	TDS	Water Type
P 1	I	DBH-36	7.8	419	20.3	2.74	52.8	11.2	7.8	5.53	248.8	0.1	354.0	Ca-Mg-HCO3
	F	DBH-52	8.2	676	62.7	1.27	44.4	10.7	9.5	6.6	366	0.2	502.2	Na-Ca-HCO3
P 2	I	DCSP-7	7.6	315	12.1	4.05	27.3	13.8	3.6	6.7	176.9	0.1	253.9	Ca-Mg-HCO3
	F	BH-8	7.8	731	94	1.65	58.5	25.6	30.3	5.1	419.6	0.4	637.7	Na-Ca-HCO3
P3	I	DBH-13	7.4	344	21.8	0.64	38	12.7	5.6	10.3	190.3	0.1	293.0	Ca-Mg-Na-HCO3
	F	DBH-72	7.7	562	66.2	1.34	47.2	11.5	13.6	12.6	341.6	0.1	496.0	Na-Ca-HCO3

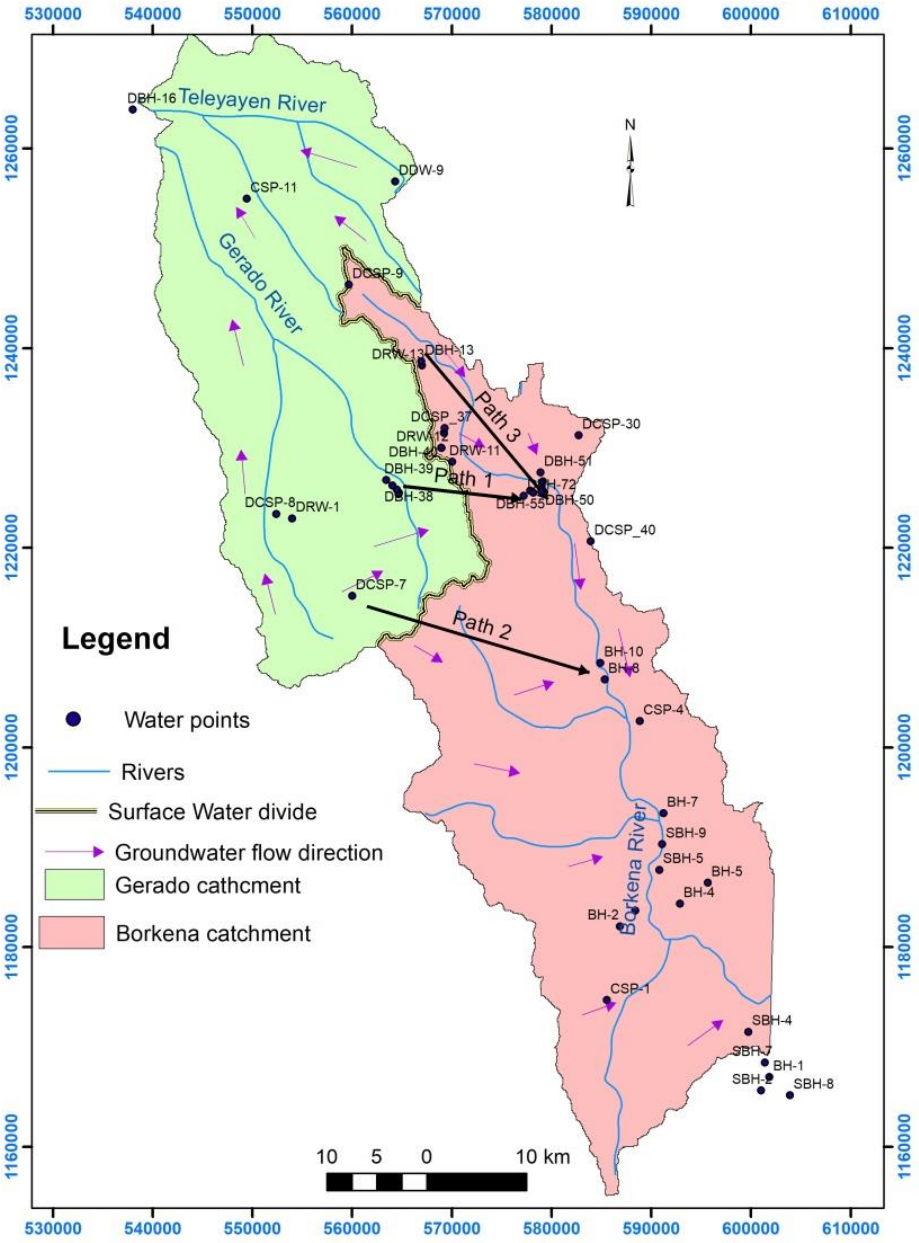

Figure 41. selected flow paths for inverse geochemical model

Mineral phase have been selected based on the geology of the study area and the predominant rock water reactions. Most of the area which is characterized by complex volcanic lithology, rocks such as basalt comprise considerable amounts of alumino silicate

minerals plagioclase, K-feldspar, pyroxene and amphiboles. These minerals are therefore thermodynamically unstable and dissolve or weather to clays and oxides when in contact with water (Freeze and Cherry,1979).

In chemically weathered volcanic rocks thermodynamic considerations dictates that the feldspar minerals are altered to clays minerals (kaolinite, montmorillonite and illite) and Al- and Fe- oxides (gibbsite, goethite and hematite) are formed (Freeze and Cherry, 1979). Calcite minerals might be found as cavity fillings in volcanic rocks as a result of precipitation during plagioclase and pyroxene weathering. Likewise, anhydrite and gypsum could also occur and fill amygdaloidal cavities of volcanic rocks.

Flow path 1

Reactant		**Phase mole transfers**
Kaolinite	Al2Si2O5 (OH) 4	1.848e+001
CO2 (g)	CO2	-1.848e+001
Calcite	CaCO3	1.848e+001
Albite	NaAlSi3O8	6.696e-005
K-feldspar	KAlSi3O8	-4.670e-004
CaX2	CaX2	-3.564e-004
Anorthite	CaAl2Si2O8	-1.848e+001
Illite	K0.6Mg0.25Al2.3Si3.5O10 (OH) 2	8.212e-004
NaX	NaX	7.129e-004

Inverse geochemical modeling was conducted from the borehole found at the Gerado well field to the Kombolcha town water supply borehole as the conceptual model shows there is a flow between those two catchments**.** The result of the model shows the dominant reaction happened on this flow path is likely to be cation exchange which Na is Exchanging Ca and dissolution of silicate minerals K- feldspar and plagioclase and gaseous CO2. Calcite and some clay minerals like illite and Kaolinite precipitated.

The general reaction equation for the flowpath one is:-

(Ca-Mg-HCO3 water)+ plageoclase + CO2+ K-Feldspar → (Na-Ca–HCO3water) + Calcite +Illite +Clay

Flow path 2

Reactants		Phase mole transfers
Kaolinite	Al2Si2O5(OH)4	1.309e-002
Ca-Montmorillonite	Ca0.165Al2.33Si3.67O10(OH)2	-1.004e-002
Calcite	CaCO3	5.962e-003
Albite	NaAlSi3O8	6.400e-003
K-feldspar	KAlSi3O8	-1.581e-004
Anorthite	CaAl2Si2O8	-4.517e-003

The second path was conducted from the Highland area spring found near to Guguftu to the low land area of Borkena plain to the Harbu. The geochemical modeling along the flow path shows the dissolution of feldspar and primary alumino-silicate mineral which results in feldspar and the formation of a secondary clay mineral-like kaolinite.

(Ca-Mg-HCO3 water) + Ca-Montmorillonite + Anorthite +K feldspar → (Na-Ca-HCO3 Water) + calcite + Kaolinite

Flow path 3

Reactants		Phase mole transfers
Kaolinite	Al2Si2O5(OH)4	2.775e+001
Ca-Montmorillon	Ca0.165Al2.33Si3.67O10(OH)2	-1.397e-003
CO2(g)	CO2	-2.775e+001
Calcite	CaCO3	2.776e+001
Albite	NaAlSi3O8	1.056e-003
K-feldspar	KAlSi3O8	-1.101e-003
Anorthite	CaAl2Si2O8	-2.775e+001
Illite	K0.6Mg0.25Al2.3Si3.5O10(OH)2	1.892e-003

This flow model was conducted along a flow path from Alsha plain through Dessie area to Kobmolcha. Selected initial water for the modeling shows a significant mixing of waters. The model shows that the dissolution of Ca-plagioclases, K-feldspars and CO2. There also precipitation of calcite, Illite and clay minerals. Those are the major chemical processes more or less responsible to the observed natural groundwater chemistry in the study area.

5.6 Isotope hydrology

Isotopes are forms of a particular element that have the same atomic number but different atomic weights due to varying numbers of neutrons in the nucleus. Stable isotopes are not involved with any natural radioactive decay process. In hydrological studies, the stable isotopes of interest commonly relate to H, C, N and O (Yitbarek, 2009).

Oxygen has three stable isotopes, ^{16}O, ^{17}O, and ^{18}O; and hydrogen has two stable isotopes ^{1}H and ^{2}H. The basic hydrological processes that affect the distribution of these isotopes through the hydrological cycle consist of Evaporation, Condensation, Re evaporation from soils and surface waters, which enriches the residual water in both isotopes and Mixing during recharge and groundwater flow.

The isotopic composition of water is expressed in comparison to the isotopic composition of ocean water. For this purpose an internationally agreed upon sample of ocean water has been selected, called Standard Mean Ocean Water (SMOW) (Craig, 1961). The isotopic composition of water is expressed in per mil % deviations from the SMOW standard. The deviations are written $\delta^{2}H$ for the deuterium, and $\delta^{18}O$ for ^{18}O.

$$\delta H\%_o = \frac{(2H/1H)sample - (2H/1H)SMOW}{(2H/1H)SMOW} * 1000$$

$$\delta O\%o = \frac{\left(\frac{18O}{16o}\right)sample - \left(\frac{18\,O}{16o}\right)SMOW}{((18o/16o)SMOW}) * 1000$$

Definite universal rules can be predictable for the distribution of these isotopes in ground water. If the isotope content does not change within the aquifer, it will reveal the source of the groundwater. If the isotopic content changes along groundwater paths, it will reveal the history of the water.

Evaporation increases the isotope concentration while transpiration does not affect or little affect isotope concentration. Tracing groundwater by means of environmental isotopes offers unique and supplementary information on the source and flow of groundwater and its dissolved constituents, as well as allows a quantitative evaluation of mixing (IAEA,2000).

5.7 Local Meteoric Water Line (LMWL)

The isotope value of precipitation is controlled by, isotope value of source, rate of evaporation of source, isotopic evolution of air mass, relative humidity during precipitation.

The meteoric line is an appropriate reference line for the understanding and tracing of local groundwater origins and movements. The composition of precipitation is reflected from composition of groundwater. The resemblance or departure from of groundwater from precipitation will be interpreted in terms of hydrological processes such as recharge source, recharge mechanism, evaporation, mixing between different waters and isotope exchange.

Apart from global meteoric water line (GMWL) it is common to plot groundwater samples against Local meteoric lines. On this study local meteoric water line is established from database of global network for isotopes in precipitation (GNIP) for Kombolcha, Weledi and Dessie. Despite the data lacks temporal variation, it has average $\delta^{18}O$ and $\delta^{2}H$ composition 0.26‰ and 15.5‰ respectively. The precipitation of the area is plotted in a scatter plot of deuterium and 18 Oxygen. The points fitted with best fit has given a regression coefficient of R^2=0.96.

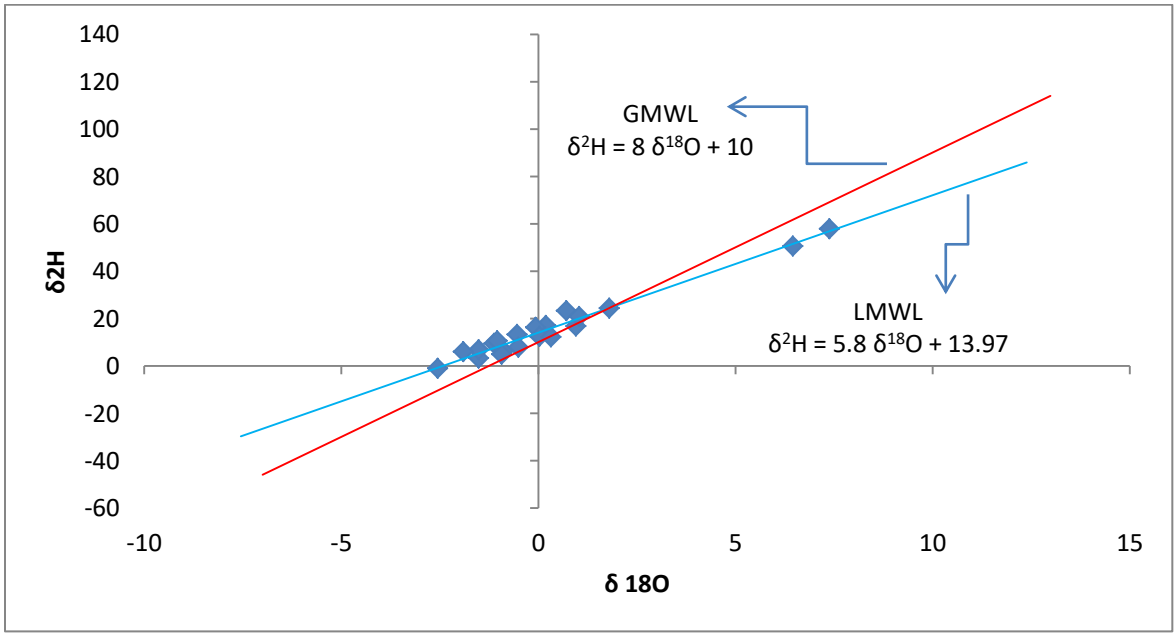

Figure 42. Local meteoric water line

The local meteoric water line placed above a global meteoric water line and eventually crossed each other at a certain point. This is because of differences in the origin of water vapor and rainout along the trajectory from the source. The main sources of moisture in Ethiopia are the monsoon from Atlantic and Indian Oceans. High sea surface temperature over north Indian Ocean favors the formation of enriched vapor coming to Ethiopia (Seifu Kebede, 2013).

The value of δ^2H and $\delta^{18}O$ is varies spatially on the study area. This might be occurred because of altitude effect. Isotopic content of rains is depleted with an altitude; this is attributed to the decline in temperature with altitude, which drives rainout and distillation of isotopes during orographic precipitation.

Mean $\delta^{18}O$ and ^2H values have been calculated from the GNIP data for each station. $\delta^{18}O$ varies from 0.06 (Weledi), 0.68 ‰ (Kombolcha) and 0.046‰ (Dessie). On the other hand an average δ^2H values become 13.15 (Weledi), 14.5 ‰ (Kombolcha) and 18.64‰ (Dessie).

5.8 Deuterium and Oxygen-18 of Ground water

Groundwaters generally reflect the isotopic signature of precipitation in the zone of recharge, although individual reservoirs may acquire signatures reflecting their mean residence time and seasonal timing of inputs, as modified by mixing between other sources, such as river water or artificial recharge (Gibson, et.al, 2005). The changes in isotopic composition are mainly the result of the recharge process.

31 Isotope samples have been obtained from secondary source which was analyzed in Addis Ababa University Isotope Laboratory. The spatial distribution of samples showed in figure 35. Oxygen (18) and deuterium for spring of both catchments have ranges from -4.73 to -1.44 and -16.85 to 3.86 respectively. The average isotope value has become -2.855 and -6.42 for oxygen and deuterium respectively. Locally enriched values have been found in springs from the escarpment.

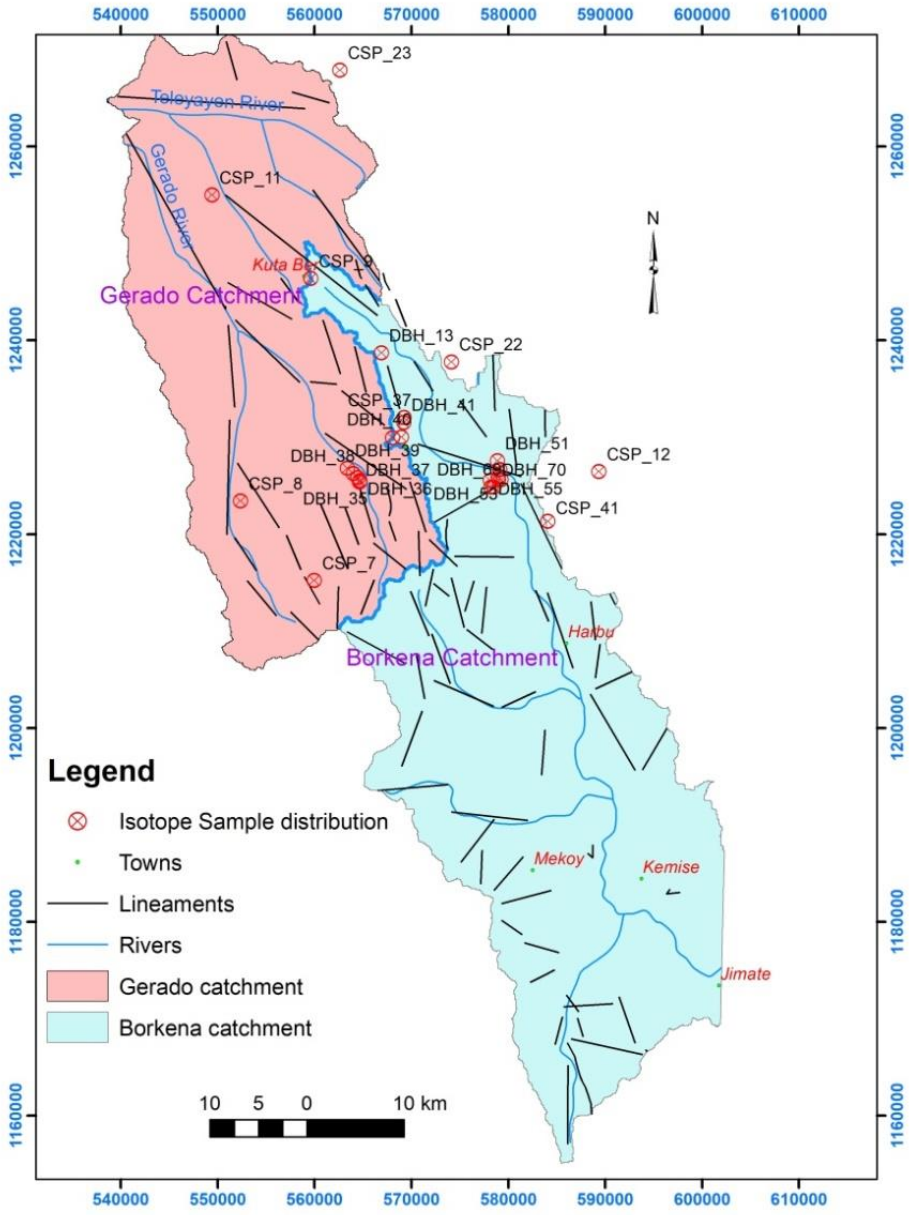

Figure 43. Environmental isotope data distribution map

Some of the springs lies on the LMWL line while most of springs deviate from the line. The possible reason for the depleted isotope signatures for most of the springs are loses water by direct evaporation and by means of water uptake by the roots and transpiration. Evaporation from the unsaturated zone and ultimately from the water table can also occur.

However the loss of water by transpiration, in contrast to evaporation, does not fractionate ^{18}O and D (Clark, 2015). .

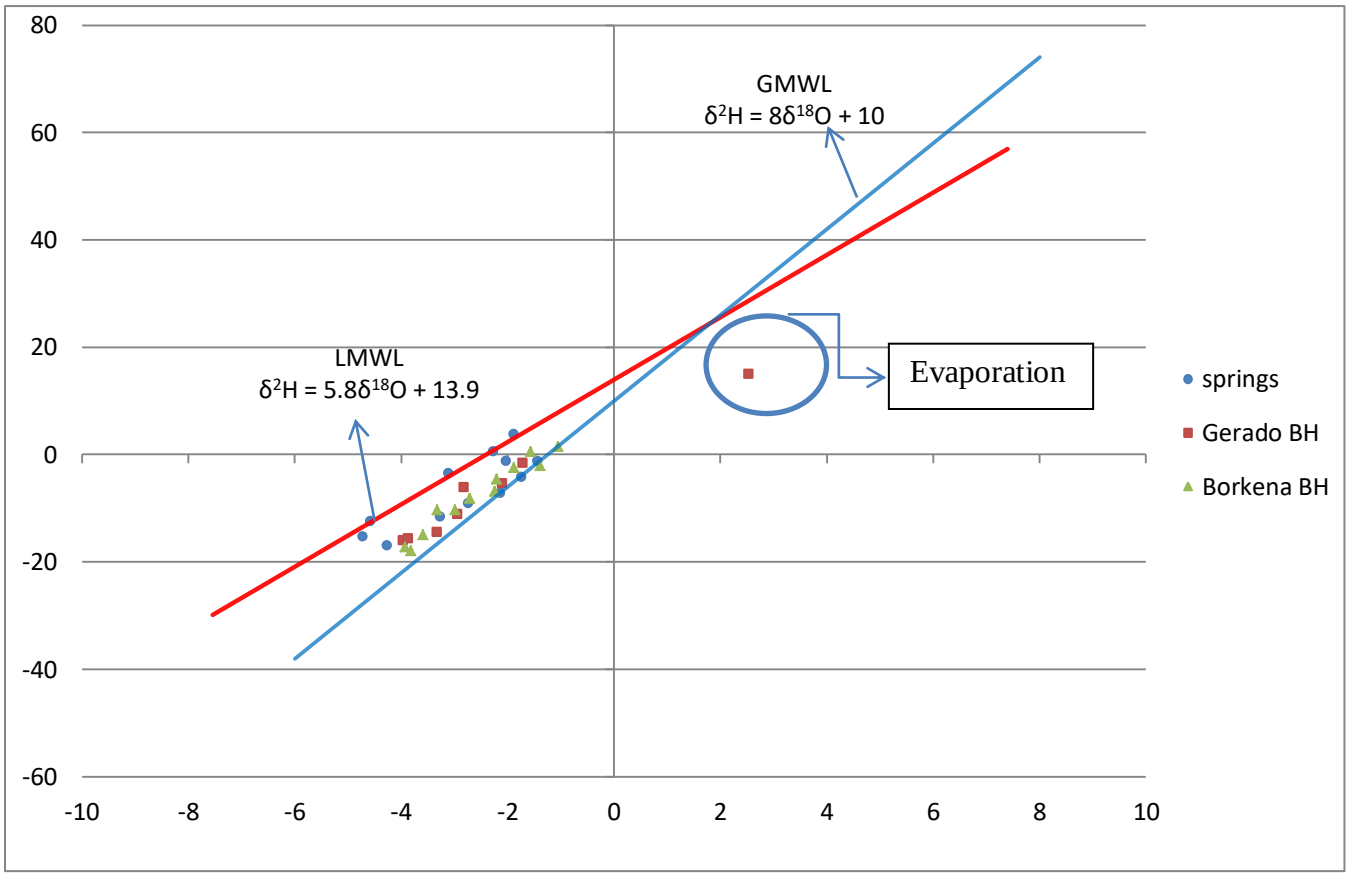

Figure 44. Groundwater sample against LMWL and GMWL

In arid regions, groundwater recharge is largely inclined toward the large precipitation events. As light rains contribute little to the weighted mean of precipitation, the isotopic composition of groundwater is well represented by the weighted mean annual or long term weighted value for precipitation (Clark, 2015). However, most of the groundwater samples from Gerado and Borkena catchments have depleted isotopic signature of ^{18}O and D from -2.28 to -6.83 and -2.5 to -7.8 respectively.

The regular trend in the isotopic signature of both catchments suggests a similarity in origin of the groundwaters. The groundwaters in the Borkena catchments are depleted in $\delta^{18}O$ and δD contents and show similar values to that of the groundwaters from the Gerado in the west, this may indicate the main source of recharge to both catchments is same.

When groundwater and rainwater data are compared, depleted water occurs in the recharge process. This might because of the amount of rainfall, with recharge occurring preferably from more intense rains. An average precipitation recorded for the summer time is 323.4 mm and 351.6 mm for July and August respectively.

The higher d-excess is related to significant evaporation of local surface waters under low humidity, and the vapour mass mixes with atmospheric reservoirs and re-condenses (Clark, 2015). The d-excess value in most of groundwater from both the catchment is low. D-excess values more than mean value for the global water line $10‰$ indicate evaporation. There is only one borehole encountered with the d- excess more than $10‰$ which is believed to be exposed to the evaporation. This Borehole is found at the Hara Wobelo Locality in the Gerado Plain.

6 Conclusion and recommendation

6.1 Conclusion

- ✓ The study area is found around Dessie Area which the capital of South Wollo. The area approximately bounded to 10^{o} 24' 0'' up to 11^{o} 30' 0'' N and 39^{o}24'0' up to 39^{o} 54' 0'' E. It is elongated in the NNW to SSE direction with a total length about 118 km and the maximum width not more than 41 km East-West direction. The study area consists of two river catchments which are Gerado and Borkena river catchments. Those rivers belong to upper Blue Nile and Lower Awash River basins.
- ✓ The main objective of the study is to understand the groundwater transfer and hydrodynamic system between Gerado and Borkena River. To achieve this objective combining evidences from conventional hydro geological investigation, geological and structural investigations, water chemistry and environmental isotope hydrology were used.
- ✓ The study area comprises two litho-stratigraphic units. These are: - Cenozoic and quaternary volcanic rocks and alluvial deposits. Volcanic rocks are highly dissected by NNE-SSW, NE-SW, EW trending faults. Numbers of intermountain Graben are formed elongated in north-south and NW-SE directions. The volcanic rocks form the mountains, escarpments and rugged terrain which act as recharge area for those intermountain valleys. The intermountain Graben is dominantly composed of poorly compacted quaternary basin fill deposits. The alluvial deposit's origin is considered to be local tectonic development forming an intermountain channels. Those alluvial deposits have different permeability from the volcanic rocks.
- ✓ From the structural observations the groundwater flow on the study area controlled by the faults which are SW to NW and WNW- trending and dipping to the northeast create the pattern for groundwater flow from the western escarpment towards the northeast. Lineaments which are related either to fractures and joints are common in the mapped area. They are N-S to NE, NW and E-W striking with the N-S and NE lineaments is predominating. Those lineaments are transected by the E-W striking lineaments. These lineaments also have a favorable condition for groundwater flow across surface water divide.

- ✓ A recharge was calculated using two methods which are chloride mass balance and Base flow separation. Based on the two methods an average areal recharge has become 174.4 mm/year for Gerado catchment and 106.2 mm/year for Borkena catchment.
- ✓ Spring patterns suggest there is an inter-basin groundwater flow between the catchment. The springs have preferential alignment in emerging with a considerable discharge which support inter-basin groundwater flow.
- ✓ Based on the dominant cation and anions waters in the study area classified in to 5 different hydro chemical facies which are: - Ca-HCO3, Ca-Mg- HCO3, Ca-Na-HCO3, Na-Ca-HCO3 and Na-HCO3. Water groups represented by Ca-Mg-HCO3 are associated with the shallow systems. Those types of waters are localized in the highland basic volcanic areas. Ca-Na- HCO3 which are more mineralized and evolved types of water with the TDS ranging from 300- 918 mg/l. this water type is found in relatively deep wells found at the Gerado graben and some of Bore holes found at the foot of eastern block of Borkena graben. Na-Ca-HCO3 groups are represented by intermediate groundwater evolution which relatively long travel distance from the recharge source and more residence time. These types of water are found at Kombolcha area along the fault line of Dessie- Muti kolo- Bati.Na-HCO3 type waters were obtained from wells and thermal fault springs. The group has range of TDS values from 204- 938 mg/l.
- ✓ From inverse Geochemical modeling results the dominant reaction happened on this flow path is likely to be cation exchange, dissolution of silicate minerals, precipitation of calcite and Illite and clay minerals. As two flow paths were crossing the surface water divide between Gerado and Borkena catchments there is a reasonable evolutionary path for the solutes.
- ✓ Environmental Isotope evidences show most of groundwater from Gerado and Borkena catchments has a highly depleted isotopic signature of ^{18}O and D from -2.28 to -6.83 and -2.5 to -7.8 respectively. The regular trend in the isotopic signature of both catchments suggests a similarity in origin of the groundwaters. The groundwaters in the Borkena catchments are depleted in δ18O and δD contents

and show similar values to that of the groundwaters from the Gerado in the west, this may indicate the main source of recharge to both catchments is same.

6.2 Recommendation

This work has limitations with regard to the spatial and temporal Distribution of hydrogeological, hydro chemical and especially an isotope data. This problem is considerate in Gerado catchment since the water points are limited to some springs and few boreholes located in the Gerado well field. To better understand and increase the knowledge on the hydrogeological framework of a complex system. Appropriate use of current data and generating new data is vital.

The following points are forwarded as useful remarks for the future works.

- ✓ Spatial and temporal coverage of Surface water, groundwater and rainfall data are very limited.
- ✓ Data monitoring is not yet started to be implemented in the area boreholes. It is essential in both resource management and to characterize temporal variation of hydro chemical and hydrogeological parameters.
- ✓ The boreholes in the study area lack full information about the history of the wells. Drilling companies should have a proper data management system.

References

Abbate, E., Bruni, P., & Sagri, M. (2015). Geology of Ethiopia: A Review and Geomorphological Perspectives,Landscapes and Landforms of Ethiopia, springer, 2nd ed., pp. 33-64.

Addisu Deressa (2012). Hydrogeochemical and Isotope Hydrology in investigating groundwater Recharge and Flow Process, South Afar. Addis Ababa: Unpuplished MSc thesis, pp.128.

Amahara Design and supervision works enterprise (ADSWE) (2013). Awash Basin (Kobo – Robit – Minjar) Groundwater Potential Assessment Project. technical Report, Bahir Dar, pp.217.

Anderson, K., Nelson , S., Mayo, A., & Tingey, D. (2006). Interbasin flow revisited: The contribution of local recharge to high-discharge springs,Death vally. Hydrol, 323, 276–302.

Asantea , J., & Kreamerb, D. K. (2018). Identifying local and regional groundwater in basins: chemical and stable isotopic attributes of multivariate classification of hydrochemical data, the Lower Virgin River Basin, Nevada Arizona and Utah, U.S.A. Isotpes In Environmental and Health Studies, https://doi.org/10.1080/10256016.2018.1444611.

Australian Government bereau of rural sceinces (AGBRS) (2007). Managing Non Renewable Groundwater Resources. Department of Agriculture Fesheries and forestery. Science for decision makers,Australia

BCEOM), French Engineering Consultants ((1999). Abay River Basin integrated master plan,main report. Addis Ababa: Ministry of water resources.

Behailu Brhanu, Tilahun Azagegn, Tenalem Ayenew, & Masertti M. (2017). Inter-Basin Groundwater Transfer and Multiple Approach Recharge Estimation of the Upper Awash Aquifer System. Journal of Geoscience and Environment Protection, 76-98.

Clark, I. (2015). Groundwater geochemistry and Isotopes. New York: Taylor & Francis Group, 442 pp.

Craig, H. (1961). Isotopic variations in meteoric waters. Science, 133: 1702-1703.

Danapou, M., Højbergt , A. L., Jensen, K. H., & Stisen, S. (2019). Assessment of regional inter-basin groundwater flow using both simple and highly parameterized optimization schemes. Hydrogeology Journal, 27:1929–1947.

Dereje, G., Nata, T., & Miruts, H. (2016). Estimation of Groundwater Recharge Using Water Balance Model: A Case Study in the Gerado Basin, North Central Ethiopia. International journal of earth sciences and engineering, 9: 942-950.

Dereje, Gidafie. (2012). Groundwater potential assessment and water quality investigation of Gerado river catchment, Amhara region, north eastern Ethiopia. Mekelle University. Mekelle, unpuplished MSc thesis, pp 181.

Dricoll, F. D. (1986). Groundwater and wells (2nd ed.). USA: H. M. Smyth Company. Inc. Minnesota.

(FAO) (1997). Global soil and terrain data base.

Fazzini, M., Bisci, C., & Billi, P. (2015). The Climate of Ethiopia. World Geomorphological Landscapes, 65-87.

Fetter J. (2001). Applied Hydrogeology (4th ed). P. Lynch, S. Hale, & B. Sturla, Eds.) United States of America: Pearson, pp 615.

Fitts, C. (2002). Groundwater science. London.Elsevier sceince Ltd. 467pp.

Freeze, A. R., & Cherry, A. J. (1979). Hydrogeology. United States of America: Prentice-Hall. Inc., Englewood Cliffs, N.J. 07632, pp 624.

Frisbee, M. D., Tysor, E. H., Stewart-Maddox, N. S., Tsinnajinnie, L. M., Wilson, J. L., Granger, D. E., et al. (2016). Is there a geomorphic expression of interbasin groundwater flow in watersheds? Interactions between interbasin groundwater flow,

springs, streams,and geomorphology. Geophysical Research Letters, 43(doi:10.1002/2015GL067082), 1158–1165.

Genereux, D. P., Jordan, M. T., & Carbonell, D. (2005). A paired-watershed budget study to quantify interbasin groundwater flow in a lowland rain forest, Costa Rica. Water Resources Research, 41:1-17.

Genereuxa, D. P., & Jordan, M. (2006). Interbasin groundwater flow and groundwater interaction with surface water in a lowland rainforest, Costa Rica A review. Journal of Hydrology, 320:385–399.

Geyh, M. A. (2000). Environmental Isotopes in the Hydrological Cycle. Hannover: International Atomic Energy Agency.

Gibson J. J., Edwards T. W, Birks, S .J., St Amour N. A, Buhay,W. M., McEachern P, Wolfe,B. B., & Peters,D. L. (2005). Progress in isotope tracer hydrology in Canada. Hydrol Process.19, 303–327.

Gilvear, D. J., & Bradley,C.,(2009). Hydrological Dynamics II: Groundwater and Hydrological Connectivity.In the wetlands Handbook, 169-193.

Glynn, P. D., & Plummer, N. L. (2005). Geochemistry and the understanding of ground-water systems. Hydrogeology Jornal, 13: 263-287.

Geological survey of Ethiopia (GSE) (2009). Geology of Were Illu Area (NC 37-7). Basic Geoscince Mapping, Addis Ababa, pp 62.

Geological survey of Ethiopia (GSE) (2010).Geology, Geochemistry and Gravity Surveyof Dessie Area. Unpublished report, Basic geosciences core process, Addis Ababa, pp 76.

Geological Survey of Ethiopia (GSE) (2017). Hydrogeological and Hydrochemical Maps of Dessie (NC 37 – 3) sheet.Unpublished report, Groundwater Resources Assessment Directorate, Addis Ababa, pp 117.

Geological Survey of Ethiopia (GSE) (2017). Hydrogeological and Hydrochemical Maps of Were Ilu NC 37 – 7 Sheet. Unpublished report, Addis Ababa, pp 74.

Hem, J. (1989). Study and Interpretation of the chemical characterstics of naatural water (3rd ed.). U.S Geological Survey Water-Supply Paper 2254,pp 271.

IAEA,(2000). Environmental Isotopes in the Hydrological Cycle (Vol. I). Veinna.

Kassa, F. (2015). Ethiopian Seasonal Rainfall Variability and Prediction Using Canonical CorrelationAnalysis(CCA).EarthSciences,4(3):112-119,doi: 10.11648/j.earth.20150403.14).

Kelly, L., Kalin, R. M., Bertra, D., Kanjaye , M., Nkhata, M., & Sibande, H. (2019) Quantification of Temporal Variations in Base Flow Index Using Sporadic River Data: Application to the Bua Catchment, Malawi. Water, 1-17.

Ketema Tadesse (1980). Hydrogeology of the Borkena River Basin Wollo- Ethiopia. Unpublished MSc Thesis, Addis Ababa University, Addis Ababa, pp 115.

Kidist Ayalew (2018). Numerical groundwater Flow Modeling of the Gerado River Catchmnet. Unpublished Msc Thesis, Addis Ababa University, Addis Ababa, pp 105.

Kovalevsky, V. S., Kruseman, G. P., & Rushton, K. R. (2004). Groundwater Studies An international guide for hydrogeological investigations. United Nations Educational, Scientific and Cultural Organization(UNESCO), pp 430.

Kresic, N. (2007). Hydrogeology and Groundwater Modelling (2nd ed.). Rixeyville, Virginia, United States of America: Taylor & Francis Group, pp 830.

Kruseman, G. P., & de Ridder, N. A. (1994). Analysis and Evaluation of Pumping Test Data (2nd ed.). International Institute for Land Reclamation and Improvement, Amsterdam, pp 372.

Marei , A., Khayat , S., Weise , S., Ghannam, S., Sbaihr, M., & Geye, S. (2010). Estimating groundwater recharge using the chloride mass-balance method in the West Bank, Palestine. Hydrological Sciences Journal, 55(5):780-791.

Mazor, E. (2004). Chemical and Isotopic Groundwater Hydrology (3rd ed.). Marcel Dekker ,Newyork, pp 463.

Mesfin Sahle (2001). Hydrogeological Investigation of the Upper and Middle Borkena River catchment,noorthern Ethiopa,Wollo. Unpublished MSc thesis,Addis Ababa, pp 156.

Ministry of Water Irrigation and Energy (MoWIE) (2018). Kobo Chefa Groundwater Resource Evaluation, pp 113.

Mohr (1983). Perspectives On The Ethiopian Volcanic Province. Bull. Volcanol, 46-1: 23-43.

Mohr (1962). The Ethiopian rift system. Bulletin of the Geophysical Observatory, 5:33-62.

Molla Demile (2000). Hydrology Hydrogeology and Hydrochemistry of Lake Systems Haiq-Ardibo , Northern Ethiopia, Unpuplished msc theisis, Addis Ababa, pp 132.

Molla Demile., Wohnlich b, S., & Tenalem Ayenew. (2008). Major ion hydrochemistry and environmental isotope signatures as a tool in assessing groundwater occurrence and its dynamics in a fractured volcanic aquifer system located within a heavily urbanized catchment, central Ethiopia. Journal of Hydrology, 176-188.

Nelson, S. T., & Mayo, A. L. (2014). The role of interbasin groundwater transfers in geologically complex terranes, demonstrated by the Great Basin in the western United States. Hydrogeology Journal, DOI 10.1007/s10040-014-1104-6.

Parkhurst, D. L., & Appelo, C. (1999). User guide to PHREEAC: A computer program for speciation, batch reaction, one dimensional transport and inverse geochemical calculations. US geological survey, water resources investigation Report 99-4259.

Pik, R., Deniel, C., Coulon, C., Yirgu, G., Hofmann, C., Ayalew, D., 1998. The northwestern Ethiopian Plateau flood basalts: Classification and spatial distribution of magma types. Jornal of Volcanology and Geothermal Research, 81: 91–111.

Plummer, L. N., Prestemon, E. C., & Parkhurst, D. L. (1994). An Interactive Code (NETPATH) for Modeling NET Geochemical Reactions Along a Flow PATH version 2.0. USGS Water Resources Investigations Report.

Rango , T., Petrini, R., Stenni, B., Bianchini, G., Slejko, F., Beccaluva, L., et al. (2010). The dynamics of central Main Ethiopian Rift waters: Evidence from δD, δ18O and 87Sr/86Sr ratios. Applied Geochemistry, 1860-1871.

Rooney, T. O. (2017). The Cenozoic magmatism of East-Africa: Part I – Flood basalts and pulsed magmatism. Lithos, doi:10.1016/j.lithos.2017.05.014.

Rushton, K. R. (2003). Groundwater Hydrology Conceptual and Computational Models. Chichester, West Sussex, England: John Wiley & Sons Ltd.

Samson T., & Woldai, G. (2013). Simple shear detachment fault system and marginal grabens in the southernmost Red Sea rift. Tectonophysics, 608:1268–1279.

Seifu Kebede, Travi Y., Assfawossen Asrat, Tamru Alemayehu, Tenalem Ayenew, & Zenaw Tessema (2008). Groundwater origin and flow along selected transects in Ethiopian rift volcanic aquifers. Hydrogeology Jornal, 55-73.

Seifu Kebede, Yves, T.,Tamiru Alemayehu, & Tenalem Ayenew. (2005). Groundwater recharge, circulation and geochemical evolution in the source region of the Blue Nile River, Ethiopia. Applied Geochemistry, 20:1658–1676.

Seifu Kebede (2013). Groundwater in Ethiopia Features, Numbers and Opportunities. Springer-Verlag Berlin Heidelberg, pp 293.

Smakhtin, V. U. (2001). Low flow hydrology: a review. Journal of Hydrology, 240(3–4): 147-186.

Tenalem Ayenew, Tamiru Alemayehu, & Seifu Kebede (2007). Environmental isotopes and hydrochemical study applied to surface water and groundwater interaction in the Awash River Basin. Wiley InterScience.

Tilahun Azagegn, Assfawossen Asrat, Seifu Kebede, & Tenalem Aynew (2015). Litho-structural control on interbasin groundwater transfer in central Ethiopia. Journal of African Earth Sciences, 101:383-395.

Tilahun, Azagegn. (2014). Groundwater Dynamics in the Left Bank Catchments of the Middle Blue Nile and the Upper Awash River Basins, Central Ethiopia.Addis Ababa University, Unpublished phD thesis, Addis Ababa, pp196.

Toth, J. (1963). A Theoretical Analysis of Groundwater Flow in Small Drainage Basins. Journal of Geophysical research, 68(16):4795-4812.

Varsanyi, I. (1989). Tracing groundwater flow using chemical data. Hydrological Sciences Journal, 34(3): 265-275.

Wolfenden, E., Ebinger, C., Yirgu, G., Renne, P. R., & Kelley, S. P. (2005). Evolution of a volcanic rifted margin: Southern Red Sea, Ethiopia. Geological Society of America Bulletin, 117, 846–864.

Yitbarek Baye (2009). Hydrogeological and hydrochemical framework of complex volcanic system in the Upper Awash River basin, Central Ethiopia : with special emphasis on inter-basins groundwater transfer between Blue Nile and Awash rivers. Unpublished phD thesis, University of Poitiers, pp233.

Zanettin B., Justin-Visentin E., Nicoletti M., Piccirillo E.M.(1980) Correlations among Ethiopian volcanic formations with special references to the chronological and stratigraphical problems of the ‘trap series’. In: Geodynamic Evolution of the Afro-Arabian Rift System Acad, Naz. Linc, 47: 231–252

Zwaan, F., Corti, , G., Keir , D., & Sani, F. (2019). A review of tectonic models for the rifted margin of Afar: implications for continental break-up and passive margin formation. Journal of African Earth Sciences (https://doi.org/10.1016/j.jafrearsci)

APPENDICES

APPENDICES 1 Hydro meteorological data

1. **Mean monthly and annual precipitation (mm) at selected stations**

Year	X	Y	Z	Station	Jan	Feb	Mar	Apr	May	Jun	Jul	Aug	Sep	Oct	Nov	Dec	Annual
2007-2017	577980	1195287	2428	Albuko	16.5	45.6	56.4	110.5	123.8	59.3	404.0	475.7	143.0	60.4	52.5	25.8	1573.6
1995-2018	550825	1256357	2720	Borumeda	17.5	24.8	66.6	94.4	55.9	34.9	337.5	351.9	127.2	51.8	18.8	27.4	1208.6
2002-2016	583672	1214036	1400	Cheffa	21.3	22.2	71.8	94.1	58.3	24.3	261.2	298.6	90.3	29.4	20.5	21.3	1013.3
2000-2018	554769	1206152	3431	Guguftu	20.1	26.2	65.0	78.6	70.6	75.2	427.6	432.0	113.0	34.9	18.3	13.4	1375.0
2001-2018	585906	1207412	1507	Harbu	15.2	22.4	87.8	96.4	40.9	32.0	259.8	293.9	98.8	19.3	19.4	28.2	1014.1
1986-2003	591029	1184568	1450	Kemise	26.2	36.1	62.5	101.3	61.1	28.0	257.5	288.3	120.5	51.3	22.8	15.4	1071.0
1986-2018	578284	1225144	1857	Combolcha	22.7	24.2	62.8	94.9	56.9	33.2	281.1	264.8	106.3	44.9	19.4	16.5	1027.6
1986-2006	569065	1229115	2553	Dessie Zuriya	25.7	35.7	77.9	91.9	70.1	39.3	322.9	339.6	160.8	54.5	24.2	21.7	1264.4
2002-2018	559087	1211355	3302	Tebasit	18.0	18.6	49.5	66.8	77.5	65.6	394.7	436.7	129.5	32.7	20.7	8.9	1319.1
2002-2018	573179	1234191	2465	Tita	20.7	28.6	75.3	91.6	78.6	36.6	287.4	334.8	96.2	50.3	25.1	12.9	1138.2

2. Average daily Sunshine hours

Year	X	Y	Z	Station	Jan	Feb	Mar	Apr	May	Jun	Jul	Aug	Sep	Oct	Nov	Dec
2000-2009	578284	1225144	1857	Combolcha	8.1	9	8.3	8.3	8.6	7.5	6.3	6.4	6.9	8.2	8.8	8.4
2003-2013	583672	1214036	1400	Cheffa	7.5	8.5	8.1	8.1	8.9	7.2	6.1	6.6	7.2	8.5	8.8	8.3
2003-2012	522833	1237894	2990	Amba Mariyam	9	9.2	8.5	8.3	8.9	7.1	5.4	6.2	7.7	9.5	9.3	9.3

3. **Relative humidity in (%)**

Year	X	Y	Z	Station	Jan	Feb	Mar	Apr	May	Jun	Jul	Aug	Sep	Oct	Nov	Dec
2013-2016	578284	1225144	1857	Cheffa	62.3	55.72	55.6	57.21	56.1	42.6	58.2	71.2	68.8	61.3	59.3	57.9
2012-2016	583672	1214036	1400	Combolcha	62.81	55.6	55.4	59.6	54.76	44.3	57.4	67.8	64.5	60.1	61.3	60
2010-2016	522833	1237894	2990	Amba Mariyam	53.9	49.1	54.7	57.7	59.4	53	75.1	81.2	70.1	61.8	59.7	55.4

4. **Maximun and minimum average temperatures in (^{o}C)**

Year	X	Y	Z	Stations	Temprature	Jan	Feb	Mar	Apr	May	Jun	Jul	Aug	Sep	Oct	Nov	Dec
2008-2018	579573	1250149		Mariye	Min	7.1	8.2	9.5	11.0	11.9	12.2	12.1	11.6	10.9	8.6	7.6	6.9
					Max	20.8	22.8	24.2	24.7	25.4	26.7	24.4	23.0	23.3	22.6	21.4	20.5
2008-2018	522833	1237894	2990	Amba Mariyam	Min	18.0	17.7	17.4	17.3	16.6	16.4	15.7	17.3	17.1	15.6	14.5	13.7
					Max	20.0	21.3	21.7	21.5	21.3	21.5	18.4	17.5	18.5	18.9	19.2	19.4
2008-2018	573179	1234191	2465	Tita	Min	18.6	18.6	18.4	18.3	17.6	17.4	16.4	17.4	17.4	16.4	15.7	15.1
					Max	20.1	21.4	22.3	22.9	23.8	25.7	24.1	22.5	22.7	21.6	20.8	19.9

2008-2018	578284	1225144	1857	Combolcha	Min	18.2	18.5	18.7	18.7	18.5	18.6	17.6	18.2	18.3	17.3	16.5	15.9
					Max	25.5	27.1	28.2	28.6	29.3	30.7	28.8	27.5	27.3	26.6	25.8	25.2
2008-2018	585906	1207412	1507	Harbu	Min	18.5	19.1	19.4	19.6	19.5	19.9	18.6	19.4	19.4	18.5	17.7	17.1
					Max	28.2	28.5	30.4	30.2	31.2	31.7	30.7	29.3	28.6	27.9	27.6	27.3
2006-2013	554769	1206152	3431	Guguftu	Max	20.9	21.5	22.1	22.1	22.2	22.7	21.3	21.1	21.2	20.3	19.7	19.2
					Min	15.6	15.7	15.6	15.6	15.7	15.8	15.1	15.4	15.2	15.2	15.4	15.4
2008-2016	583672	1214036	1400	Cheffa	Min	20.7	21.3	21.9	22.0	22.2	22.8	21.6	21.3	21.3	20.5	19.9	19.4
					Max	27.9	29.9	31.4	31.6	33.0	35.0	32.5	29.9	30.0	29.7	29.2	28.0

APPENDICES 2 hydro geological data

X	Y	Altitude(m)	Static water level (m)	Well_field	Well depth(m)	Dynamic water Level(m)	Discharce (L/S)	Transmissivity (m2/day	Conductivity m/day	Aquifer type
582837	1207610	1500	5.04	Harbu	268	86.21	20	20.5	0.22	alluvial deposits (sand and gravel)
587540	1182638	1450	8.32	Mekoye	252	11.59	60	1690	20.2	alluvial deposits (sand and gravel)
590050	1185850	1423	0	Kemissie-gerbi	260	28.25	66	316	4.07	alluvial deposits (sand and gravel)
565035	1226086	2229	0	Gerado	62.5	19.93	35	246	12.3	alluvial deposits
566864	1226390	2226	0		123	23.35	22.51	56.4	1.34	alluvial deposits
564424	1226780	2223	0		115.5	18.4	15	25.8	0.677	alluvial deposits
565035	1225946	2229	0		120	16.2	39.9	118	2.4	alluvial deposits
564073	1227366	2220	0		80.87	27.87	16.5	21.1	0.571	alluvial deposits
569303	1224795	2257	0	Kelina	109	40.32	35	65.7	1.43	alluvial deposits
569755	1194212	2475	4.76	Degaga	121	21.66	13.4	142.2	3.93	basalt
578537	1226089	1850	0	Kombolcha	112	15.86	14.3	81.42	1.69	alluvial deposits
578231	1226297	1852	0		97.5	12.23	14.3	135	2.64	alluvial deposits
579350	1226465	1840	0		110.7	7.16	14.4	201	3.9	alluvial deposits
579379	1226203	1830	0		140	25.69	51	216	5.18	alluvial deposits

578913	1226081	1837	2.3		144	19.28	30	149	3.14	alluvial deposits
584805	1208278	1485	0	Harbu	146	56.67	26	405	1.12	alluvial deposits
584465	1208654	1485	0		121	53.63	27	81.4	2.01	alluvial deposits
596618	1186473	1480	7.91	Kemissie	147.6	69.08	5	4.89	0.068	alluvial deposite and rhyolite
595618	1186264	1455	6.25		149.5	38.35	13.5	49	0.742	alluvial deposite and rhyolite
569164	1239609	2609	41.05	Hoteh	133	42.16	6.8	744	18.1	Fractured Basalt
595092	1185850	1444	8.1	Kemisse	150	83.28	10.35	71.12	1.07	alluvial deposits and weathered rhyolite
595618	1186473	1480	6.81	Kemisse	147.6	69.08	5	4.62	0.07	alluvial deposits and Highly to completely weathered and fractured rhyolitic basalt
595618	1186264	1480	6.25	Kemisse	150	38.35	13.5	35.16	0.53	alluvial deposits and Highly fractured and weathered rhyolitic basalt
595373	1186685	1463	6.33	Kemisse	146	18.49	6.5	44.64	0.62	alluvial deposits and Highly fractured and moderately weathered rhyolite
597030	1184800	1481	9.25	Kemisse	145	23.27	19	130.2	1.97	Highly fructured and weathered rhyolite
590842	1185334	1415	0	Kemisse	260	0			0	alluvial deposits and Moderately fractured and weathered trachyte
579345	1226470	1836	0	Dewey	110	0	25	333.5/86.4	0	alluvial deposits
578542	1226092	1840	0	Sheshaber	112	40	20.5	88.4/101	0	alluvial deposits
578233	1226301	1844	0	Sheshaber	97	41	18.7	207.4/173.8	0	alluvial deposits
579376	1226205	1835	1.66		140	24.03		125.14	2.98	alluvial deposits and Highly fractured & weathered basalt
578936	1226045	1843	2.3		144	14.68		125.71	2.67	alluvial deposits
578718	1226240	1859	0	Sheshaber	112.5	15.86	14.3	81.4	2.01	alluvial deposits
578528	1226346	1850	0	Sheshaber	105	12.3	14.3	135	2.61	alluvial deposits

579565	1226611	1848	0	Dewey	110.7	7.16	14.4	201	3.89	alluvial deposits
579066	1226301	1838	6.96	Dewey	152.5	80.4	43	64.92	6.29	Alluvial
578915	1226614	1850	0	Dewey	258	78.8	63	552	7.27	Alluvial

APPENDICES 3 hydrochemistry data

ID	Na+	K+	Ca2+	Mg2+	HCO3-	Cl-	F-	SO2-4	NO-3	Br-	pH	EC, µS/Cm	X	Y	Z
DBH-13	21.8	0.64	38	12.7	190.32	5.67	0.1	10.3	13.29	0.2	7.46	344	566927	1238698	2609
DCSP-7	12.1	4.05	27.3	13.8	176.9	3.62	0.19	6.7	8.86	0.37	7.6	315	560001	1215214	2933
DCSP-8	21.5	1.27	73.8	14.7	300.12	12.83	0.11	11.2	23.92	0.52	7.31	577	552397	1223421	2578
DCSP-9	10.1	2.23	39.9	10.4	184.22	5.39	0.12	9.4	6.64	0.27	6.88	524	559655	1246384	2743
CSP-11	16.8	1.43	49.3	12.8	224.48	4.89	0.28	17.3	12.85	0.29	6.69	417	549444	1254991	2059
DRW-1	15	1.26	28.3	8.3	170.8	8.15	0.2	8.1	0.1	0.03	8.19	261	554001	1222972	2407
DBH-69	57.5	0.73	44.5	9.7	232.6	12.7	0.26	11	0.1	0	7.8	514	578230	1224874	1831
DBH-70	65.9	0.44	11.6	1.7	152.5	10.98	0.35	5.5	0.1	0	8.14	330	578543	1224851	1852
DBH-71	67	0.37	9.8	0.8	155.6	5.25	0.36	5.2	0.1	0	8.24	310	578675	1224673	1846
DBH-72	66.25	1.34	47.2	11.5	341.6	13.61	0.1	12.6	1.77	0	7.79	562	577191	1225245	1863
DRW-11	46.6	9.17	74.2	20.5	305	56.72	0.33	16.15	20.37	0	7.35	757	570025	1228657	2368
DRW-12	44.99	7.76	69.9	17.9	292.8	35.1	0.5	12.74	5.32	0	7.55	655	568928	1230048	2453
DRW-13	15.5	2.38	42.3	15	231.8	5.88	0.31	3.92	0.1	0	7.67	391	567009	1238290	2597
DCSP-30	14.9	0.85	60.9	18	309.88	6.09	0.15	7.9	6.2	0.32	7.9	496	582728	1231280	2257
DCSP_37	19.1	1.41	44.8	11.5	213.5	4.96	0.17	8.4	11.52	0.3	8.06	367	569287	1232031	2514
DCSP_38	8.6	0.49	38.2	8.1	195.2	3.19	0.19	5.4	2.21	0.22	7.81	309	568084	1229960	2584
DCSP_40	23.6	0.74	65.7	20.5	323.2	10.14	0.24	11.8	62.46	0.37	7.49	555	583910	1220692	2157
DDW-9	5.9	1.99	26.3	9	100.04	9.78	0.28	24.79	7.97	0.35	7.14	270	564333	1256732	2342
DBH-35	30.2	3.25	33.9	5.7	207.4	4.96	0.24	4.56	2.22	0.16	8.05	333	564670	1225399	2235
DBH-36	20.3	2.74	52.8	11.2	248.88	7.8	0.18	5.53	4.43	0.17	7.82	419	564708	1225536	2233
DBH-37	19.7	1.42	48	10	244	6.24	0.2	5.91	4.87	0.19	7.78	417	564494	1225842	2230
DBH-38	26.4	1.12	35.1	7.1	207.4	6.03	0.21	7.16	0.1	0.64	8.09	418	564050	1226264	2222
DBH-39	37.5	1.11	26	4.2	192.76	5.96	0.3	4.09	0.1	0.47	8.24	341	563411	1226816	2219
DBH-40	32.5	1.95	74.5	18.6	305	34.74	0.2	19.78	18.16	1.1	7.84	316	568979	1230036	2461
DBH-41	22.5	1.68	62.3	15.6	275.72	11.7	0.18	13.93	5.76	0.46	7.82	659	569224	1231526	2490
DBH-42	26.1	8.97	40.9	8.9	195.2	6.95	0.21	8.42	4.43	0.31	7.7	478	568760	1231553	2495
DBH-49	61	1.84	63.4	17.2	378.2	15.6	0.3	19.59	0.89	1.3	7.62	484	579283	1225622	1832
DBH-50	58.1	1.37	40.9	11.4	305	9.93	0.25	28.76	2.22	0.69	8.26	666	579015	1225653	1837
DBH-51	35.9	1.46	60.3	21.7	439.2	7.8	0.26	6.38	1.77	0.48	8.04	559	578907	1227572	1860
DBH-52	62.7	1.27	44.4	10.7	366	9.5	0.29	6.68	0.1	0.53	8.27	676	579154	1226670	1843

DBH-53	57	1.58	79.1	23.6	397.72	12.05	0.33	18.62	4.43	0.57	8.35	574	578982	1225920	1836
DBH-54	53.1	2.13	56.6	14.5	341.6	12.62	0.27	13.53	3.1	0.5	8.15	723	577860	1225749	1848
DBH-55	58.1	1.69	68.3	19.5	342.82	12.76	0.31	16.11	4.43	0.47	8.34	561	578170	1225540	1860
SBH-3	16.25	6.47	55.8	10.25	161	20.21	0.33	25.08	15.58	0.45	6.64	369	600805	1170977	1445
SBH-4	91.8	6.87	167.2	24.7	411.14	163.07	0.48	27.95	21.26	4.48	6.96	1394	599749	1171529	1415
SBH-5	59.7	21.38	132.4	25.4	247	100.68	0.64	111.85	62.02	2.52	6.93	898	590812	1187759	1447
SBH-6	41.9	3.58	150.8	41.5	356	90.18	0.33	101.39	86.39	1.46	7.23	1050	586670	1188168	1444
SBH-9	24.5	9.27	35	7.5	176.9	14.46	0.4	17.64	16.83	0.52	6.73	340	591099	1190335	1443
SBH-10	45	2.34	77.5	25.1	406.26	34.67	0.35	20.02	15.5	0.85	7.35	706	589035	1200408	1486
BH-2	32.9	1.81	109.45	40.5	477	10.35	0.27	12.77	20.38	0.96	7.74	787	586839	1182109	1467
BH-4	64.25	0.72	0.3	1.75	117.12	11.06	1.1	6.64	0.89	0.56	8.9	272	592875	1184375	1425
BH-5	60.6	7.44	99.9	20.7	452.62	22.76	0.51	27.57	0.44	0.45	7.48	678	595679	1186467	1466
BH-6	37	11.41	101.8	18.2	429.44	18.72	0.47	16.21	12.4	0.73	7.76	641	594267	1185353	1439
BH-7	153.5	8.58	25.8	6	389.18	32	1.21	50.6	4.43	1.06	7.82	720	591221	1193425	1463
BH-8	94	1.65	58.5	25.6	419.68	30.34	0.4	5.1	1.35	1.1	7.89	731	585349	1206825	1484
BH-9	0.2	2.2	55.3	19.7	366	65.58	0.41	31.22	10.63	1.81	7.75	784	584559	1208864	
BH-10	98.7	1.83	22.1	7.2	270.84	28.43	0.4	35.16	3.1	1.33	8.04	515	584897	1208484	1489
HSP-1	231.8	4.26	16.5	1.8	265	48.35	12.7	192	0.44	1.45	8.1	1025	601554	1175482	1417
HSP-2	267.3	2.82	11	1.6	464.82	32.05	2.57	155.9	0.1	0	8.02	1102	588396	1208522	1565
CSP-1	11.22	0.91	22.36	7.24	107	0.57	0.5	14.59	0.44	0.26	8.29	188	585556	1174709	1722
CSP-3	17.6	0.8	57.3	16.4	269.62	1.91	0.31	6.6	3.5	0	7.69	433	588396	1183662	1991
CSP-4	79.7	2.08	45.3	21.6	314.76	37.65	0.35	35.2	18.6	0	7.77	330	588855	1202670	1473
SBH-7	40	6.49	26.05	11.4	226	15.03	0.64	19.58	13.29	0.86	7.02	506	601405	1168458	1456
SBH-8	47.75	7.39	21.85	18.5	262.23	10	0.45	16.86	0.89	0.54	7.49	426	603913	1165181	1458
SBH-2	39.1	8.04	59.2	30.6	363	7.23	1.09	9.77	0.4	0.44	7.33	561	601032	1165645	1449
BH-1	33	9.87	49.05	9.9	203	12.12	0.46	30.26	12.85	0.49	6.72	410	601858	1167012	1481
BH-3	17.8	4.04	40.3	11.15	187	3.4	0.64	3.9	2.22	0.32	7.56	308	600512	1163039	1466
DBH-16	16.9	0.94	57.1	13	217.16	9.43	0.25	16.3	11.08	0.18	7.57	427	537991	1263934	1736

Isotope data

ID	x	y	z	Locality	^{2}H	^{18}O
CSP_8	552397	1223421	2578	Gandera	-8.99	-2.75
CSP_9	559655	1246384	2743	wela wela	-11.55	-3.27
CSP_11	549444	1254991	2059	Kundi	-4.07	-1.74
CSP_22	574139	1237782	2360	Mededo	-3.43	-3.12
CSP_23	562651	1267865	1873	Robit	3.86	-1.89
CSP_37	569287	1232031	2514	Dessie/Kurkur	-15.17	-4.73
CSP_38	568084	1229960	2584	Dessie/Sire	-12.29	-4.59
CSP_41	584094	1221342	2287	Ancharo/sholla	-1.11	-2.04
CSP_7	560001	1215214	2933	Dessie	-16.85	-4.27
CSP_12	589367	1226447	1921	Kalu	-1.18	-1.44
CSP_29	596589	1237831	2183	023 Kebele/Kalu	0.7	-2.28
CSP_53	517869	1254740	2394	Tenta	-7.04	-2.14
DBH_35	564670	1225399	2235	Dessie	-6.06	-2.83
DBH_36	564708	1225536	2233	Dessie	15.03	2.52
DBH_37	564494	1225842	2230		-1.53	-1.72
DBH_38	564050	1226264	2222	Dessie	-11.03	-2.95
DBH_40	568979	1230036	2461	Dessie	-2.45	-1.88
DBH_49	579283	1225622	1832	kombolcha	-6.87	-2.24
DBH_50	579015	1225653	1837	kombolcha	-10.33	-2.98
DBH_13	566927	1238698	2609	Kalu	-8.12	-2.71
DBH_14	599142	1231220	1483	Kalu	1.5	-1.05
DBH_18	573979	1279765	1518	Habru	0.55	-1.57
DBH_39	563411	1226816	2219	Gerado	-14.38	-3.33
DBH_41	569224	1231526	2490	Gerado	-5.26	-2.11
DBH_51	578907	1227572	1860	Kombolca	-10.33	-3.32
DBH_52	579154	1226670	1843	kombolcha	-14.95	-3.59
DBH_53	578982	1225920	1836	kombolcha	-4.58	-2.2
DBH_55	578170	1225540	1860	kombolcha	-2.13	-1.38
DBH_62	523376	1238731	2918	Tenta	-15.91	-3.97
DBH_65	525736	1240584	2889	Tenta	-15.52	-3.87
DBH_69	578230	1224874	1831	kombolcha	-17.92	-3.82
DBH_70	578543	1224851	1852	kombolcha	-17.26	-3.92